Quorum Sensing Cooperation and Conflict in *Pseudomonas aeruginosa*

A Dissertation Presented to
The Academic Faculty

By

Kathleen O'Connor

In Partial Fulfillment
of the Requirements for the Degree Doctor of Philosophy in Biological Sciences

Georgia Institute of Technology

December 2023

Quorum Sensing Cooperation and Conflict in *Pseudomonas aeruginosa*

Approved by:

Stephen P. Diggle, PhD (Advisor)
Biological Sciences
Georgia Institute of Technology

Marvin Whiteley, PhD
Biological Sciences
Georgia Institute of Technology

Sam Brown, PhD
Biological Sciences
Georgia Institute of Technology

Kendra Rumbaugh, PhD
Department of Surgery
Texas Tech University

Joanna Goldberg, PhD
Department of Pediatrics
Division of Pulmonary, Asthma, Cystic Fibrosis, and Sleep
Emory University School of Medicine

“Does the path choose the walker, or the walker the path?” – Garth Nix, Sabriel

I dedicate this thesis to my family: chosen family, blood family, and family through law.

Acknowledgements

I would like to first and foremost acknowledge the continued support of my advisor, Dr. Stephen P. Diggle. I admired your work from afar for years, and I am so grateful to have done my doctorate under your supervision. I would like to thank to my committee members, Dr. Kendra Rumbaugh, Dr. Marvin Whiteley, Dr. Sam Brown, and Dr. Joanna Goldberg. Thank you especially to Dr. Whiteley who gave me a healthy reality check at the beginning of my PhD and pushed me to be the student I am today. Thank you also for the use of your lab's confocal microscope. Without that piece of equipment, I would have a much shorter thesis. Thank you to Dr. Rumbaugh for acting as a supporting mentor and meeting with me monthly – you caught me during a difficult time while coming out of the pandemic and got me out of my rut.

Thank you to both past and current Diggle lab members for your training, support, and laughter. Thank you especially to Dr. Madeline Mei and Dr. Jelly Vanderwoude, with whom I overlapped the most with at Georgia Tech. Thank you for sharing your opinions and knowledge and for giving me a greater understanding of both science and myself. Thank you to Dr. Sheyda Azimi for training me on the confocal microscope, and additionally for driving me to and from work while I was without a car.

I am grateful for to the greater CMDI research community. Thank you to the many grad students, professors, and post-docs who offered advice, reagents, and shared equipment. It takes a village.

Thank you to Chung Kim, a constant administrative support during my doctorate. You were endlessly patient with me while I navigated with the administrative aspects of academia. Thank

you also for your patience and help during interview weekend back in 2018, I was very nervous and you were so kind to me.

Thank you to my dear wife, Kay Heffernan. You took a leap of faith and moved to a new city with a near stranger, and I am forever grateful that you took that chance. Your constant support kept me going during this process. Thank you for your patience, your love, and your humor. I am so proud to share my life with you and I know my PhD would have looked a lot different without your support. Thank you also to our dear cat, Paprika. You made a great emotional support animal while I was writing.

Thank you to my parents for their support, emotionally and financially during my PhD. I am grateful for the safety net you provided, your constant reassurance and pride, and for always patiently listening to me explain my work. Thank you also to my in-laws, who have become a source of support and love in recent years. Thank you for welcoming me into your family and showing so much support during this process. Thank you to my extended family for your unconditional love and constant cheerleading. You believed I'd go on to win the Nobel Prize before I had even achieved candidacy.

Thank you to my chosen family, both those based in Atlanta and those distributed across the globe. Your coffee meet-ups, dinner dates, phone calls and visits have kept me grounded and sane during a challenging process. Thank you dear friends new and old.

TABLE OF CONTENTS

List of Tables

List of Figures

LIST OF SYMBOLS AND ABBREVIATIONS

3O-C12-HSL *N*-3-oxo-C12-homoserine lactone

AHLs *N*-acyl homoserine lactones

AQs alkyl-quinolones

bp basepair

BLAST Basic Local Alignment Search Tool

C Celsius

C4-HSL *N*-butanoyl-homoserine lactone

CF cystic fibrosis

CFU colony forming units

DNA deoxyribonucleic acid

HHQ 3-hydroxy-4-quinolone

h hours

IPCD International Pseudomonas Consortium Database

L liter

LB lysogeny broth

LBA lysogeny broth agar

LPS lipopolysaccharide

µL microliter

µM micromolar

mM millimolar

mL milliliter

nm nanometers

OD optical density

OSA O-specific antigen

PBS phosphate buffered saline

PCR polymerase chain reaction

PQS Pseudomonas Quinolone Signal, 2-heptyl-3-hydroxy-4-quinolone

QS quorum sensing

t time

WT wild type

Summary

Bacteria are single celled organisms capable of making great changes to their environment. They accomplish this by working together – using social behaviors to collectively affect the world they live in. Bacterial cells are capable of both cooperation and conflict, flip sides of social behaviors that either benefit or harm the overall population. Social behaviors can only be maintained when the trait benefits both producing cells and closely-related neighbors, and are not overly costly to fitness. The social evolution in microbes field was born from looking at intra-species *Pseudomonas aeruginosa* social behaviors in liquid media, studying theory established by evolutionary biologists and economists and applying it to real organisms. Social studies in bacteria have now expanded to inter-species and even inter-kingdom social interactions. The field has also begun studying the importance of spatial structure for social traits, and it has been suggested that proximity is essential for social interactions in microbes. In this thesis, I focus on the social behavior quorum sensing (QS) in *P. aeruginosa*. I first investigate the variation in phenotypic and genotypic QS traits in *P. aeruginosa* across different environments, and then I study the impact of spatial structure and proximity on QS-regulated cooperation and spite.

Chapter 1: Introduction

1.1 *Pseudomonas aeruginosa:* A Clinically Important Opportunistic Pathogen

Pseudomonas aeruginosa is a Gram-negative Gammaproteobacteria that engages in a range of social traits and is a common model organism for studying social behaviors, in addition to being a pathogen of interest in human infections [1]. *P. aeruginosa* can be isolated widely from animal and human-associated sources [2–5]. It is often associated with moist surfaces and is frequently found on medical devices in hospital environments, including respirators and in-dwelling devices like catheters [6–9]. *P. aeruginosa* causes chronic lung infections in individuals with chronic obstructive pulmonary disease (COPD) or cystic fibrosis (CF), eye infections in contact-wearers, virulent skin infections in burn patients, and is responsible for difficult to treat infections of implanted surgical devices [10–13]. In addition to being a social organism that works cooperatively to cause disease, *P. aeruginosa* has a large genetic tool kit – with a large genome and an even larger pan-genome across different strains [14]. Once in a host, *P. aeruginosa* genetically diversifies, making it difficult to target by both the host's immune system and the patient's treating clinician [15–18]. *P. aeruginosa* has a lipopolysaccharide (LPS) structure which varies by strain serotype, and which can render cells resistant to multiple antibiotics [19]. The bacterium also rapidly evolves resistance against new antimicrobials [20]

P. aeruginosa is considered an opportunistic pathogen because it rarely infects healthy humans. Instead, it infects those already ill, elderly, immunocompromised or otherwise predisposed to disease. In some types of infection, *P. aeruginosa* is a secondary pathogen. In chronic wounds, *Staphylococcus aureus* often initially establishes an infection, causing tissue destruction which

creates a niche for *P. aeruginosa* to establish itself. Once inside a host, *P. aeruginosa* expresses virulence factors that cause tissue decay and ultimately disease [21–24]. *P. aeruginosa* uses quorum sensing (QS), which is described in more detail below, to socially coordinate the production of secreted products. The bacterium secretes phenazine products which act as reactive oxygen species, leading to host cell death [25, 26]. *P. aeruginosa* also produces volatile hydrogen cyanide gas which inhibits cell respiration in host cells [27–30]. Complicating immune response and treatment, *P. aeruginosa* forms multi-cellular surface attached biofilms and free-floating aggregates which are coated in extracellular polymers and proteins [31]. This type of growth protects the cells from the immune system and changes their interactions with antibiotics due to changes in growth rate and oxygen availability [32]. *P. aeruginosa* causes difficult to treat biofilm-related infections on implanted medical devices, often requiring costly and uncomfortable replacement of the device after failed treatment attempts [33, 34]. The bacterium is perhaps most notoriously known for causing morbidity and mortality in people with CF, where it causes chronic lung infections. Before the development of tobramycin, an inhaled antibiotic, *P. aeruginosa* was once responsible for CF patients having a life expectancy of under 30 years.

Many virulence factors produced by *P. aeruginosa* can be considered social behaviors, including protease excretion, siderophore production, biofilm formation, antibiotic resistance mechanisms, QS, and phenazine secretion [35–40]. Protease secretion is essential for the cell to feed on large proteins, and causes destruction of human host tissues. Siderophores, iron-chelating molecules which are secreted extracellularly, are essential for the cells' proliferation in the host [41]. *P. aeruginosa* grows as a social community in biofilms, making it difficult to eradicate chronic infections. These social behaviors are important for *P. aeruginosa* to establish infection and have

implications for disease outcomes. It is important to understand the complex dynamics that impact social behaviors such as cooperation and spite in *P. aeruginosa* and other social bacteria.

1.2 The Evolution and Maintenance of Social Behaviors

Social behaviors have evolved throughout the tree of life, allowing individuals to work as a group to make changes to their collective environment. In the event of biotic or abiotic stressors, individuals must work cooperatively to obtain nutrients and reproduce as they are incapable of surviving alone. Social behaviors encoded by a heritable gene are maintained when individuals selectively benefit others with the same gene, increasing the fitness of the receiver and ensuring the gene is passed on.

Table 1. Microeconomics defines 4 types of "goods" based on whether they are rivalrous or excludable. Common goods (referred to as public goods in the sociomicrobiology field) have been commonly studied in bacteria. Public goods which are non-rivalrous have not yet been studied in bacteria. (*) Siderophores and QS could be argued as common goods or club goods based on whether they are considered excludable and/or rivalrous. They are private to a strain or species, but if cheating takes place intra-specifically then the goods are rivalrous and excludable.

	Rivalrous	Excludable	Bacterial Examples
Common Good	Yes	No	Anibiotic resistance, protease secretion, siderophores*, quorum sensing*
Public Good	No	No	Not yet documented
Private Good	Yes	Yes	Cyanide resistant cytochrome oxidase, adenosine metabolism
Club Good	No	Yes	Siderophore* (strain specific), quorum sensing* (species specific)

The microbiology field has used the theory and language of evolutionary biology and economics to describe social behaviors in living creatures. Sociobiology focuses on cooperative behaviors and social interactions, while economics studies the exchange of "goods" in human populations. In economics, goods can be categorized into 4 categories based on whether they are rivalrous and/or excludable: common goods, public goods, club goods, and private goods (**Table 1**) [42].

Common goods and public goods are both freely available, but only common goods are rivalrous. An example of a common good would be a field that multiple sheep herders would use to graze their sheep – anyone can use it, but if too many sheep graze, then the resource will be depleted. Public goods are non-rivalrous, meaning they cannot be used up and will remain freely available – like a dam used to block a river or the use of calculus. Private and club goods are excludable, meaning they must be purchased in some way to be accessed. Private goods are rivalrous and excludable - they must be purchased to be used and they can run out; an example would be a purchased good like a car or a piece of furniture. A club good is excludable, and is accessed through membership to a community, but they are not rivalrous and will not run out. Club goods might look like access to a private swimming pool or golf course that can be used exclusively by club members. Microbiologists therefore use economics theory to describe social behaviors in bacteria based on whether the behaviors are rivalrous or excludable.

As far as we know, bacteria do not operate complex economies using currency to trade goods like what we see in human communities. Instead, we study the social behaviors bacterial cells exhibit and how neighboring cells are affected. Perhaps best studied in bacteria are publicly available and rivalrous behaviors that can be considered the production of "common goods." These common goods are secreted outside of the cell so they are available to producing and non-producing neighbors alike, but they can be used up if there are not enough producers, making them rivalrous. The authors are not aware of examples of true "public goods" (which are non-rivalrous) that have been discovered in bacterial populations. Common goods observed in bacteria have tended to be named (incorrectly) as "public goods." For the remainder of this thesis, public goods as described in bacterial populations will refer to the production of non-excludable and rivalrous products. We

predominantly use the term public goods for consistency with the current literature. Private goods in bacteria can only be used by the producing cell, often because the behavior is kept intracellularly. Club goods can be loosely attributed to bacterial behaviors, if the reader accepts a few caveats. An example of a club good would be a secreted product that is only available to a select group of bacteria, and which would be non-rivalrous. Siderophore production by *P. aeruginosa* could be considered a club good because only closely related individuals sharing the receptor for the siderophore can use the good – they are in a quasi-club together [43, 44]. QS signals, which are specific to a species can also be considered a club good from the perspective that non-species members cannot use it [45]. However, in both the case of siderophore production and QS signal production, these traits are rivalrous and will be depleted if there are not enough producing cells [46, 47]. Therefore, while a case could be made to describe some bacterial traits as club goods, but the field has primarily focused on categorizing bacterial behaviors as private or public/common.

Figure 1. Cheating in spatial structure: here we illustrate how *P. aeruginosa* cheats on QS-regulated protease secretion. Cooperators (green) produce a localized public good: exoprotease which breaks down large proteins into amino acids for consumption. The denser cooperators, the more active QS is and the more exoprotease they secrete. Cheaters (red) that are close to many cooperators receive the most benefit. Cheaters next to a single cooperator or next to know cooperators receive less public good.

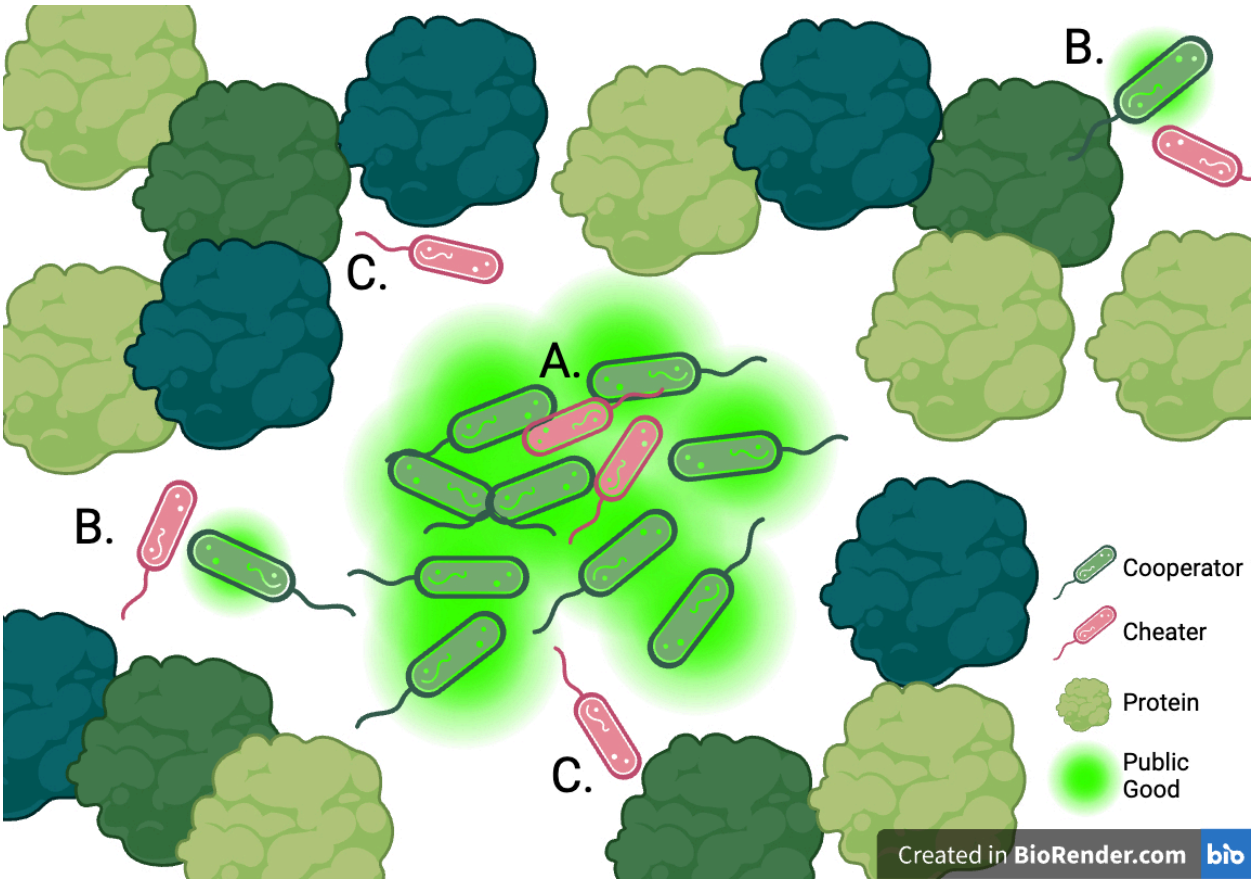

In bacteria, public goods are secreted by the producing "cooperator" cell and are available both to the producing cell and to nearby neighbors. If cells are assorted by social behavior, then only cooperators benefit from public goods. In a mixed population, cooperators may have no way to exclude cooperation from "cheaters." Cheaters are cells that receive a fitness benefit from the cooperative behavior but do not contribute to producing public goods. An example of public goods cheating - exoprotease cheating in bacterial populations - is illustrated in **Figure 1**. Green cooperators secrete public goods (green gradient) when they are densely packed (A); cheaters receive the greatest benefit when they are close by to numerous cooperators. The fewer cooperators present, the less public goods they produce, and the lower the fitness benefit for cheaters (B). When cheaters are far from cooperators, they are not exposed to any public goods and will perish (C).

Cheaters do not bear the cost of cooperation, so they have more resources to devote to reproduction. Because of this, cheaters can take advantage of cooperators and overtake the population. When there are too many cheats in an environment where social behaviors are required to survive, there will not be enough public goods to sustain life, and the population will crash. When cheaters take over and all cells suffer, it results in a "tragedy of the commons," where the entire population collapses, leading to the loss of the cooperative trait. To maintain cooperation, cooperators must selectively benefit themselves and suppress the growth of cheaters [48–51].

Cooperation dynamics are affected by 3 factors, as described by Hamilton's rule: $rb - C > 0$ [51, 52]. Relatedness is represented by r, and is a quantification of how related individuals are. The second defining factor is C, the cost of cooperating. The more costly a behavior, the more at-risk cooperators are to cheat invasion. The third factor is benefit, or the mutual benefit that recipients receive from the cooperative behavior. Larger benefit and relatedness will lead to the maintenance of cooperation while increased cost will decrease the maintenance of cooperation. Hamilton's rule informs the evolutionary outcome for 4 types of interactions: cooperation where both actor and receiver are benefitted (+,+), altruism where the actor is harmed and the receiver benefits (-,+), selfishness where the actor is benefitted and the receiver is harmed (+,-), and spite where both the actor and receiver are harmed (-,-). [53]

Cheaters are individuals in a cooperative population that do not contribute to the cooperative behavior yet receive a fitness benefit. In microbiology experiments, cheater and cooperator cells are often isogenic except for a single gene which controls the cheating behavior. Cheaters are

defined as having r = -1, while fellow cooperators are defined as having r = 1 and they can arise through spontaneous mutation of the cooperative gene, rendering it non-functional. Cooperation is energy intensive, and individuals contributing to cooperation have fewer energetic resources to devote to reproduction. Cheaters therefore reproduce more quickly than cooperators and overtake the gene pool. To maintain cooperation, cooperators need to selectively benefit individuals carrying the cooperative gene. In social animals, intelligent cooperators remember who in the community is cooperative and can selectively benefit them through reciprocity [54]. Cooperation is not only seen in sentient animals though, but also in single celled organisms, which presumably cannot remember which individuals are fellow cooperators. Bacteria, single celled prokaryotes, need another mechanism to differentiate between cooperator and non-cooperator and selectively avoid cheaters. One method is assortment: spatially dividing cooperators and cheaters so that only fellow cooperators are nearby. If the social behavior is localized, then only close by cooperators will receive that beneficial behavior. Another mechanism is "pleiotropy," linking the control of cooperation with another gene essential for function. That way if a cell loses the cooperative trait, there is a mechanism to suppress its growth.

Bacteria make ideal models to study social dynamics. Unlike multi-cellular organisms, they can be grown in large batches, manipulated, and killed without ethical research restraints. In addition to being convenient models for study, bacteria use social behaviors to cause disease, so it is essential we study social behaviors in bacteria.

1.3 Social Behaviors in the Bacterial Domain

Social behaviors in bacteria take many forms, whether it be interactions that increase or decrease the fitness of neighbors, or whether it be a secreted product or collective change in behavior. One of the more complex social behaviors seen in bacteria is QS, which is selectively expressed based on cell density [55–60]. QS has been well studied in *P. aeruginosa* where is varies greatly between strains and rapidly evolves in infections. QS is a density-dependent controlled social behavior that controls both cooperation and spite in some bacteria. It is seen in Gram-positive and Gram-negative cells, although the two types are mechanistically very different from one another. It is complex enough that it calls for further exploration it its own section, seen below. Another change in behavior cooperatively regulated by cell density is growth rate in liquid cultures. In late phase growth in liquid cultures *in vitro*, the availability of food decreases and the media acidifies [61] Cells collectively slow their growth and reproduction so that the population can continue to survive. Bacteria often use stimuli from their environment to regulate the expression of social behaviors, because it would be costly to constitutively express them.

In addition to responding to density with behavioral changes, bacteria work socially to secrete products essential for survival. Many well-studied cooperative behaviors are secreted products that are available to the producer cell and neighbors. Certain antibiotic resistance mechanisms are cooperatively produced [62]. Beta-lactamases break down beta-lactam antibiotics and are secreted by the cell, so that they can be shared collectively with neighbors. Bacteria are unable to bring large proteins into the cell, so they secrete proteases – enzymes that work extracellularly to break down proteins in the environment [63] Proteases serve the dual function of also breaking down host tissues during infections. In the host environment, iron is an essential but limited resource. Cells secrete iron-chelating molecules called siderophores to bind and sequester iron for bacterial

use [41]. They are produced by cooperators and are widely available to neighboring cells. Bacteria grow in collective communities called biofilms, which are formed through the secretion of extracellular products. Growth of bacteria in biofilms changes their resistance to antibiotics, their growth rate, their susceptibility to predation, and their exposure to oxygen and other diffusible nutrients [32]. The secretion of extracellular matrix and protein components of the biofilm has been described as a cooperative behavior [64].

Bacteria also demonstrate selfish and spiteful behaviors, which are used to harm neighbors, and incidentally is neutral or harms the producing cell, respectively. Bacteriocins are spite molecules produced by cells which kill other bacteria by punching through the cell wall and leading to cell lysis [65]. *P. aeruginosa* produces multiple forms of bacteriocins, more specifically called pyocins used for intra-species competition [66]. In addition to killing neighbors with secreted bacteriocins, *P. aeruginosa* uses membrane-located Type VI secretion system (T6SS) to punch holes in the cell wall of neighboring cells of different species, such as *Vibrio* bacteria [67]. T6SS is seen in intra-Domain inter-species competition between bacteria. Another form of secretion system, Type III secretion system (T3SS) is used by *P. aeruginosa* and *Salmonella* to cause virulence in inter-Domain interactions in humans by delivering toxins into host tissues [68]. Complex mechanisms regulating the expression of T3SS are essential for its maintenance as a costly social trait [69, 70]. In addition to molecular mechanisms to perforate the cell wall and cause lysis, *P. aeruginosa* also produces diffusible spite molecules that act as reactive oxygen species or cell respiration inhibitors – such as phenazines and hydrogen cyanide [40, 71].

Many of these social behaviors seen in *P. aeruginosa* are controlled through a complex hierarchical QS system.

1.4 Quorum Sensing: A Social Behavior Regulating Other Social Behaviors

QS is a chemical communication system used by bacteria to coordinate behaviors. It is a social behavior that controls both cooperative and spiteful behaviors [71–73]. The best studied form of QS is acyl-homoserine lactone (AHL) signaling, which is a form of one-component signaling involving a transcriptional regulator which alters DNA expression once bound to a cognate signal [58]. The signal is produced by a signal synthase, which is encoded on the genome close by to the transcriptional regulator. AHL-dependent QS was first described in *Aliivibrio fischeri* (previously a member of the *Vibrio* genus) where is controls the production of bioluminescence [74]. Luminescence turns on in *A. fischeri* when there is a critical accumulation of autoinducer, which is an AHL signal. QS is now well studied in many bacterial species, especially *P. aeruginosa,* due to its importance in regulating virulence determinants during human infection.

Figure 2. QS in *P. aeruginosa* is composed of 3 interconnected systems. *Las* hierarchical regulates *rhl* and *las* and previously was attributed to total control over the system. New research shows that the *rhl* system can also regulate the *las* system and the *rhl* and *pqs* system regulate each other independently from *las.*

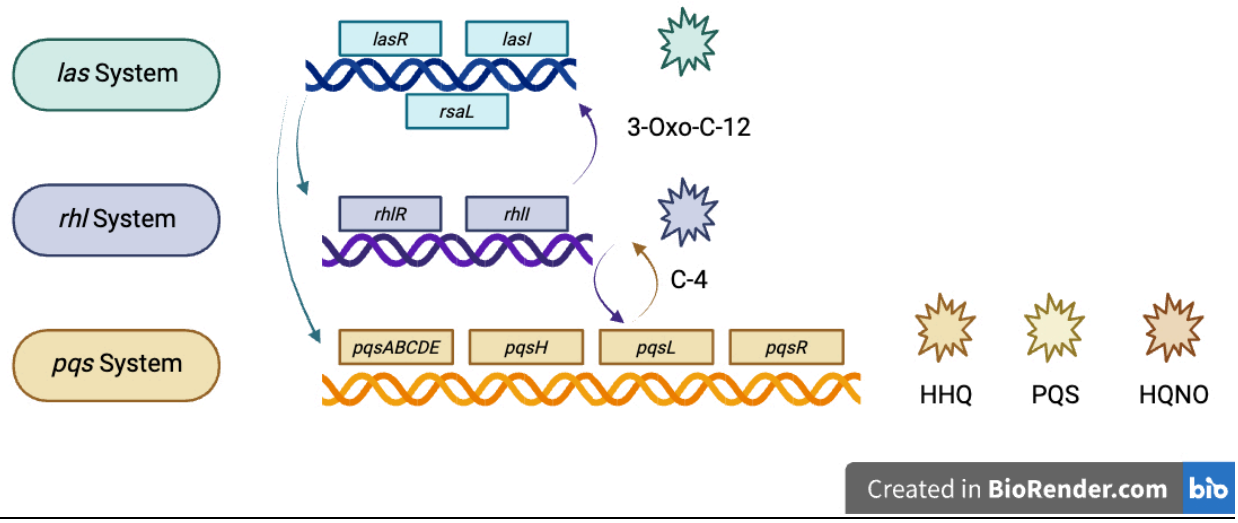

P. aeruginosa has 3 interconnected QS systems – 2 AHL systems, and a 3rd quinolone-dependent system termed the PQS system (**Fig. 2**) [73, 75–83]. Throughout the 1990s, the *las* AHL system was established as the hierarchical controller of the *rhl* and *pqs* systems. Recent work has shown that rather than a simple hierarchy, the *las, rhl* and *pqs* systems have interconnected control over one another, and that control varies between different strains [84]. Traditionally, *las* was seen as having total control over the *rhl* system - when *las* was deleted, it was assumed that all AHL QS behavior was lost. More recent studies have shown that RhlR is capable of regulating *lasI* expression, reversing the traditional hierarchy [85]. *Las* still appears to have the upper hand and its control over *rhl* makes for bigger changes in transcriptional regulation than when RhlR regulates *lasI*. (**Fig. 3**)

Intriguing new data has also shown a complex interconnected relationship between the *pqs* and *rhl* systems that functions independently of *las*. PqsE, part of the *pqs* operon, is an important regulator of virulence during infection. PqsE appears to cooperate with RhlR through either direct protein-protein interactions or through another more complex and unknown mechanism [86–92]. Because

las was seen as the top of the hierarchy, behaviors controlled by *rhl* and *pqs* were also attributed to be under *las* control. When *P. aeruginosa* was isolated showing colony autolysis or a lack of exoprotease production, it was attributed to a loss of the *lasR* gene [93–96].

In addition to reversing the hierarchy, *rhl* can function independently of *las* in certain evolved isolates from the CF lung, possibly through growth as aggregates in the CF lung, because *P. aeruginosa* is exposed to a high volume of extracellular QS signals from large neighboring aggregates. *In vitro* exposure of *lasR*- cells to high levels of C4-HSL (the cognate signal of the *rhl* system) leads to independent expression of the *rhl* system. We hypothesize that through its growth as aggregates in the CF lung, *lasR*- *P. aeruginosa* aggregates are exposed to C4-HSL, leading to independent *rhl* function.

P. aeruginosa commonly loses the *lasR* gene, and no longer excretes protease or other QS-regulated traits. Some works have suggested that these cells are social cheats, but we would argue that there is no data to support that, as cells likely do not need to cheat or be social to survive in the CF lung. The CF lung is rich in amino acids and other carbon sources, so *lasR*- strains do not need to socially cheat on proteases produces by wildtype strains [97]. Instead, it is likely the fittest adaptation for the cell because QS is energy intensive, and not necessary for chronic infection.

A portion of evolved *lasR*- strains maintain some QS function through changes to the *mexT* gene, or through changes in the interactions between the *rhl* system and *pqsE* [84, 98]. The *mexT* gene is constitutively overexpressed in MPAO1, a common lab strain used in cheating experiments and experiments to study the evolution of QS. *mexT* regulates the expression of the *mexEF-oprN*

operon, an efflux pump that incidentally effluxes HHQ, and *pqs* system produced QS signal [99, 100]. In our limited understanding of the interactions between the *rhl* and *pqs* system, upregulating efflux of a *pqs* signal likely suppresses the activity of the *rhl* system [101]. Through the loss of MexT, *rhl* is likely upregulated, allowing it to function independently of *las* in evolved strains. I hypothesize that inactivating MexT leads to an accumulation of HHQ in the cell, which upregulates the expression of the *pqs* system and leads to increased PqsE protein levels. With increasing PqsE levels, PqsE and RhlR form a protein-protein interaction and lead to the independent *rhl* system activity (**Fig. 3**). Specific molecular experiments are needed to confirm the hypotheses proposed in this section.

Figure 3. When the cell loses MexT function, *rhl* can function independently from *las*, but the exact mechanism that allows this to happen has not been defined. Other works have shown that MexT regulated MexEF-OprN will efflux HHQ, a quinolone intermediate and alternative *pqs* system signal. HHQ activates the *pqsABCDE* operon, which activates the *pqsR* regulator, which leads to a *pqs* positive feedback loop. With increased *pqs* system activity, the PqsE protein is expressed in excess. This has not been experimentally shown, but by linking findings from multiple recent papers, I suggest that increased PqsE intracellular levels leads to an interaction between RhlR and PqsE and independent function of the *rhl* system.

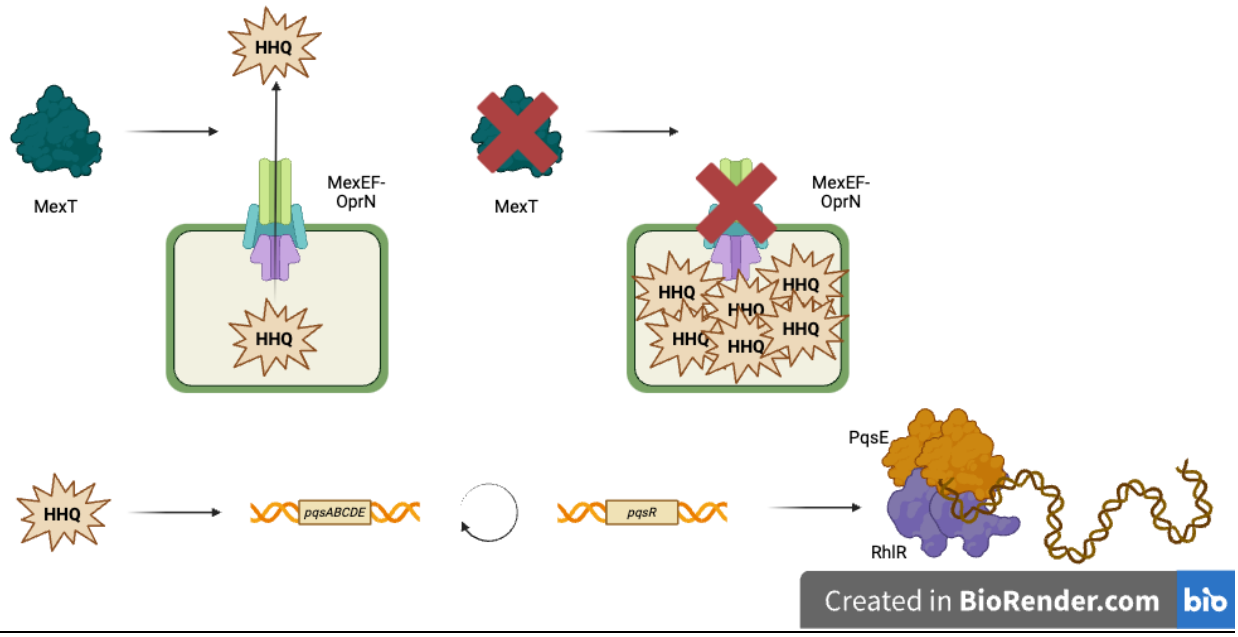

QS in *P. aeruginosa* controls behaviors important to establishing itself in an environment. *P. aeruginosa* uses QS to sense population density and respond collectively when it reaches a critical density. Some works have also shown that the multiple signals *P. aeruginosa* uses can help the bacterium sense the diffusibility of the environment, potentially informing social behaviors [102]. QS regulates the expression of toxins, proteases, biofilm formation, and antibiotic resistance mechanisms. QS is considered a social trait not only because it is impacted by the presence of other organisms, but because it also regulates the expression of other social traits.

At one time, it was suggested that QS was not a social trait and was just a response to diffusion [103, 104]. It was theorized that diffusion-related response to density was a means to preserve secreted products which would wastefully diffuse away if cells were not living densely enough. If QS was indeed social, it should be cheatable – susceptible to the rise of QS-negative cells which benefit from public goods but do not contribute to them. Papers soon showed that QS was cheatable, supporting that it is a social trait [35, 36]. Beyond showing that it is social, because QS is a social trait controlling a complex combination of spiteful and cooperative behaviors, it has become the focus of many cheating experiments in bacteria. Studies have looked at the different factors that affect cheating, focusing on Hamilton's rule in early experiments, and more recently expanding to studying spatial structure and cheating.

1.5 Bacterial Social Cheating and the Implications for Cooperation

Hamilton's rule introduces the importance of relatedness, cooperative cost, and cooperative benefit for the maintenance of cooperation. Through the introduction of spatial structure in cheating studies, we find factors like diffusion, density and distance are also important factors for the evolution of cooperation. Cheating in bacteria began in well-mixed liquid cultures due to its feasibility and reproducibility. Publicly available secreted proteins are susceptible to cheaters. In liquid media where cells are well mixed, it is assumed that cheaters and cooperators have equal access to public goods. Bacteria secrete numerous products that enable them to survive in their environment, such as antibiotic resistance proteins, metal chelators, and proteases. In a liquid well-mixed environment, public goods freely diffuse and cooperators and cheaters alike have unfettered access to secreted products. When spatial structure is introduced, how cells mix and grow changes. The addition of agar or polymers changes the diffusibility of the media, limiting how public goods travel – especially if public goods are large or charged [105]. Cells may also be more likely to grow clonally because cells will divide and remain in place due to spatial structure. This might increase the distance between cooperator and cheater, potentially impacting their access to public goods.

Kicking off the field of bacterial cheating, were two papers published within months of each other in 2007 on protease cheating in *P. aeruginosa* [35, 36]. Δ*lasR* mutants are QS-negative and do not secrete extracellular protease. QS-dependent secretion of protease is required for growth in a protein-based media, and Δ*lasR* cells must cheat on wildtype protease production to survive. Δ*lasR* cells have higher fitness than wildtype because they do not contribute towards QS, an energy intensive behavior. Cheaters overtake the population and there is no longer enough protease secreted, leading to a population crash and the tragedy of the commons. A similar dynamic is seen

in siderophore cheating in iron-limited environments, where a secreted product is susceptible to the invasion of cheats which ultimately leads to a population crash [106]. Beta-lactamase cheating follows the same dynamic where cheaters cheat on publicly available antibiotic resistance enzymes in the presence of antibiotics [39]. In these cases, the relatedness is r=-1 because cheaters do not share the cooperative trait, although they are otherwise isogenic. These are examples of intra-species cheating on cooperative behaviors that bear a fitness cost for the cooperator and offer a fitness benefit to both cooperator and non-cooperator alike. Cooperation fails because r is low.

Social cheating has been studied in spatially structured populations by growing cells on agar plates, or using agar to create spatial structure. Decreasing the diffusibility of the media using agar decreases the fitness of cheaters [107]. It is assumed that in addition to limiting the distance public goods can travel, the agar also increases the space between cooperators and cheaters. Here, distance between cells was not quantified, so it could only be assumed that distance in addition to diffusion was an important factor for cheater fitness. To better understand the importance of distance for cheaters, the Kummerli group studies siderophore cheating on agar plates. Cells grow as surface attached biofilms on agar plates and spread out from each other on a single dimension. Cheaters have highest fitness when they are closest to cooperators, and the fitness of cheaters decreases with distance. Agar limits how cells can interact with one another because they can only expand on a single plane. Additionally, the density of the cells changes from the center of the aggregate to edges. It is important to expand on these studies by looking at the effects of spatial structure where cells can structure themselves across 3 dimensions.

P. aeruginosa grows in the CF lung in spatially structured aggregates, which are free-floating rather than surface attached [97, 108–114]. Depending on the LPS structure of the cell, *P. aeruginosa* will form either stacking or clumping aggregates in spatially structured environments mimicking the CF lung [114, 115]. The LPS coats the outer surface of Gram-negative cells, including *P. aeruginosa*. Wildtype *P. aeruginosa* LPS is hydrophilic in nature, and cells form stacking aggregates through entropic de-aggregation in the presence of polymers. Polymers gently push the cells to line-up side-to-side, with their poles forming honeycomb-like structures. When the LPS is mutated such that it becomes hydrophobic – for example *ssg* or *wbpL* mutations – the cells form sticky clumping aggregates. Because of their differences in cell surface hydrophobicity, wildtype *P. aeruginosa* and LPS mutants form distinct aggregates similarly to oil and water. In flow cells, *Vibrio* similarly grows as spatially structured free-floating aggregates [38]. In these aggregates we see that non-producers cheat on biofilm extracellular matrix components. Cheating in this environment is dependent on the flow rate and the distance between cells. In *Vibrio,* the farther cheaters are from cooperators, the worse their fitness outcomes. Here, producers form separate clusters and cheater cells cluster nearby [116].

In addition to relatedness and proximity, the cost of the cooperative trait can determine whether bacterial cheats are able to overtake the population. Siderophore production is more costly when carbon or nitrogen is limited [117]. When C is high due to nutrient limitation, cheaters overtake cooperators and successfully cheat on siderophore secretion. Similarly to what we see in liquid, in spatial structure, cost matters for whether cheats can invade in *Bacillus subtilis* populations [64]. When a behavior is costly, non-cooperative cheats can invade and overtake the population. However public goods that do not have a cost cannot be cheated on. In this environment, diffusion

is also important for determining the fitness of cheats. Cooperation is especially costly when cooperators are contributing to multiple public goods simultaneously. It is possible for cheaters to cheat on multiple social behaviors at once, earning them the moniker "super-cheats." They receive a high fitness benefit by avoiding contributing to multiple costly behaviors. Protease and biofilm production are both cheatable traits, which are susceptible to cheats. Cheats invade more quickly when they are super-cheats because they are escaping contributing to a greater cost than if they were to cheat on one trait alone.

The 3rd factor in Hamilton's rule: b, or the benefit that cooperation provides has not yet been directly explored in the field of bacterial social science. It is presumed that increasing b will stabilize cooperation. Papers have found that privatizing b, making it so that producing cells selectively benefit more than neighbors can stabilize cooperation. However, so far, the study of benefit privatization is more directly looking at the relatedness factor, r, than b. Privatizing benefit means ensuring only individuals with high r – individuals that are related to the cooperator – are receiving the benefit. However, the field has not yet looked at the effects of changing b on the maintenance of cooperation in bacteria. Based on Hamilton's rule, I can assume that increasing b will maintain cooperation, but this must be directly investigated. It cannot be certain that b will universally impact cooperative traits, and it is not known how other factors like spatial structure will impact benefit.

Pleiotropy can maintain cooperation by co-regulating other behaviors in addition to cooperation. In *P. aeruginosa*, QS co-regulates public secretion of protease and private metabolism on adenosine. Adenosine metabolism is considered "private" because the enzymes are expressed

intracellularly, where they are only available – privately – to the producing cell. When cells are grown on adenosine, the rise of cheats is suppressed because they are unable to share metabolism of adenosine. However, it is unlikely that *P. aeruginosa* will ever find itself growing on adenosine as a sole carbon source in the environment or in a host [118–120]. A form of pleiotropy that is more likely to successfully maintain cooperation in natural environments or infections is the co-regulation of spite and cooperation, and the co-regulation of spite and resistance to spite. Spite molecules like hydrogen cyanide and pyocyanin are found in the lung of CF patients with *P. aeruginosa* infections, indicating that spiteful behaviors are active during infection. QS in *P. aeruginosa* co-regulates hydrogen cyanide production (*hcnABC*) and hydrogen cyanide resistance (*cioAB*) [121–123]. Hydrogen cyanide production is public – affecting the producer and neighbors, while hydrogen cyanide resistance is private, only able to benefit the producer. Also tied with hydrogen cyanide production and resistance is cooperatively secreting protease. By tying the 3 traits together, *P. aeruginosa* uses QS to pleiotropically constrain the evolution of cheats, which can help maintain cooperation.

The microbiology world has primarily focused on intra-species cheating that happens within a species, often where a cell is defined as a cheater by a single gene change, leading to the loss of the cooperative behavior. Cheating also happens between individuals of different species [116, 118]. *Bdellovibrio bacteriovorus* is a bacterial predator that targets and kills Gram-negative bacteria. *Vibrio* biofilms are uniquely adept at resisting *B. bacteriovorus* predation due to its extracellular matrix. *Escherichia coli* does not have the same type of biofilm structure and is susceptible to *B. bacteriovorus* predation. When mixed, *E. coli* can invade *Vibrio* biofilms and gain a fitness benefit by surviving predation better within *Vibrio* biofilms. *Vibrio* in turn has worse

fitness when mixed with *E. coli* under *B. bacteriovorus* predation. Spatial structure is critically important for determining the survival of these two species under predation. *E. coli* can also survive phage killing through structuring with *Vibrio* biofilms [124]. Not only are inter-species interactions impacted by spatial structure, but also inter-Domain interactions (Bacteria and non-living phages).

In addition to cheating, spatial structure is important for understanding interactions between different species. Polymicrobial communities structure themselves in specific ways that can be quantified at the micron scale. Their structuring leads to changes in their response to antimicrobials, impacting human health outcomes. This structuring is impacted by social behaviors like secreted anti-*Staph* products, or anti-*Vibrio* T6SS [67, 125]. Conversely, spatial structure also affects social behaviors such as communication between neighboring aggregates depending on aggregate size and proximity [105]. It is essential to study spatially structured populations of bacteria to better understand the physiology of bacteria in infection. Studying bacterial spatial structure will increase our understanding of cheating dynamics and other social behaviors in bacteria, as well as inform treatment of complex bacterial infections.

The field began by focusing on the cooperative behaviors regulated by QS that benefitted the population and were susceptible to traits. Newer works have begun investigating the dynamics of spite behaviors controlled by *P. aeruginosa* QS. Spiteful behaviors are costly to the cooperating cell and cause harm to recipients, acting opposite of cooperation. Spite appears to play an important role in maintaining cooperation, and it is important to explore the dynamics affecting spite from a

social lens. Spite appears to play a key role in suppressing cheats in intra-species interactions and suppressing the growth of neighbors of a different species.

1.6 Spiteful behaviors in *P. aeruginosa*

Unlike cooperation which benefits the producer and receiver, spite harms both producer and receiver. It is costly to produce the spite behavior and it harms neighbors. Often the producer is resistant to the spite behavior. Its maintenance follows the same Hamilton's rule requirements. Similarly to the maintenance of cooperation, spite can only be maintained if criteria surrounding cost, relatedness, and benefit are met. Although this has not been studied *in vitro* for spite behaviors to the extent that cooperation has. Hamiltonian spite happens within a species and is spiteful where the cooperator experiences a cost for producing the spite behavior and the recipient has a negative fitness impact. The key to maintaining spite is that the harmful behavior must differentially harm non-relatives over relatives. The spite behavior must offer a positive fitness benefit for the producer through the harm of the recipient [40, 126].

P. aeruginosa produces multiple spite behaviors, including secreting hydrogen cyanide, phenazines, and bacteriocins. Pseudomonas uses spiteful behaviors to "police" the rise of cheats in a population. In a population where QS-negative cheats arise and overtake the population, spite can maintain cooperation. The key to this maintenance is pleiotropy. QS in Pseudomonas pleiotropically co-regulates cooperative behaviors such as protease production and spiteful behaviors like hydrogen cyanide and phenazine production [86]. Importantly, in addition to co-regulating spite and cooperation, QS also controls producer's resistance to spite.

Hydrogen cyanide inhibits cellular respiration by targeting cytochrome c oxidase, and is seen as a spiteful behavior in both liquid and spatially structured environments, as well as in inter- and intra-species interactions [127]. Wildtype *P. aeruginosa* is resistant to hydrogen cyanide killing through its production of a cyanide-resistant cytochrome oxidase, encoded by *cioAB* [122]. Production of hydrogen cyanide through the *hcnABC* operon and resistance to hydrogen cyanide through *cioAB* is pleiotropically co-regulated by QS. For this reason, some QS-negative cheaters are susceptible to cyanide poisoning, although the outcome varies depending on the study. By pleiotropically linking cooperation and spite-resistance, cooperators are able to "police" cheats through spiteful behaviors without experiencing spite themselves [123]. It is costly to produce hydrogen cyanide, but so long as it differentially harms cheaters, it can help maintain cooperation. In liquid well mixed cultures, cooperators police cheats using hydrogen cyanide to maintain cooperation [123, 128]. Hydrogen cyanide is also seen in inter-species non-Hamiltonian spite. *P. aeruginosa* and *S. aureus* commonly co-infect the CF lung, a spatially structured and nutritionally complex environment. Hydrogen cyanide is used by *P. aeruginosa* to suppress the growth of *S. aureus*. In spatially structured populations, *P. aeruginosa* produces hydrogen cyanide and suppresses the growth of *S. aureus* [30].

P. aeruginosa produces another anti-staphylococcal agent through the control of QS called HQNO, which has high activity against *S. aureus* in well mixed cultures [129]. HQNO production is regulated by QS, a costly trait. We can for this reason see HQNO as a form of spite, in that it is costly to produce, and harms the receiver. In a spatially structured environment mimicking the CF lung and in a murine wound infection, *S. aureus* and *P. aeruginosa* co-exist despite this anti-staphylococcal compound. Despite HQNO being anti-Staphyloccocal, it seems essential for their

close structuring, showing the complex dynamics of spatially structured populations [125]. Additionally, interactions between *S. aureus* and *P. aeruginosa*, potentially related to excreted spite factors, alters bacterial response to certain antibiotics [130].

Another form of QS-regulated spite that is seen to affect intra-species cheating is phenazine production. *P. aeruginosa* produces multiple phenazines including pyocyanin, which is redox-active and kills through the creation of reactive oxygen species [40, 131, 132]. QS controls the response to reactive oxygen species, pleiotropically protecting cooperators from pyocyanin spite. The production of pyocyanin polices the rise of QS cheats in well mixed liquid cultures. Interestingly, pyocyanin impacts *S. aureus* in a wound environment, showing that it can act as an intra- and inter-specific spite molecule [133].

The ability of cells to cheat on spite has not yet been investigated. Cheating experiments have focused on the invasion of cooperative populations, and spite as seen as a tool to maintain cooperation. However, if behaviors like pyocyanin and hydrogen cyanide production are indeed social, they should potentially be cheatable. It is essential that the field investigates the factors described by Hamilton's rule for the maintenance of spite. It would require using a cheat that is not itself susceptible to spite – perhaps studying how non-spiteful individuals survive amongst a spiteful population when spite is required to eliminate a neighbor of a different species. For example, *P. aeruginosa* that does not produce T6SS should gain a fitness benefit by invading a T6SS+ population which is competing against *Vibrio*. QS-negative *P. aeruginosa* that does not contribute to HQNO production would additionally be expected to see a fitness benefit when

mixed with QS+ cells competing against *S. aereus.* The "cheatability" of spite should be investigated first in liquid, and then in spatially structured populations.

1.7 Conclusions

Social behaviors in bacteria pose a challenge for evolutionary biologists as they are costly behaviors that are susceptible to cheating and provide a threat to the entire population. Despite this, we see diverse social behaviors across the Bacterial Domain. Bacteria use social behaviors to create a niche and survive in large, variable environments. The field began by studying these behaviors primarily in liquid media, where cooperation is widely lost to cheats. The world at large is not well mimicked by well-mixed liquid cultures growing in aerated flasks – it is therefore essential to introduce spatial structure to cheating studies. In studying social behaviors in spatial structure, we can better understand how cooperation is maintained. In addition to spatial structure impacting social behaviors, conversely, we see that social behaviors determine how cells spatially structure. Inter- and intra-species cooperation and spite behaviors are responsible for bacterial spatial arrangement. These sometimes subtle changes in spatial arrangement due to social behaviors, impact how bacteria respond to the immune system and antimicrobials. In addition to the influence of spatial structure and the complications it introduces – through changes in environment diffusion, cell-to-cell proximity, and aeration – cooperation is still impacted by the factors described by Hamilton's rule. Hamilton's rule describes the impact relatedness, r, benefit, b, and cost, C has on the evolution of cooperation. When r and b are high, cooperation is assumed to be maintained, while rising C will lead to a loss of cooperation. However only r and C have been investigated *in vitro* in bacterial populations – it is still necessary for the field to investigate the direct effect of b on the maintenance of cooperation. Cooperation is also maintained through

the pleiotropic regulation of spite behaviors and private benefits for cooperators. In some cases, pleiotropy links the production of public and private behaviors, ensuring that cooperation is maintained. There is a private benefit that only cooperators receive, that is not cheatable. In an environment where the private good is required, cheaters cannot overtake the population. When bacteria link publicly expressed spiteful behaviors with private resistance to spite, they are able to police the rise of cheaters, ensuring cooperation is maintained. A key example of this is seen in *P. aeruginosa* QS pleiotropically links cooperation, spite, and resistance to spite, which helps the bacterium maintain cooperation in the face of cheats. Spite is considered a social trait, but its susceptibility to cheating has not yet been investigated. To truly consider spiteful traits like *P. aeruginosa* secretion of HQNO or *Vibrio* expression of T6SS social, the field must test cheating on spite. The field of bacterial social biology began simply by testing intra-species cheating on QS and has now expanded to include looking at inter-species and inter-Domain social interactions, spite, social behaviors in spatial structure, and the different factors that affect the maintenance of cooperation. *P. aeruginosa* is perhaps the best studied bacterium in the field, because of its QS system and multiple inter- and intra-species social interactions. Social behaviors in bacteria include virulence traits, which impacts the health of human hosts during infection. It is essential we continue exploring social behaviors in all bacteria, with special attention towards difficult to treat pathogens.

1.8 Summary of Thesis Findings

In this thesis I explore QS variation and social dynamics in *P. aeruginosa*. *P. aeruginosa* is an opportunistic pathogen with a large genetic tool kit, and large genotypic and phenotypic heterogeneity between strains. Once it enters the host, it evolves and diversifies, worsening

infection and complicating treatment. An important factor for virulence is the regulation of QS, a complicated network of chemical communication used by the bacterium to coordinate social behaviors. The QS system is commonly mutated in *P. aeruginosa* strains isolated from wound infections, the CF lung, and the environment. It is key that we understand what aspects of the QS system are mutated or conserved to target it as a virulence factor. Also important for study is how the dynamics of QS change in spatially structured environments, which better mimic infection environments than typically used well-mixed liquid cultures.

The evolution of QS in the CF lung during chronic infection has long been recognized. *P. aeruginosa* isolated from the CF lung diversifies in a multitude of ways, including the loss of the QS transcriptional regulator, LasR. LasR was previously viewed as the hierarchical controller of QS, and it was assumed that all QS activity was lost in these strains. Indeed, *lasR*- strains isolated from the CF lung frequently showed phenotypic evidence of QS-loss through the lack of protease secretion and through the production of colony sheen (HHQ over accumulation). We now know that QS is not always completely lost in *lasR*- strains, and is sometimes re-regulated, perhaps through *P. aeruginosa's* exposure to high levels of C4-HSL production in the lung from neighboring QS+ aggregates. In investigating isolates from environment, CF, and wound sources, I found that LasR is the most commonly mutated QS protein in *P. aeruginosa*. It appears to be a key mutation for *P. aeruginosa,* regardless of its isolation source and is not specific to CF. This finding was consistent with another publication looking at *lasR* mutations across environment isolates. In addition to being a frequent target for mutation, early stops leading to a truncated protein were common, unlike *pqs* genes which were a target for frequent but smaller changes in protein code. It appears that not only is it beneficial to mutate *lasR*, it is beneficial to completely

inactivate the protein. On the opposite end of the mutation frequency spectrum from LasR was the transcriptional regulator RsaL. RsaL is part of the *las* QS system, and negatively regulates the *las* system, serving the opposite function of the positive regulatory function of LasR. In the majority of studied strains, LasR resides at the top of the QS hierarchy, turning QS expression on. For this reason it is interesting that the positive QS regulator LasR is most frequently mutated, while the negative regulator RsaL is conserved.

pqsA, H and *L* were frequently mutated, albeit not commonly truncated. When I looked at the effect of protein length on mutation frequently, I found that it was likely that *pqs* genes were frequently mutated due to their length and not necessarily for fitness reasons – the longer the amino acid sequence, the more opportunities for mutation accumulation. Consistent with a theoretical paper exploring the evolution of QS transcriptional regulators and signal synthases, I found that signal synthases were more conserved than their partnered transcriptional regulator (RhlI, RhlR; LasI, LasR). I found that the *pqs* system, specifically the *pqsH* and *pqsL* genes were responsible for the colony autolysis and sheen phenotype previously attributed to *lasR*- mutants isolated from the CF lung. Previous publications had shown that *pqsL*- mutations would lead to colony sheen, attributed to HHQ-accumulation, but they had not linked by it was attributed to *las* system mutations. I showed that deleting *pqsA*, which is the first gene responsible for downstream quinolone production, including HHQ production, would prevent the colony autolysis phenotype in Δ*lasR*. A recent publication expanded upon this work, further confirming my findings. After studying the variation in QS genes, I turned my focus to the social dynamics of QS in spatial structure, using confocal microscopy.

After studying the QS variation in *P. aeruginosa,* I wanted to look at the effects of spatial structure on QS social dynamics. *P. aeruginosa* forms multi-cellular surface detached aggregates in the CF lung. Similar aggregates are seen from other organisms in animal and plant hosts, indicating it might be a common way to cells to grow in nature. *P. aeruginosa* is capable of forming two types of aggregates depending on its cell surface: clumping aggregates and stacking aggregates. Wildtype *P. aeruginosa* has a hydrophilic cell surface due to its LPS structure and forms stacking aggregates due to entropic de-aggregation. When the LPS is mutated, in the case of an Δ*ssg* or Δ*wbpL* mutation, the cell surface becomes hydrophobic and cells form clumping aggregates. I reasoned that mixing hydrophobic and hydrophilic cells would lead to separate aggregate forms with limited interactions between different aggregate types in spatial structure. Indeed, when Δ*ssg* or Δ*wbpL* cells are mixed with PAO1, they assort by LPS-type and have reduced mixing like oil and water. I used this to manipulate the distance between cells to test the effects of proximity on cheating in *P. aeruginosa,* by mixing cells of the same or different surfaces. I found that when mixing cheaters and cooperators of the same cell surface, then cheaters cluster together with cooperators closely but have poor fitness. Already this first result surprised us, because we assumed that with close proximity, cheaters would have high fitness and take over the population. Previous *in vitro* experiments in spatial structure suggested that the closer cheats are, the fitter they are. We knew at this early point that there was likely another behavior besides cooperation at play – we suspected spite. We then mixed cooperators and cheats with different cell surfaces and found two divergent results: when Δ*lasR*Δ*rhlR* hydrophilic cheats were mixed with Δ*ssg* they had high fitness, and when Δ*lasR*Δ*rhlR*Δ*ssg* hydrophobic cheats were mixed with PAO1 they had low fitness. The hydrophobic-hydrophilic mixes were on either ends of the spectrum compared to cooperator-cheat mixes of the same surface charge. Δ*lasR*Δ*rhlR* cheaters clustered an intermediate

distance from Δ*ssg* cooperators, in an area we dubbed the "goldilocks zone." We hypothesized that this intermediate distance was a key distance from cooperators where cheaters experienced the greatest benefit, but it was not immediately clear why. Δ*lasR*Δ*rhlR*Δ*ssg* cells were very far away from PAO1 cooperators and had low fitness that was not frequency dependent. One explanation for the "goldilocks zone" was that spite was acting on the smaller distance scale where cheaters of the same cell surface aggregated with cooperators. Perhaps cooperation happened over an intermediate distance – reaching cells of close or intermediate distance, while spite happened on a small distance – reaching only cells that shared the same surface.

To study the distance between cells, we took 3-D images of aggregates using a confocal microscope. We assessed the location of the cells using MicrobeJ to locate cells and assign them an X, Y, and Z position. After assigning cells a location, we found the mean nearest neighbor distance using Spatstat, a Geolocation R Studio plugin. The spatial location analysis shown in Chapter 2 is preliminary analysis and will be completed post-defense before submitting the work for publication.

In this thesis I worked with colleagues to explore QS in *P. aeruginosa* by looking at its variation and social dynamics. I found that there is an apparent benefit to losing the genes that activates QS and maintaining the genes that deactivate QS. Despite QS being attributed to important virulence traits, it seems there is a benefit to losing QS activity in many environments. Some works have attributed loss of QS to be an adaptation for social reasons because the QS- mutants are acting as cheats. This argument is based off the many liquid studies performed with protein-based mediums, but likely does not translate to natural environments. Natural environments have multiple food

sources that are not protein based, and they are spatially structured. For this reason, I wanted to study the social dynamics of QS in spatial structure, to better understand how cells function in natural environments. I found that closely aggregating cheaters do not have great fitness, which was unexpected based on previous work. It was assumed that the closer cheaters clustered to cooperators, the fitter they would be. In fact, we saw that cheaters that were an intermediate distance from cooperators in the "goldilocks zone" had the highest fitness. Cells experience the "goldilocks zone" when cheaters are close enough to experience the benefit cooperation but are too far away from cooperators to experience the harm of spite. The introduction of spatial structure complicated how cooperators and cheaters interact, emphasizing how important it is for us as a field to study bacteria in spatially structured populations. Liquid studies serve as a good introduction to study basics like QS regulatory cascades, but to understand complex social interactions and the importance of proximity, we must introduce spatial structure. This thesis expands our understanding of QS variation across different environments, and how *P. aeruginosa* interacts socially in spatial structure.

1.9 References

1. **Diggle SP, Whiteley M**. Microbe profile: Pseudomonas aeruginosa: Opportunistic pathogen and lab rat. *Microbiology (United Kingdom)* 2020;166:30–33.
2. **Hoadley AW, McCoy E**. Studies of certain Gram-negative bacteria from surface waters. *Health Lab Sci* 1966;3:20–32.
3. **Lányi B, Gregács M, Adám MM**. Incidence of Pseudomonas aeruginosa serogroups in water and human faeces. *Acta Microbiol Acad Sci Hung*;13:319–26.

4. **Ayliffe GA, Barry DR, Lowbury EJ, Roper-Hall MJ, Walker WM**. Postoperative infection with Pseudomonas aeruginosa in an eye hospital. *Lancet* 1966;1:1113–7.

5. **Akatov AK**. [Hospital infection caused by the pyocyaneus bacillus]. *Zh Mikrobiol Epidemiol Immunobiol* 1966;43:38–41.

6. **Phillips I, Spencer G**. Pseudomonas aeruginosa cross-infection due to contaminated respiratory apparatus. *Lancet* 1965;2:1325–7.

7. **Fierer J, Taylor PM, Gezon HM**. Pseudomonas aeruginosa epidemic traced to delivery-room resuscitators. *N Engl J Med* 1967;276:991–6.

8. **Beck A, Zadeh JA**. Infection by anaesthetic apparatus. *Lancet* 1968;1:533–4.

9. **Collins RN, Braun PA, Zinner SH, Kass EH**. Risk of local and systemic infection with polyethylene intravenous catheters. A prospective study of 213 catheterizations. *N Engl J Med* 1968;279:340–3.

10. **KATZNELSEN D, VAWTER GF, FOLEY GE, SHWACHMAN H**. BOTRYOMYCOSIS, A COMPLICATION CYSTIC FIBROSIS. REPORT OF 7 CASES. *J Pediatr* 1964;65:525–39.

11. **JACKSON DM, LOWBURY EJL, TOPLEY E**. Pseudomonas pyocyanea in burns; its role as a pathogen, and the value of local polymyxin therapy. *Lancet* 1951;2:137–47.

12. **GOULD HL, INGLIMA R**. CORNEAL CONTACT LENS SOLUTIONS. *Eye Ear Nose Throat Mon* 1964;43:39–49.

13. **Bryan CS, Sutton JP, Saunders DE, Longaker DW, Smith CW**. Endocarditis related to transvenous pacemakers. Syndromes and surgical implications. *J Thorac Cardiovasc Surg* 1978;75:758–62.

14. **Freschi L, Vincent AT, Jeukens J, Emond-Rheault JG, Kukavica-Ibrulj I, *et al.*** The Pseudomonas aeruginosa Pan-Genome Provides New Insights on Its Population Structure, Horizontal Gene Transfer, and Pathogenicity. *Genome Biol Evol* 2019;11:109–120.

15. **Darch SE, McNally A, Harrison F, Corander J, Barr HL, *et al.*** Recombination is a key driver of genomic and phenotypic diversity in a Pseudomonas aeruginosa population during cystic fibrosis infection. *Sci Rep* 2015;5:1–12.

16. **Govan JR, Harris GS**. Pseudomonas aeruginosa and cystic fibrosis: unusual bacterial adaptation and pathogenesis. *Microbiol Sci* 1986;3:302–8.

17. **Marshall BC, Carroll KC**. Interaction between Pseudomonas aeruginosa and host defenses in cystic fibrosis. *Semin Respir Infect* 1991;6:11–8.

18. **Polack B, Dacheux D, Delic-Attree I, Toussaint B, Vignais PM**. Role of manganese superoxide dismutase in a mucoid isolate of Pseudomonas aeruginosa: adaptation to oxidative stress. *Infect Immun* 1996;64:2216–9.

19. **Huszczynski SM, Lam JS, Khursigara CM**. The role of Pseudomonas aeruginosa lipopolysaccharide in bacterial pathogenesis and physiology. *Pathogens*;9. Epub ahead of print 2020. DOI: 10.3390/pathogens9010006.

20. **Pang Z, Raudonis R, Glick BR, Lin TJ, Cheng Z**. Antibiotic resistance in Pseudomonas aeruginosa: mechanisms and alternative therapeutic strategies. *Biotechnol Adv* 2019;37:177–192.

21. **Feshchenko LG**. [Comparison of the virulence factors in freshly isolated and museum strains of bacillus pyocyaneus]. *Mikrobiol Zh* 1969;31:644–7.

22. **Muszyński Z, Kedzia WB**. Some biological and biochemical properties of toxins (extracellular proteolytic enzymes) of Pseudomonas aeruginosa strains. *J Hyg Epidemiol Microbiol Immunol* 1974;18:310–2.

23. **Baker NR**. Role of exotoxin A and proteases of Pseudomonas aeruginosa in respiratory tract infections. *Can J Microbiol* 1982;28:248–55.

24. **Snell K, Holder IA, Leppla SA, Saelinger CB**. Role of exotoxin and protease as possible virulence factors in experimental infections with Pseudomonas aeruginosa. *Infect Immun* 1978;19:839–45.

25. **Nutman J, Berger M, Chase PA, Dearborn DG, Miller KM, *et al.*** Studies on the mechanism of T cell inhibition by the Pseudomonas aeruginosa phenazine pigment pyocyanine. *J Immunol* 1987;138:3481–7.

26. **Kanthakumar K, Taylor G, Tsang KW, Cundell DR, Rutman A, *et al.*** Mechanisms of action of Pseudomonas aeruginosa pyocyanin on human ciliary beat in vitro. *Infect Immun* 1993;61:2848–53.

27. **CONTRERAS AA, EVANS BW, MONCRIEF JA, LINDBERG RB, VILLARREAL Y, *et al.*** SOME ASPECTS OF CYANIDE-PRODUCING CAPABILITIES OF PSEUDOMONAS AERUGINOSA STRAINS ISOLATED FROM BURNED PATIENT INFECTIONS. *J Trauma* 1963;3:527–33.

28. **GOLDFARB WB, MARGRAF H**. CYANIDE PRODUCTION BY PSEUDOMONAS AERUGINOSA. *Surg Forum* 1964;15:467–9.

29. **Reimmann C, Beyeler M, Latifi A, Winteler H, Foglino M, *et al.*** The global activator GacA of Pseudomonas aeruginosa PAO positively controls the production of the autoinducer N-butyryl-homoserine lactone and the formation of the virulence factors pyocyanin, cyanide, and lipase. *Mol Microbiol* 1997;24:309–319.

30. **Létoffé S, Wu Y, Darch SE, Beloin C, Whiteley M, *et al.*** Pseudomonas aeruginosa Production of Hydrogen Cyanide Leads to Airborne Control of Staphylococcus aureus Growth in Biofilm and In Vivo Lung Environments. *mBio* 2022;13:e0215422.

31. **Moreau-Marquis S, Stanton BA, O'Toole GA**. Pseudomonas aeruginosa biofilm formation in the cystic fibrosis airway. *Pulm Pharmacol Ther* 2008;21:595–9.

32. **Nichols WW, Evans MJ, Slack MP, Walmsley HL**. The penetration of antibiotics into aggregates of mucoid and non-mucoid Pseudomonas aeruginosa. *J Gen Microbiol* 1989;135:1291–303.

33. **Hsieh P-H, Lee MS, Hsu K-Y, Chang Y-H, Shih H-N, *et al.*** Gram-negative prosthetic joint infections: risk factors and outcome of treatment. *Clin Infect Dis* 2009;49:1036–43.

34. **Zmistowski B, Fedorka CJ, Sheehan E, Deirmengian G, Austin MS, *et al.*** Prosthetic joint infection caused by gram-negative organisms. *J Arthroplasty* 2011;26:104–8.

35. **Diggle SP, Griffin AS, Campbell GS, West SA**. Cooperation and conflict in quorum-sensing bacterial populations. *Nature* 2007;450:411–414.

36. **Sandoz KM, Mitzimberg SM, Schuster M**. Social cheating in Pseudomonas aeruginosa quorum sensing. *Proc Natl Acad Sci U S A* 2007;104:15876–15881.

37. **Kümmerli R, Brown SP**. Molecular and regulatory properties of a public good shape the evolution of cooperation. *Proc Natl Acad Sci U S A* 2010;107:18921–18926.

38. **Tai JSB, Mukherjee S, Nero T, Olson R, Tithof J, *et al.*** Social evolution of shared biofilm matrix components. *Proc Natl Acad Sci U S A* 2022;119:1–10.

39. **Perlin MH, Clark DR, McKenzie C, Patel H, Jackson N, *et al.*** Protection of Salmonella by ampicillin-resistant Escherichia coli in the presence of otherwise lethal drug concentrations. *Proceedings of the Royal Society B: Biological Sciences* 2009;276:3759–3768.

40. **Castañeda-Tamez P, Ramírez-Peris J, Pérez-Velázquez J, Kuttler C, Jalalimanesh A, *et al.*** Pyocyanin Restricts Social Cheating in Pseudomonas aeruginosa. *Front Microbiol* 2018;9:1348.

41. **Zygiel EM, Nelson CE, Brewer LK, Oglesby-Sherrouse AG, Nolan EM**. The human innate immune protein calprotectin induces iron starvation responses in Pseudomonas aeruginosa. *J Biol Chem* 2019;294:3549–3562.

42. **Mankiw NG**. *Principles of microeconomics*. 7th ed. Cengage; 2014.

43. **Smith P, Schuster M**. Public goods and cheating in microbes. *Current Biology* 2019;29:R442–R447.

44. **Schalk IJ, Mislin GLA, Brillet K**. *Structure, Function and Binding Selectivity and Stereoselectivity of Siderophore-Iron Outer Membrane Transporters*. Elsevier. Epub ahead of print 2012. DOI: 10.1016/B978-0-12-394390-3.00002-1.

45. **Wellington S, Peter Greenberg E**. Quorum sensing signal selectivity and the potential for interspecies cross talk. *mBio*;10. Epub ahead of print 2019. DOI: 10.1128/MBIO.00146-19.

46. **Harrison F, Buckling A**. Hypermutability impedes cooperation in pathogenic bacteria. *Current Biology* 2005;15:1968–1971.

47. **Xavier JB, Foster KR**. Cooperation and conflict in microbial biofilms. *Proc Natl Acad Sci U S A* 2007;104:876–881.

48. **Wade MJ**. Kin selection: its components. *Science* 1980;210:665–7.

49. **Boyd R, Richerson PJ**. Effect of phenotypic variation on kin selection. *Proc Natl Acad Sci U S A* 1980;77:7506–9.

50. **Uyenoyama MK, Feldman MW, Mueller LD**. Population genetic theory of kin selection: Multiple alleles at one locus. *Proc Natl Acad Sci U S A* 1981;78:5036–40.

51. **Hamilton WD**. The Evolution of Altruistic Behavior. *Am Nat* 1963;97:354–356.

52. **Hamilton W**. The genetical evolution of social behaviour. *J Theor Biol*;7(1):17-52.

53. **Bourke AFG**. Hamilton's rule and the causes of social evolution. *Philosophical Transactions of the Royal Society B: Biological Sciences* 2014;369:20130362.

54. **Gerald S. Wilkinson**. Reciprocal food sharing in the vampire bat Gerald. *Nature* 1984;13:576.

55. **Waters CM, Bassler BL**. Quorum sensing: Cell-to-cell communication in bacteria. *Annu Rev Cell Dev Biol* 2005;21:319–346.

56. **Popat R, Cornforth DM, McNally L, Brown SP**. Collective sensing and collective responses in quorum-sensing bacteria. *J R Soc Interface*;12. Epub ahead of print 2015. DOI: 10.1098/rsif.2014.0882.

57. **Papenfort K, Bassler BL**. Quorum sensing signal-response systems in Gram-negative bacteria. *Nat Rev Microbiol* 2016;14:576–588.

58. **Schuster M, Joseph Sexton D, Diggle SP, Peter Greenberg E**. Acyl-homoserine lactone quorum sensing: From evolution to application. *Annu Rev Microbiol* 2013;67:43–63.

59. **Williams P, Cámara M**. Quorum sensing and environmental adaptation in Pseudomonas aeruginosa: a tale of regulatory networks and multifunctional signal molecules. *Curr Opin Microbiol* 2009;12:182–191.

60. **Scholz RL, Peter Greenberg E**. Positive autoregulation of an Acyl- homoserine lactone quorum-sensing circuit synchronizes the population response. *mBio* 2017;8:1–12.

61. **Bacun-Druzina V, Cagalj Z, Gjuracic K**. The growth advantage in stationary-phase (GASP) phenomenon in mixed cultures of enterobacteria. *FEMS Microbiol Lett* 2007;266:119–127.

62. **ERIKSEN KR, HANSEN D**. Observations on the extracellular nature of staphylococcal penicillinase. *Acta Pathol Microbiol Scand* 1954;35:169–74.

63. **BORN G V**. The extracellular bacteriolytic enzymes of a species of Streptomyces. *J Gen Microbiol* 1952;6:244–51.

64. **Jautzus T, van Gestel J, Kovács ÁT**. Complex extracellular biology drives surface competition during colony expansion in Bacillus subtilis. *ISME J* 2022;16:2320–2328.

65. **RAMON G, RICHOU R, RAMON P**. [On the diastatic, bacteriostatic, bactericidal and bacteriolytic properties of bacillus culture filtrates subtilis]. *C R Hebd Seances Acad Sci* 1945;220:543–7.

66. **Michel-Briand Y, Baysse C**. The pyocins of Pseudomonas aeruginosa. *Biochimie* 2002;84:499–510.

67. **Basler M, Ho BT, Mekalanos JJ**. Tit-for-tat: type VI secretion system counterattack during bacterial cell-cell interactions. *Cell* 2013;152:884–94.

68. **Diard M, Hardt W-D**. Basic Processes in Salmonella-Host Interactions: Within-Host Evolution and the Transmission of the Virulent Genotype. *Microbiol Spectr*;5. Epub ahead of print September 2017. DOI: 10.1128/microbiolspec.MTBP-0012-2016.

69. **Czechowska K, McKeithen-Mead S, Al Moussawi K, Kazmierczak BI**. Cheating by type 3 secretion system-negative Pseudomonas aeruginosa during pulmonary infection. *Proc Natl Acad Sci U S A* 2014;111:7801–6.

70. **Diard M, Garcia V, Maier L, Remus-Emsermann MNP, Regoes RR, *et al.*** Stabilization of cooperative virulence by the expression of an avirulent phenotype. *Nature* 2013;494:353–6.

71. **Wang M, Schaefer AL, Dandekar AA, Greenberg EP**. Quorum sensing and policing of Pseudomonas aeruginosa social cheaters. *Proc Natl Acad Sci U S A* 2015;112:2187–91.

72. **Lesic B, Starkey M, He J, Hazan R, Rahme LG**. Quorum sensing differentially regulates Pseudomonas aeruginosa type VI secretion locus I and homologous loci II and III, which are required for pathogenesis. *Microbiology (Reading)* 2009;155:2845–2855.

73. **Pearson JP, Pesci EC, Iglewski BH**. Roles of Pseudomonas aeruginosa las and rhl quorum-sensing systems in control of elastase and rhamnolipid biosynthesis genes. *J Bacteriol* 1997;179:5756–67.

74. **Nealson KH, Platt T, Hastings JW**. Cellular control of the synthesis and activity of the bacterial luminescent system. *J Bacteriol* 1970;104:313–22.

75. **Déziel E, Gopalan S, Tampakaki AP, Lépine F, Padfield KE, *et al.*** The contribution of MvfR to Pseudomonas aeruginosa pathogenesis and quorum sensing circuitry regulation: multiple quorum sensing-regulated genes are modulated without affecting lasRI, rhlRI or the production of N-acyl-L-homoserine lactones. *Mol Microbiol* 2005;55:998–1014.

76. **Xiao G, Déziel E, He J, Lépine F, Lesic B, *et al.*** MvfR, a key Pseudomonas aeruginosa pathogenicity LTTR-class regulatory protein, has dual ligands. *Mol Microbiol* 2006;62:1689–99.

77. **Diggle SP, Matthijs S, Wright VJ, Fletcher MP, Chhabra SR, *et al.*** The Pseudomonas aeruginosa 4-quinolone signal molecules HHQ and PQS play multifunctional roles in quorum sensing and iron entrapment. *Chem Biol* 2007;14:87–96.

78. **Fletcher MP, Diggle SP, Crusz SA, Chhabra SR, Cámara M, *et al.*** A dual biosensor for 2-alkyl-4-quinolone quorum-sensing signal molecules. *Environ Microbiol* 2007;9:2683–93.

79. **Pesci EC, Pearson JP, Seed PC, Iglewski BH**. Regulation of las and rhl quorum sensing in Pseudomonas aeruginosa. *J Bacteriol* 1997;179:3127–32.

80. **Pesci EC, Iglewski BH**. The chain of command in Pseudomonas quorum sensing. *Trends Microbiol* 1997;5:132–4; discussion 134-5.

81. **Pearson JP, Passador L, Iglewski BH, Greenberg EP**. A second N-acylhomoserine lactone signal produced by Pseudomonas aeruginosa. *Proc Natl Acad Sci U S A* 1995;92:1490–4.

82. **Gray KM, Passador L, Iglewski BH, Greenberg EP**. Interchangeability and specificity of components from the quorum-sensing regulatory systems of Vibrio fischeri and Pseudomonas aeruginosa. *J Bacteriol* 1994;176:3076–80.

83. **Wade DS, Calfee MW, Rocha ER, Ling EA, Engstrom E, *et al.*** Regulation of Pseudomonas quinolone signal synthesis in Pseudomonas aeruginosa. *J Bacteriol* 2005;187:4372–80.

84. **Cruz RL, Asfahl KL, Bossche S Van den, Coenye T, Crabbé A, *et al.*** RhlR-Regulated Acyl-Homoserine Lactone Quorum Sensing in a Cystic Fibrosis Isolate of Pseudomonas aeruginosa. *mBio*;11. https://doi.org/10.1128/mBio.00532-20 (2020).

85. **Thomas S, El-Zayat AS, Gurney J, Rattray J, Brown SP**. The las and rhl Quorum Sensing Systems in Pseudomonas aeruginosa Form a Multi-Signal Reciprocal Network Which Can Tune Reactivity to Variations in Physical and Social Environments. *bioRxiv*. Epub ahead of print 2023. DOI: 10.1101/2023.02.23.529764.

86. **Letizia M, Mellini M, Fortuna A, Visca P, Imperi F, *et al.*** PqsE Expands and Differentially Modulates the RhlR Quorum Sensing Regulon in Pseudomonas aeruginosa. *Microbiol Spectr* 2022;10:e0096122.

87. **Taylor IR, Paczkowski JE, Jeffrey PD, Henke BR, Smith CD, *et al.*** Inhibitor Mimetic Mutations in the Pseudomonas aeruginosa PqsE Enzyme Reveal a Protein-Protein Interaction with the Quorum-Sensing Receptor RhlR That Is Vital for Virulence Factor Production. *ACS Chem Biol* 2021;16:740–752.

88. **García-Reyes S, Cocotl-Yañez M, Soto-Aceves MP, González-Valdez A, Servín-González L, *et al.*** PqsR-independent quorum-sensing response of Pseudomonas aeruginosa ATCC 9027

outlier-strain reveals new insights on the PqsE effect on RhlR activity. *Mol Microbiol* 2021;116:1113–1123.

89. **Simanek KA, Taylor IR, Richael EK, Lasek-Nesselquist E, Bassler BL, *et al.*** The PqsE-RhlR Interaction Regulates RhlR DNA Binding to Control Virulence Factor Production in Pseudomonas aeruginosa. *Microbiol Spectr* 2022;10:e0210821.

90. **Feathers JR, Richael EK, Simanek KA, Fromme JC, Paczkowski JE**. Structure of the RhlR-PqsE complex from Pseudomonas aeruginosa reveals mechanistic insights into quorum-sensing gene regulation. *Structure* 2022;30:1626-1636.e4.

91. **Borgert SR, Henke S, Witzgall F, Schmelz S, Zur Lage S, *et al.*** Moonlighting chaperone activity of the enzyme PqsE contributes to RhlR-controlled virulence of Pseudomonas aeruginosa. *Nat Commun* 2022;13:7402.

92. **Farrow JM, Sund ZM, Ellison ML, Wade DS, Coleman JP, *et al.*** PqsE functions independently of PqsR-Pseudomonas quinolone signal and enhances the rhl quorum-sensing system. *J Bacteriol* 2008;190:7043–51.

93. **D'Argenio DA, Wu M, Hoffman LR, Kulasekara HD, Déziel E, *et al.*** Growth phenotypes of Pseudomonas aeruginosa lasR mutants adapted to the airways of cystic fibrosis patients. *Mol Microbiol* 2007;64:512–533.

94. **D'Argenio DA, Calfee MW, Rainey PB, Pesci EC**. Autolysis and autoaggregation in Pseudomonas aeruginosa colony morphology mutants. *J Bacteriol* 2002;184:6481–6489.

95. **Déziel E, Lépine F, Milot S, He J, Mindrinos MN, *et al.*** Analysis of Pseudomonas aeruginosa 4-hydroxy-2-alkylquinolines (HAQs) reveals a role for 4-hydroxy-2-heptylquinoline in cell-to-cell communication. *Proc Natl Acad Sci U S A* 2004;101:1339–1344.

96. **Hazan R, Que YA, Maura D, Strobel B, Majcherczyk PA, *et al.*** Auto Poisoning of the Respiratory Chain by a Quorum-Sensing-Regulated Molecule Favors Biofilm Formation and Antibiotic Tolerance. *Current Biology* 2016;26:195–206.

97. **Palmer KL, Aye LM, Whiteley M**. Nutritional cues control Pseudomonas aeruginosa multicellular behavior in cystic fibrosis sputum. *J Bacteriol* 2007;189:8079–8087.

98. **McKnight SL, Iglewski BH, Pesci EC**. The Pseudomonas quinolone signal regulates rhl quorum sensing in Pseudomonas aeruginosa. *J Bacteriol* 2000;182:2702–2708.

99. **Köhler T, Epp SF, Curty LK, Pechère JC**. Characterization of MexT, the regulator of the MexE-MexF-OprN multidrug efflux system of Pseudomonas aeruginosa. *J Bacteriol* 1999;181:6300–6305.

100. **Lamarche MG, Déziel E**. MexEF-OprN efflux pump exports the Pseudomonas quinolone signal (PQS) precursor HHQ (4-hydroxy-2-heptylquinoline). *PLoS One* 2011;6:e24310.

101. **Köhler T, Van Delden C, Curty LK, Hamzehpour MM, Pechere JC**. Overexpression of the MexEF-OprN multidrug efflux system affects cell-to-cell signaling in Pseudomonas aeruginosa. *J Bacteriol* 2001;183:5213–5222.

102. **Cornforth DM, Popat R, McNally L, Gurney J, Scott-Phillips TC, *et al.*** Combinatorial quorum sensing allows bacteria to resolve their social and physical environment. *Proc Natl Acad Sci U S A* 2014;111:4280–4284.

103. **West SA, Winzer K, Gardner A, Diggle SP**. Quorum sensing and the confusion about diffusion. *Trends Microbiol* 2012;20:586–594.

104. **Redfield RJ**. Is quorum sensing a side effect of diffusion sensing? *Trends Microbiol* 2002;10:365–70.

105. **Darch SE, Simoska O, Fitzpatrick M, Barraza JP, Stevenson KJ, *et al.*** Spatial determinants of quorum signaling in a Pseudomonas aeruginosa infection model. *Proc Natl Acad Sci U S A* 2018;115:4779–4784.

106. **Kümmerli R**. Cheat invasion causes bacterial trait loss in lung infections. *Proc Natl Acad Sci U S A* 2015;112:10577–10578.

107. **Mund A, Diggle SP, Harrison F**. The Fitness of Pseudomonas aeruginosa Quorum Sensing Signal Cheats Is Influenced by the Diffusivity of the Environment. 2017;8:1–8.

108. **Bjarnsholt T, Alhede M, Alhede M, Eickhardt-Sørensen SR, Moser C, *et al.*** The in vivo biofilm. *Trends Microbiol* 2013;21:466–474.

109. **Alhede M, Kragh KN, Qvortrup K, Allesen-Holm M, van Gennip M, *et al.*** Phenotypes of non-attached pseudomonas aeruginosa aggregates resemble surface attached biofilm. *PLoS One*;6. Epub ahead of print 2011. DOI: 10.1371/journal.pone.0027943.

110. **Darch SE, Kragh KN, Abbott EA, Bjarnsholt T, Bull JJ, *et al.*** Phage inhibit pathogen dissemination by targeting bacterial migrants in a chronic infection model. *mBio*;8. Epub ahead of print 2017. DOI: 10.1128/mBio.00240-17.

111. **Kragh KN, Alhede M, Jensen P, Moser C, Scheike T, *et al.*** Polymorphonuclear leukocytes restrict growth of Pseudomonas aeruginosa in the lungs of cystic fibrosis patients. *Infect Immun* 2014;82:4477–4486.

112. **Kragh KN, Hutchison JB, Melaugh G, Rodesney C, Roberts AEL, *et al.*** Role of multicellular aggregates in biofilm formation. *mBio*;7. Epub ahead of print 2016. DOI: 10.1128/mBio.00237-16.

113. **Bjarnsholt T, Jensen PØ, Fiandaca MJ, Pedersen J, Hansen CR, *et al.*** Pseudomonas aeruginosa biofilms in the respiratory tract of cystic fibrosis patients. *Pediatr Pulmonol* 2009;44:547–558.

114. **Azimi S, Thomas J, Cleland SE, Curtis JE, Goldberg JB, *et al.*** O-specific antigen-dependent surface hydrophobicity mediates aggregate assembly type in pseudomonas aeruginosa. *mBio*;12. Epub ahead of print 2021. DOI: 10.1128/mBio.00860-21.

115. **Azimi S, Lewin GR, Whiteley M**. The biogeography of infection revisited. *Nat Rev Microbiol*;0123456789. Epub ahead of print 2022. DOI: 10.1038/s41579-022-00683-3.

116. **Wucher BR, Winans JB, Elsayed M, Kadouri DE, Nadell CD**. Breakdown of clonal cooperative architecture in multispecies biofilms and the spatial ecology of predation. *Proc Natl Acad Sci U S A* 2023;120:e2212650120.

117. **Sexton DJ, Schuster M**. Nutrient limitation determines the fitness of cheaters in bacterial siderophore cooperation. *Nat Commun* 2017;8:230.

118. **Dandekar AA, Chugani S, Greenberg EP**. Bacterial quorum sensing and metabolic incentives to cooperate. *Science (1979)* 2008;23:1–7.

119. **Schuster M, Sexton DJ, Hense BA**. Why Quorum Sensing Controls Private Goods. *Front Microbiol* 2017;8:885.

120. **Feng X, Kostylev M, Dandekar AA, Greenberg EP**. Dynamics of cheater invasion in a cooperating population of Pseudomonas aeruginosa. *Sci Rep* 2019;9:10190.

121. **Cunningham L, Pitt M, Williams HD**. The cioAB genes from Pseudomonas aeruginosa code for a novel cyanide-insensitive terminal oxidase related to the cytochrome bd quinol oxidases. *Mol Microbiol* 1997;24:579–91.

122. **Frangipani E, Pérez-Martínez I, Williams HD, Cherbuin G, Haas D**. A novel cyanide-inducible gene cluster helps protect Pseudomonas aeruginosa from cyanide. *Environ Microbiol Rep* 2014;6:28–34.

123. **Yan H, Asfahl KL, Li N, Sun F, Xiao J, *et al.*** Conditional quorum-sensing induction of a cyanide-insensitive terminal oxidase stabilizes cooperating populations of Pseudomonas aeruginosa. *Nat Commun* 2019;10:4999.

124. **Winans JB, Wucher BR, Nadell CD**. Multispecies biofilm architecture determines bacterial exposure to phages. *PLoS Biol* 2022;20:e3001913.

125. **Barraza JP, Whiteley M**. A pseudomonas aeruginosa antimicrobial affects the biogeography but not fitness of staphylococcus aureus during coculture. *mBio*;12. Epub ahead of print 2021. DOI: 10.1128/mBio.00047-21.

126. **García-Contreras R, Nuñez-López L, Jasso-Chávez R, Kwan BW, Belmont JA, *et al.*** Quorum sensing enhancement of the stress response promotes resistance to quorum quenching and prevents social cheating. *ISME Journal* 2015;9:115–125.

127. **Castric PA**. Hydrogen cyanide, a secondary metabolite of Pseudomonas aeruginosa. *Can J Microbiol* 1975;21:613–18.

128. **Smalley NE, An D, Parsek MR, Chandler JR, Dandekar AA**. Quorum Sensing Protects Pseudomonas aeruginosa against Cheating by Other Species in a Laboratory Coculture Model. *J Bacteriol* 2015;197:3154–9.

129. **Fugère A, Lalonde Séguin D, Mitchell G, Déziel E, Dekimpe V, *et al.*** Interspecific small molecule interactions between clinical isolates of Pseudomonas aeruginosa and Staphylococcus aureus from adult cystic fibrosis patients. *PLoS One* 2014;9:e86705.

130. **Ibberson CB, Barraza JP, Holmes AL, Cao P, Whiteley M**. Precise spatial structure impacts antimicrobial susceptibility of S. aureus in polymicrobial wound infections. *Proc Natl Acad Sci U S A* 2022;119:e2212340119.

131. **Hassett DJ, Charniga L, Bean K, Ohman DE, Cohen MS**. Response of Pseudomonas aeruginosa to pyocyanin: mechanisms of resistance, antioxidant defenses, and demonstration of a manganese-cofactored superoxide dismutase. *Infect Immun* 1992;60:328–36.

132. **Britigan BE, Roeder TL, Rasmussen GT, Shasby DM, McCormick ML, *et al.*** Interaction of the Pseudomonas aeruginosa secretory products pyocyanin and pyochelin generates hydroxyl radical and causes synergistic damage to endothelial cells. Implications for Pseudomonas-associated tissue injury. *J Clin Invest* 1992;90:2187–96.

133. **Noto MJ, Burns WJ, Beavers WN, Skaar EP**. Mechanisms of Pyocyanin Toxicity and Genetic Determinants of Resistance in Staphylococcus aureus. *J Bacteriol*;199. Epub ahead of print 1 September 2017. DOI: 10.1128/JB.00221-17.

Chapter 2: Frequency of quorum sensing mutations in *Pseudomonas aeruginosa* strains isolated from different environments

Kathleen O'Connor, Conan Y. Zhao, Madeline Mei & Stephen P. Diggle

2.1 Abstract

Pseudomonas aeruginosa uses quorum sensing (QS) to coordinate the expression of multiple genes necessary for establishing and maintaining infection. It has previously been shown that *lasR* QS mutations frequently arise in cystic fibrosis (CF) lung infections, however, there has been far less emphasis on determining whether other QS system mutations arise during infection or in other environments. To test this, we utilized 852 publicly available sequenced *P. aeruginosa* genomes from the *Pseudomonas* International Consortium Database (IPCD) to study *P. aeruginosa* QS mutational signatures. To study isolates by source, we focused on a subset of 654 isolates collected from CF, wounds, and non-infection environmental isolates, where we could clearly identify their source. We also worked a small collection of isolates *in vitro* to determine the impact of *lasR* and *pqs* mutations on isolate phenotypes. We found that *lasR* mutations are common across all environments and are not specific to infection nor a particular infection type. We also found that the *pqs* system proteins PqsA, PqsH, PqsL and MexT, a protein of increasing importance to the QS field, are highly variable. Conversely, RsaL, a negative transcriptional regulator of the *las* system, was found to be highly conserved, suggesting selective pressure to repress *las* system activity. Overall, our findings suggest that QS mutations in *P. aeruginosa* are common and not limited to the *las* system; however, LasR is unique in the frequency of putative loss-of-function

mutations.

2.2 Introduction

Pseudomonas aeruginosa is a Gram-negative opportunistic pathogen that can be problematic in a number of infection types and environments [1]. One of the major adaptations of *P. aeruginosa* during chronic infection is the loss of quorum sensing (QS) [2–8]. In *P. aeruginosa,* QS regulates the expression of hundreds of genes, including those that encode for secreted products and virulence factors [9, 10]. It is regulated via a complex hierarchical network, composed of two *N*-acyl homoserine lactone (AHL) circuits known as LasR-LasI and RhlR-RhlI, two orphan regulators termed QscR and VqsR, and a negative transcriptional regulator of the *las* system, RsaL [9–19]. The Las and Rhl systems are composed of LuxR-LuxI pairs, which are homologous to other Gram-negative bacterial QS systems. The LuxR-type receptors (LasR, RhlR) act as transcriptional regulators, and the LuxI-type proteins (LasI, RhlI) are signal synthases. LasI produces 3-oxo-dodecanoyl-L-homoserine lactone (3OC12-HSL), and RhlI produces N-butanoyl-L-homoserine lactone (C4-HSL). Both signals can function in a combinatorial manner to synergistically regulate genes [20, 21]. Working in conjunction with the two AHL systems, is an alkyl-quinolone (AQ) system, comprising the *pqsABCDE* operon and *pqsH, pqsL* and *pqsR* (*mvfR*) genes. These genes drive the synthesis and response of 2-heptyl-3-hydroxy-4-quinolone (the *Pseudomonas* quinolone signal; PQS) [22, 23].

LasR was first identified in 1991 as a regulator of the *lasB* (elastase) gene [24]. It has since been described as a key QS regulator in the well-studied laboratory strains PAO1 and PA14*,* where it

has been shown to sit at the top of the QS hierarchy, regulating both the *rhl* and *pqs* systems [9, 11–15]. *lasR* mutants have frequently been isolated from cystic fibrosis (CF) lungs and more recently, it has been shown that some CF strains use RhlR to regulate the *rhl* and *pqs* systems in the absence of functional LasR [25–30]. The decoupling of the AHL QS hierarchy reportedly requires the inactivation of MexT [25, 27, 31], a regulator of the multi-drug efflux pump operon MexEF-OprN [32, 33]. It has also been shown that *mexT* mutation in PAO1 can decouple public *rhlR*-regulated traits from private metabolic *lasR*-regulated traits [20]. PqsE and RhlR have also been suggested to function as a ligand:receptor pair in some QS 're-wired' strains [34–36].

Previous work has shown that *lasR* mutations are also found outside the CF lung, but the extent and variation of these mutations is still being elucidated [26, 30]. The degree of mutation in other QS genes in infection and environmental strains of *P. aeruginosa* remains unknown. In this study, we explored the diversity and frequency of QS mutations across a range of ecologically distinct environments to determine (i) which QS genes are frequently mutated; (ii) mutational signatures, or patterns in other genes associated with *lasR* mutations; (iii) *lasR* gene mutation frequency specific to isolate source; and (iv) the phenotypic outcome of QS mutations.

2.3 Results

We utilized the published sequences of 852 *P. aeruginosa* isolates from the International *Pseudomonas* Consortium Database (IPCD); a database representing a range of *P. aeruginosa* strains from different sources including rivers, human infection and plants [37]. We queried key QS genes from the *las*, *rhl and pqs* systems, as well as the QS regulators *qscR, rsaL* and *vqsR*

against gene sequences from PAO1 (GCF_000006765.1) for all 852 isolates; the PAO1 referenced used for bioinformatics analysis is the closed genome sequence available for PAO1 available on BLAST and Pseudomonas.com. However for *in vitro* analysis, we used our lab strain Nottingham PAO1 (NPAO1), which has some variations.. For some analyses, we additionally looked at *mexT* and *psdR,* two genes that have been associated with *lasR* mutations *in vitro* [25, 31, 38, 39]. We used two analysis pipelines to look at the variation in QS genes in *P. aeruginosa.* One pipeline used NCBI BLASTn [40] and BLOSSUM80 [41], and the second analysis utilized GAMMA [42]. All analyses were conducted in R version 4.3 [43]. In this manuscript we report on protein dissimilarity scores generated by BLOSSUM80, which are a measure of how much the amino acid sequence varies from the wildtype sequence, with 0 being identical to wildtype. We additionally report codon similarity scores which were generated with GAMMA, with 1 being a protein identical to wildtype. Codon similarity is inversely related to the protein dissimilarity score, and is a measure of how similar amino acid sequence is to the wildtype sequence.

Quorum sensing genes are highly variable at the nucleotide level. We first analyzed the diversity of nucleotide sequence for each QS gene for all 852 isolates and looked at which isolates had mutations in multiple QS-related genes. We found a large diversity in sequences and that few isolates had QS genes identical to PAO1 (GCF_000006765.1). The *rhl* system was especially variable, with 849 and 847 isolates differing from PAO1 for *rhlR* and *rhlI* respectively (Fig. 1A). The *las* system was more conserved, with 553 and 290 isolates varying from PAO1 for *lasR* and *lasI* respectively (Fig. 1A). Genes involved in 2-alkyl-4-quinolone (AQ) biosynthesis and response showed a large variation in mutations between genes, with *pqsE* as the least variable (479 mutated isolates), and *pqsH* and *pqsL* as the most variable (845, 847 respectively) (Fig. 1C). The orphan

QS transcriptional regulators *qscR* and *vqsR* were highly variable (772 and 559 respectively). However, the negative *las* system transcriptional regulator *rsaL* was relatively conserved (218 mutated isolates) (Fig. 1D).

Fig. 1.
Comparison of nucleotide sequence variation among QS genes of P. aeruginosa isolates of the IPCD. There is a high degree of variation in nucleotide sequences in many of the QS genes, obscuring patterns in mutation overlap between genes within an isolate. (a) A Venn diagram of las and rhl system genes are plotted together, showing how many isolates share mutations in multiple genes. In total, 246 isolates are mutated for all four genes, and few isolates have mutations in only a single gene. (b) A Venn diagram for pqsABCD shows a similar pattern and 683 isolates are mutated in all four genes, while few isolates are mutated in only one pqs gene. (c) Few isolates have only one pqs gene mutation, and 430 isolates have mutations in all pqsEHLR genes. (d) A Venn diagram of the negative QS regulators vqsR, rsaL and qscR show that 132 isolates share mutations in all three genes.

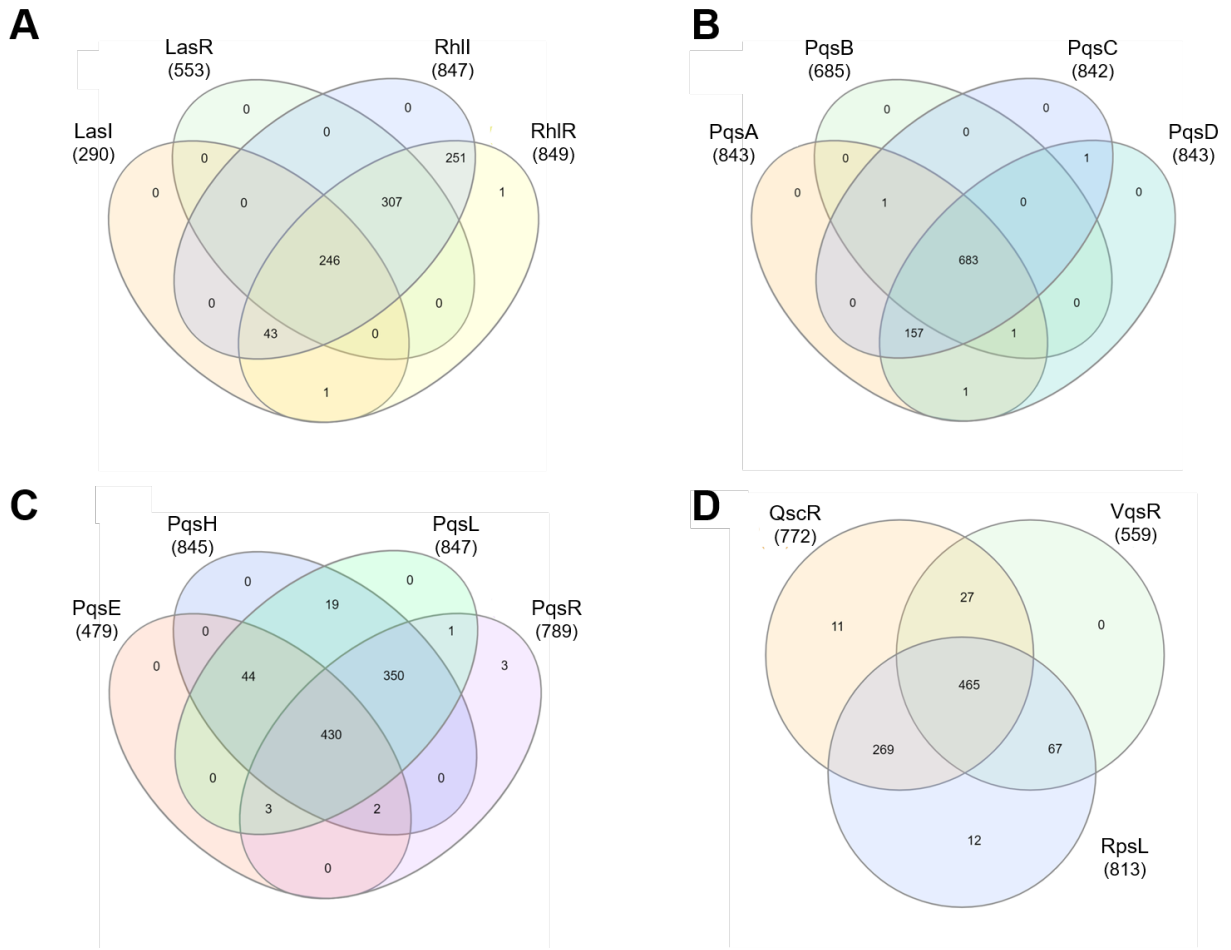

Negative and positive regulators of the *las* system are antipodal in sequence variation. We counted the number of unique protein sequences found in our database for each QS gene. We added *mucA* to our analysis as a reference gene that is frequently mutated in CF lung infections [44, 45], and *rpsL,* which encodes the 30S ribosomal protein S12; a conserved housekeeping gene [46, 47]. When we queried each QS gene nucleotide sequence against the 852 isolates using BLASTn, the query returned less than 852 sequences for each gene. This disparity is likely due to gaps in sequences, gene deletions, and extensive mutations, preventing BLASTn from returning a query. Additionally, for this analysis, we removed all truncated nucleotide sequences from the analysis, to avoid including sequencing near the end of a contig. Fig. 2A shows the number of protein sequences analyzed for each gene. After MucA, a LasR query returned the fewest number of sequences – 756 out of 852 isolates, suggesting that there are many strains that contain large deletions in LasR, truncations, or are lacking the LasR gene entirely. After translating the sequences, we found that LasR had the most unique protein sequences (259) across 852 isolates (Table 1, Fig. 2A) compared to other QS genes and MucA. The next most variable QS proteins, PqsH, PqsA, and PqsL contained 189, 170, and 169 unique protein sequences, respectively (Table 1; Fig. 2A). We found that AHL signal synthases were highly conserved; LasI and RhlI had only 61 and 87 unique protein sequences respectively. RsaL was the most conserved of all studied proteins, with only 18 unique sequences. Compared to LasR, the other key QS proteins were more conserved across isolates. Our protein sequence findings appear to contrast with our nucleotide sequence analysis, but this is likely due to primarily silent mutations in the *rhl* system. To control for possible bias due to differences in protein length, we normalized gene sizes to PAO1 by dividing the lengths of each gene by the PAO1 reference gene length. We found that the shortest proteins, RspL and RsaL were the most conserved, while the longest genes, PqsH, PqsA, and PqsL

were all highly variable. The most variable protein, LasR is of intermediate length, compared to RsaL and Pqs proteins (Table 1).

Fig. 2.
Determining variability in QS proteins between P. aeruginosa isolates from the IPCD. (a) We created a database of 852 isolates and used PAO1 to search for the QS proteins of each isolate. Due to the variation in each isolate's genome and due to gaps in sequencing, each protein queried returned fewer than 852 sequences (shown in grey). We also determined the number of unique sequences for each protein and found that LasR had the highest number of unique sequences (in colour). The next highest were PqsH, PqsA and PqsL. RsaL had the fewest number of unique sequences. (b) Using a custom dissimilarity metric (BLOSUM80), we calculated mean dissimilarity scores. We found that LasR had the highest mean dissimilarity score compared to all QS proteins, and the largest variation.

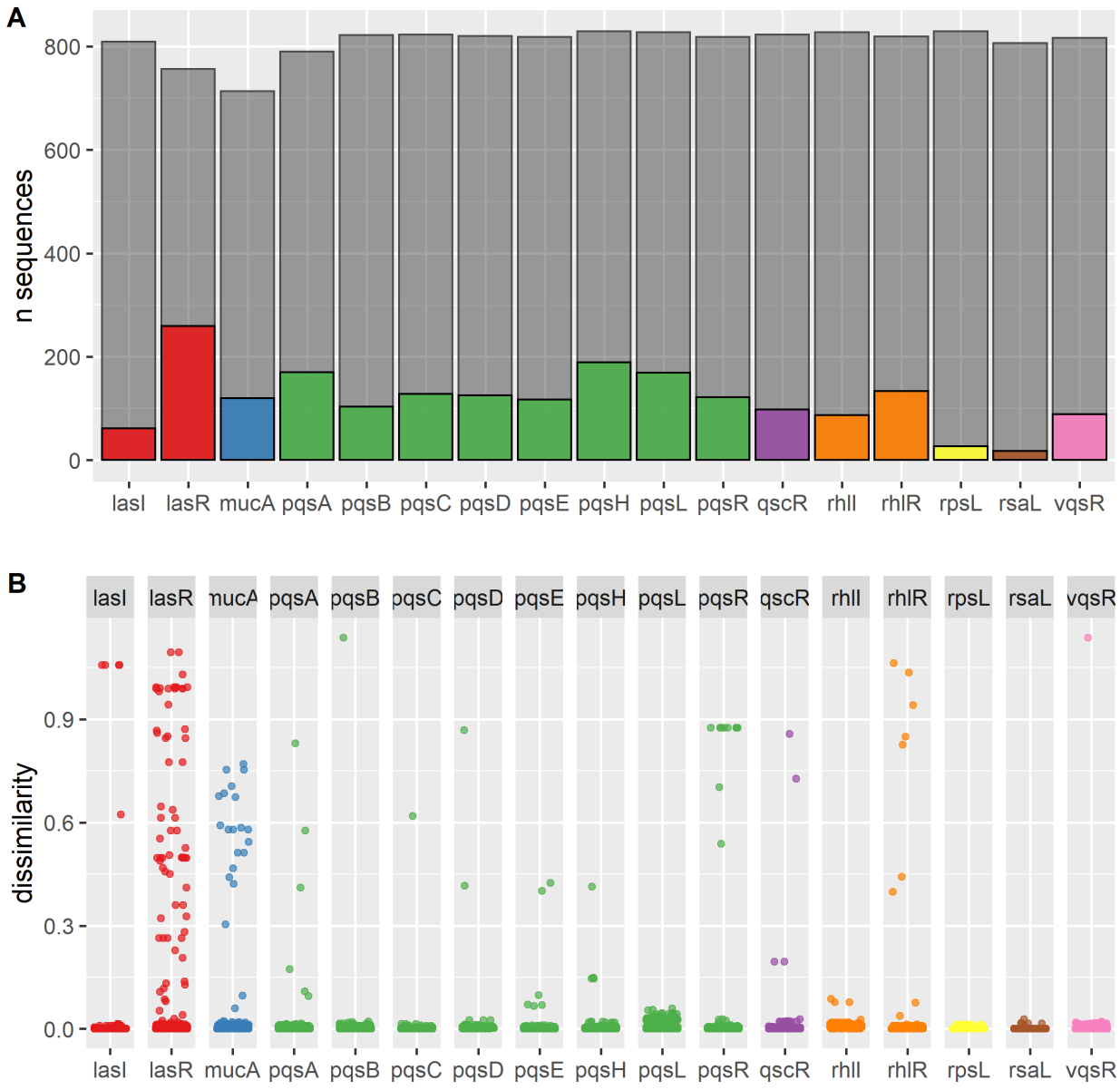

Table 1.
Variation in protein sequence encoded by P. aeruginosa isolates. Using the sequences returned by blastn, we translated genes with full-length nucleotide sequences to determine the number of unique protein sequences encoded by the isolates in the database. We found that LasR had the most unique sequences across queried isolates, and RsaL encoded the fewest unique sequences

Table 1. Protein Data				
Gene	Gene Length	Genes Returned	Unique Protein Sequences	Unique Sequences/ Gene Length
rsaL	243	806	18	0.07
rpsL	372	829	27	0.07
lasI	606	809	61	0.10
rhlI	606	827	87	0.14
vqsR	807	816	89	0.11
qscR	714	823	98	0.14
pqsB	852	822	103	0.12
pqsE	906	818	117	0.13
mucA	585	713	120	0.21
pqsR	999	818	122	0.12
pqsD	1014	820	125	0.12
pqsC	1047	823	128	0.12
rhlR	726	819	133	0.18
pqsL	1197	827	169	0.14
pqsA	1554	790	170	0.11
pqsH	1149	829	189	0.16
lasR	720	756	259	0.36

We next plotted the BLOSUM80 dissimilarity scores for all isolates for each gene and found that LasR had a large number of highly dissimilar sequences (Fig. 2B). The highly dissimilar scores

are caused by truncation mutations due to an early stop site leading to a shortened protein. Transcriptional regulators PqsR and RhlR also have a number of truncation mutations, however, there are fewer than LasR. While PqsA, PqsL and PqsH all encode many unique protein sequences, most isolates cluster towards the bottom, indicating that they have dissimilarity scores close to 0, indicating that the proteins have a near identical function.

MexT, PqsL and LasR have the highest mutation rates. We used the protein sequence data from GAMMA to look at the mutation rate of each QS protein (Table 2). For this analysis, we were able to include truncated nucleotide sequences, and only excluded sequences where it was indicated that the gene was located at the contig edge. We included MexT and PsdR proteins in this analysis. For the majority of genes, we compared isolates to the PAO1 (GCF_000006765.1) gene sequence, with the exception of PqsD and RhlI which we compared to the PAK strain of *P. aeruginosa*. The MexT sequence for PAO1 has an 8 bp insertion sequence, which was not commonly found in the IPCD database of isolates, as well as many other coding mutations. We instead used the sequence for isolate U0330A as it coded for a protein shared by 128 other isolates, the highest number of strains sharing one MexT sequence. The MexT gene is highly variable, and is mutated in our Nottingham PAO1 lab strain (NPAO1) and the PAO1 reference used (GCF_000006765.1). Among the QS genes, we found that PqsL had the highest mutation rate, followed by LasR. We defined mutation rate in this analysis as the percentage of non-wildtype protein sequences out of queried isolates. RsaL and LasI were highly conserved, with low mutation rates.

Table 2.
Mutation rate and mean codon similarity of QS proteins in P. aeruginosa . We used GAMMA to query QS genes against 852 isolates. We used PAK as a reference for RhlI and PqsD, U0330A as a reference for MexT and PAO1 as a reference for all other genes. GAMMA assigns isolates with

a codon similarity measure, which reflects the type of amino acid change or truncation. A low score reflects a likely change in function of the protein, and a score of 1 reflects the isolate is identical to the reference. We found that LasR had the lowest mean codon similarity and RsaL the highest

Table 2. Mutation Rate (Continued on Page 58)

Gene	Total	Mutant	Percent Mutant	Codon Similarity
LasR	826	425	51.45%	0.9343
MucA	850	257	30.24%	0.9450
MexT	847	719	84.89%	0.9687
RhlR	850	104	12.24%	0.9925
PqsA	826	302	36.56%	0.9945
LasI	832	33	3.97%	0.9949
PqsE	844	101	11.97%	0.9951
PqsD	847	240	28.34%	0.9953
PqsL	850	447	52.59%	0.9953
VqsR	849	256	30.15%	0.9955
QscR	848	101	11.91%	0.9967
PqsR	852	200	23.47%	0.9970
RhlI	850	198	23.29%	0.9981
PqsB	847	260	30.70%	0.9984
PqsH	848	336	39.62%	0.9986
PsdR	844	38	4.50%	0.9990
PqsC	847	164	19.36%	0.9993
RpsL	852	21	2.46%	0.9998

RsaL	830	6	0.72%	0.9999

Using GAMMA generated protein mutation data, we next calculated the average codon similarity of all isolates to a reference (Table 2). High codon similarity suggests similar protein function, while low codon similarity indicates a change or loss of protein function. For the majority of genes we used PAO1 (GCF_000006765.1) as a reference, however the codon similarity average for several proteins were low. To address this, for RhlI and PqsD we used PAK as the reference strain, and for MexT we used U0330A as these strains were likely to be better models based on higher similarity averages for each protein. Similar to our analysis using BLOSUM80, we found that LasR had the lowest average protein similarity of all QS genes, followed by MexT, which we attributed to the high rate of truncation mutations. All other QS proteins had a codon similarity average of greater than 0.99, indicating that while there is variation in the protein sequence, many of these mutations likely lead to a similarly functioning protein.

LasR protein mutations are common across all environments but are more divergent in human wounds. In agreement with previous studies, LasR was the most variable gene in our protein analysis (Table 1; Fig. 2), and we found that the highly dissimilar LasR sequences were due to protein truncations [2, 30, 48]. To determine if LasR mutations vary by environment, we categorized the strains by source. Using data from the IPCD, we selected a subset of 654 strains labeled as “environmental”, “cystic fibrosis” or “CF”, and “wound” or “ulcer” or “burn” and reclassified them as environmental (209 strains), CF (396 strains), or wound (wound, ulcer, and burn) (49 strains); 654 total. The remaining 198 strains from the original set of 852 strains were of uncertain origin and therefore excluded from this analysis. To establish a threshold by which a

protein could be deemed functional or not, we looked at truncated LasR proteins within each environment. We compared the amino acid length of LasR in the IPCD strains to the PAO1 LasR protein – which is equal in length to many commonly researched strains including PA14, PAK and the Liverpool epidemic CF strain LESB58. Our assumption was that a truncated protein due to an early stop site, would lead to a nonfunctional protein. We used a stringent 100% length as a cut-off, and any protein shorter than full-length was considered truncated. Fig. 3A shows the proportion of each group that had truncated LasR proteins with CF, environmental, and wound isolates having 20%, 11% and 30% truncations respectively. We then plotted the protein sequence dissimilarities categorized by isolate source, and found highly dissimilar isolates, primarily in CF and wounds (Fig. 3B). Overall, we found that *lasR* mutations are ubiquitous across all environments, but there is a larger percentage of strains with truncated LasR proteins found in infection environments. We additionally calculated the mean and median codon similarity scores for each environment, with 1 being a protein identical to PAO1. We found that the wound group was the most dissimilar compared to PAO1, with the lowest mean similarity score (0.893), and CF and environmental were similar (CF: 0.953, Env: 0.948). The wound group also had the lowest median similarity score (0.995), followed by CF (0.996) and environmental had the highest median similarity score (1.0). An additional analysis of a second collection of *P. aeruginosa* genomes could allow for the performance of statistics on the significance of the difference between genes, however that was unfortunately not possible for this study.

Fig. 3.
LasR truncations are found in isolates from all sources. To observe the fraction of truncated proteins across all environments, we categorized the isolates into three groups: cystic fibrosis (CF), environmental (ENV) or wound (WND). (a) We show the number of truncated proteins out of the total number of isolates in each group. The protein variation plot (b) depicts the similarity scores for all groups compared, and we see the highly dissimilar truncated proteins consisted primarily of CF and WND isolates.

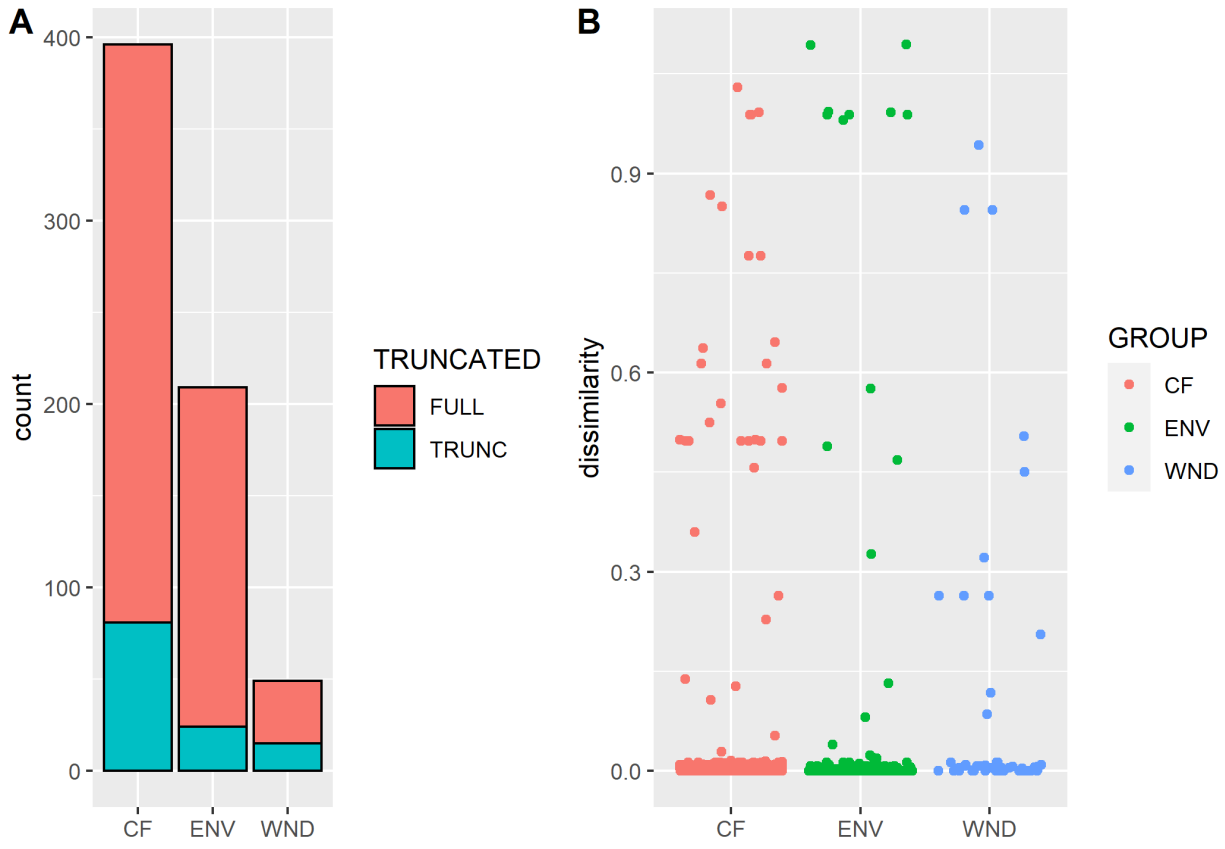

***lasR* mutation is not a predictor of exoprotease production or colony autolysis in selected environmental and infection isolates**. To accompany our genomic analysis, selected 20 isolates from the IPCD, in order to perform phenotypic assays to assess QS function. We had over 100 isolates available from the Gabriel Perron collection and we chose a collection of isolates to represent wildtype, truncated, and mutated LasR proteins from environmental, wound, and CF isolates. After Sanger sequencing the *lasR* gene to confirm isolated identification, we found that the 8 isolates with "truncated" nucleotide sequences had incorrect sequences (data not shown), likely because the sequence was at the end of a contig rather than a true truncation. We decided to move forward with 12 out of 20 isolates with correct sequence identity. We included our lab strain NPAO1 as well as the clean deletion mutants PAO1Δ*lasR*, PAO1Δ*rhlR*, PAO1Δ*lasR*Δ*rhlR*,

PAO1Δ*lasI*. Our PAO1Δ*lasR* strain made high levels of protease that were not significantly lower than NPAO1 (89 % of NPAO1 levels, $p = 0.338$). A *lasR* gentamicin insertion mutant made 75 % of the protease levels of NPAO1 ($p = 0.113$) (Fig. 4). We found that unlike mutations in LasR, mutations in RhlR had a significant effect on the protease levels produced compared to NPAO1 (PAO1Δ*rhlR*: 45 %, $p = 0.013$; PAO1Δ*lasR*Δ*rhlR* double mutant: 20 %, $p = 0.011$). Compared with both Δ*lasR* mutants, NPAO1Δ*lasI* made lower amounts of protease (60 %, $p = 0.025$) (Fig. 4). Isolates with mutated LasR proteins that produce significantly less protease than wildtype included A17, CND03, CPHL2000, Jp115 (*p* values respectively: 0.01, 0.01, 0.02, 0.01). PT31M, a German environmental isolate contains a truncation mutation in LasR, yet it produced an intermediate amount of protease compared to NPAO1 with an intact LasR (69 %, $p = 0.062$). The Belgian river environmental strain W15Dec14 also produced an intermediate amount of protease (67 %, $p = 0.065$) and is wildtype for LasR, but does contain coding mutations in RhlI. All other isolates with wildtype LasR proteins produced protease levels that were not significantly different from NPAO1 (Fig. 4).

Fig. 4.

Exoprotease secretion by environmental and clinical isolates. We measured the supernatant exoprotease levels produced by stationary phase isolates, compared to PAO1, PAO1ΔlasR and PAO1ΔlasRΔrhlR. We normalized the readings by optical density (OD 600nm) and compared all isolates and clean mutants to PAO1. * denotes a strain is significantly different from NPAO1, $P<0.05$. Strain origin abbreviated are listed after strain names as follows: environmental (E), wound, burn or ulcer (W), cystic fibrosis (CF).

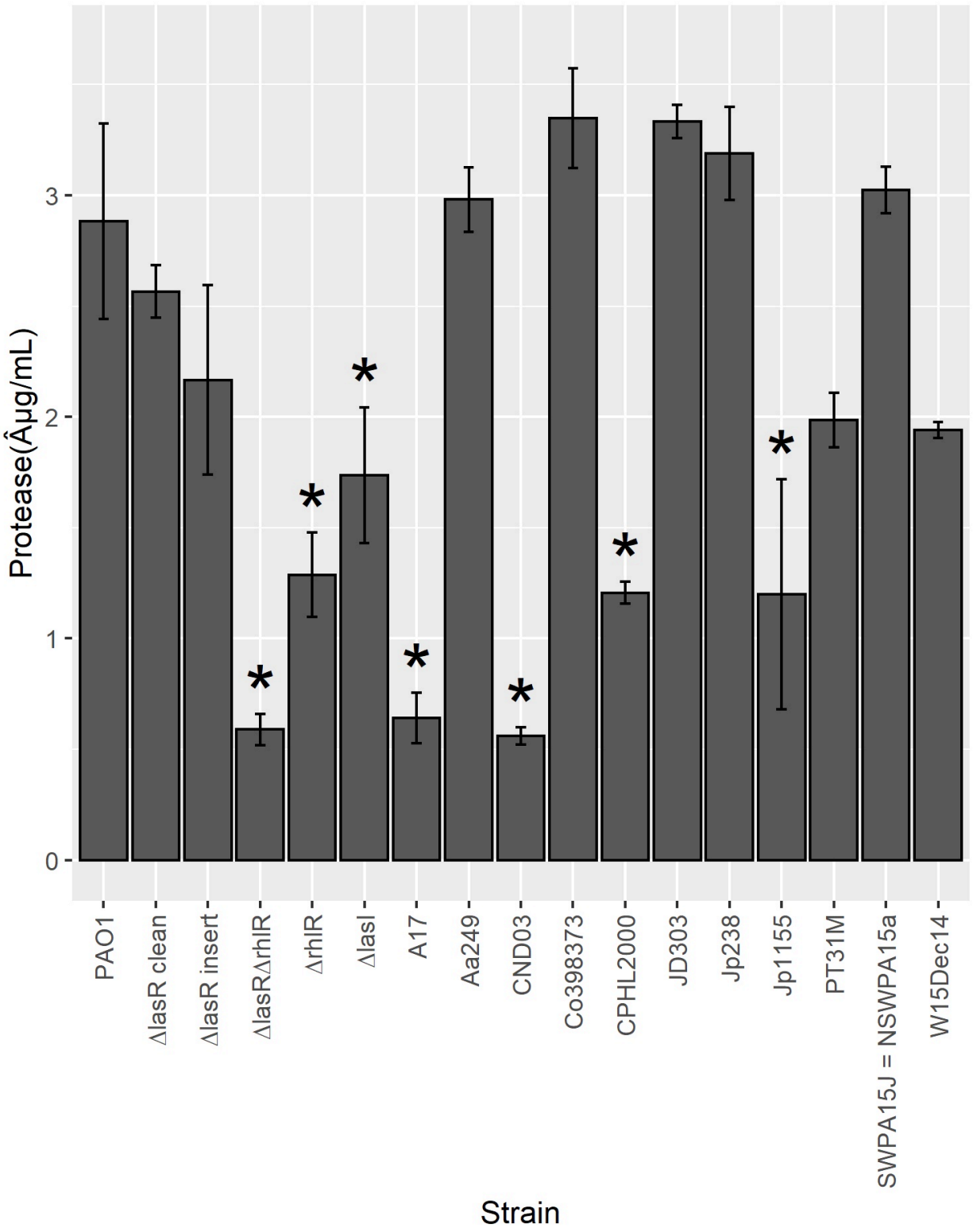

Fig. 5.
Colony autolysis phenotypes of isolates compared to lab strain QS mutants. We spotted overnight cultures on LBA plates to observe the colony autolysis phenotypes exhibited by clean QS deletion

mutants alongside environmental and clinical isolates. Colony autolysis and colony plaquing were quantified by eye, by looking for the characteristic iridescent sheen or uneven colony texture normally associated with phage activity. Strain SWPA15J=NSWPA15 a is labelled as SWPA15J. Strain origin abbreviated are listed after strain names as follows: environmental (E),wound, burn or ulcer (W),cystic fibrosis (CF).

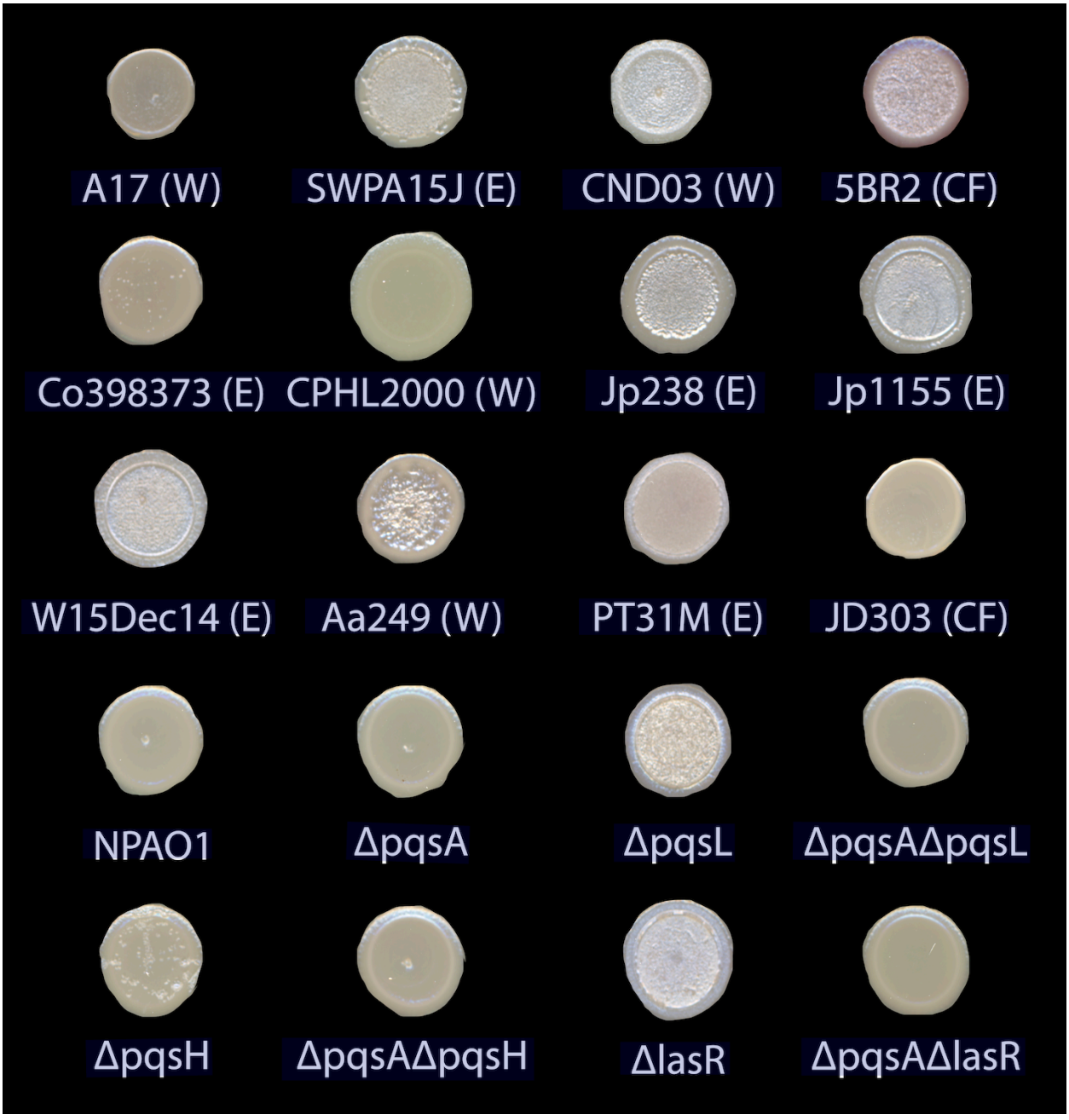

Lysis in QS mutants has long been observed in the lab, specifically in *lasR*, *lasI* and/or *pqs* mutants [48–51]. The lysis phenotype is characterized by an iridescent sheen on the colony surface, and an uneven lysed texture; some *pqs* mutants alternatively show plaquing similar to phage activity. The iridescent sheen typically seen in *lasR* mutants is attributed to HHQ accumulation [48]. We used QS deletion mutant strains to determine how QS mediates colony autolysis. PAO1Δ*lasR* and PAO1Δ*pqsL* showed similar lysis phenotypes and a metallic sheen, while PAO1Δ*pqsH* caused colony plaquing (Fig. 5). PAO1Δ*pqsA*Δ*lasR,* PAO1Δ*pqsA*Δ*pqsH* and PAO1Δ*pqsA*Δ*pqsL* mutations led to a loss of colony autolysis (Fig. 5). We found that all LasR wildtype strains we tested from the IPCD showing lysis or plaquing, contained multiple mutations in the *pqs* quinolone system, as follows: SWPA15J=NSWPA15a (PqsC,D,E), 5BR2 (PqsD,L), Co398373 (PqsD,L), Jp238 (PqsB,D,L), W15D14 (PqsE,D,L), Aa249 (PqsB,D,L), JD303 (PqsA,B,D). Strains with wildtype LasR showing lysis were from mixed environmental, wound and CF sources. There were two *lasR* mutant isolates that showed no lysis - A17 and CPHL2000, both sourced from human wounds (Fig. 5). Isolates A17 and CPHL2000 have 1 and 2 SNPs in LasR respectively, both creating a change in amino acid sequence (A17: L110P, CPHL2000: E196G). As expected, the 3 isolates with truncated LasR (CND03, Jp1155, and PT31M) demonstrated lysis.

2.4 Discussion

In *P. aeruginosa*, *lasR* QS mutants are frequently isolated from human chronic infection and environmental sources, but less is known about other QS genes [2, 48, 52]. Using a publicly available database of 852 fully sequenced isolates from CF, wounds and non-human associated (environmental) strains [37], we determined the mutation frequency and variation of *lasR* and other

QS genes in *P. aeruginosa*. To determine how QS genotype impacts phenotypic function, we used 12 strains that were sequenced as part of the IPCD study [37]. We found that (i) by multiple metrics, LasR is the most variable QS protein; (ii) LasR mutations are found in isolates across all environments, suggesting that any environment can drive the evolution of these mutations; (iii) the negative *las* system regulator RsaL is well-conserved; (iv) signal synthases LasI and RhlI are conserved compared to their transcriptional regulator pairs; (v) coding mutations in *pqs* system genes are common and may impact colony autolysis, however they are less divergent than LasR mutations; (vi) MexT is highly variable and mutations are common.

Our work supports the long-held belief that LasR is a commonly mutated QS protein as we showed that LasR has the highest number of unique protein sequences compared to other QS genes. A high number of isolates carried mutations in LasR compared to the PAO1 reference protein sequence. The IPCD strains also had the lowest average codon similarity for the LasR gene when compared to other QS regulon genes, which we attributed to nonsense mutations leading to protein truncation, and other large changes in amino acid sequence. Our results also highlight that LasR mutations are found in environmental isolates and are not specific to human infections. Truncation mutations are more commonly found in human wound infections, suggesting that there might be some selective pressure to evolve loss of function mutations. Mean and median similarity scores suggest there is not a large difference between CF and environmental isolates, and instead we found that wound isolates are enriched for loss of function mutations. The wound group was the smallest group of isolates we queried thus a larger exploration of wound strains could provide a deeper understanding of this phenomenon.

Interestingly, the most highly conserved QS protein was RsaL, which negatively regulates the *las* QS system [16, 53, 54]. RsaL and LasR are antipodal in variation across isolates and perform opposite jobs in regulating the *las* system. There may be a benefit to tightly conserving the "off" switch of the *las* system while frequently mutating and losing the function of the "on" switch, suggesting that a key element of the QS regulatory cascade is down-regulating *las*-controlled QS in *P. aeruginosa.* Given this complexity, it remains a challenge to understand why the *las* system evolved and what fitness benefits it provides *P. aeruginosa* in different environments. There may be evolutionary benefits for both the maintenance and loss of LasR so that both *lasR* positive and negative strains can stably coexist in heterogenous populations and contribute to an overall community function. In support of this idea, it has been shown that (i) *lasR*- strains overproduce Rhl-associated factors and cross-feed wild type cells in low iron environments, which will likely impact infection dynamics of mixed populations [55]; (ii) mixed *lasR* +/- populations display decreased virulence in mouse models of infection [56]; and (iii) mixed populations exhibit enhanced tolerance to beta-lactam antibiotics [57]. These data suggest there are likely considerable fitness advantages to cells growing in heterogeneous QS populations, perhaps as a bet-hedging mechanism for future disturbance events.

The signal synthases of the two AHL QS systems in *P. aeruginosa* are conserved compared to their transcriptional regulator pairs. It has been hypothesized that there could be evolutionary mechanisms to conserve signal synthases while mutating transcriptional regulators [58]. We saw a significant difference in protease production by the clean deletion of the regulator mutant LasR and the signal synthase mutant LasI, where deletion of LasI resulted in a larger decrease in protease production. The reason for this could be further explored and may be impacted by the MexT

mutation in NPAO1, common to other PAO1 lab strains, or the fact that the 3' end of RsaL is also deleted in a clean LasR deletion mutation [59]. There could also be an evolutionary benefit to maintaining some protease function in the absence of fully functioning QS, supporting the maintenance of signal synthases while mutating positive transcriptional regulators.

Recent studies on QS in *P. aeruginosa* has revealed that the complex and intertwined *las*, *rhl* and *pqs* systems can be re-wired if *lasR* becomes mutated [25, 27, 31, 34–36]. It is not always clear whether these strains are entirely QS-null or if they have re-wired their QS systems to circumvent the loss of *lasR*. In our *in vitro* work, we looked at lysis and protease secretion as indicators of QS function, which have previously been used to screen for LasR function [48, 60]. We found an environmental isolate, PT31M, with a truncated *lasR* that produces high levels of protease. PT31M may be an example of a re-wired isolate showing QS independent of LasR, suggesting this adaptation is not specific to CF lung infections. Colony lysis has been used as a predictor for *las* system function, however this study has shown little correlation between lysis and *lasR* genotype, potentially due to *pqs* mutation mediated lysis seen in NPAO1Δ*pqsH* and NPAO1Δ*pqsL*.

Overall, our work shows that LasR is uniquely mutated compared to other QS genes, future work should more strongly focus on the ecology of mixed QS-phenotypes to better understand QS-involvement in infection and other environments. With ongoing work identifying QS-inhibitors targeting the *las* QS system, the frequency of *lasR* mutated strains found in our study suggests that this particular pursuit might be improved by targeting a less variable QS gene, such as *rhl* system genes or RsaL.

2.5 Materials and Methods

Querying QS genes from the International *Pseudomonas* Consortium Database. Using nucleotide sequences from PAO1 (GCF_000006765.1), we queried QS genes using BLASTn for isolates from the IPCD [37]. We chose this strain because it is a fully sequenced, frequently used lab strain. We first compared strains with nucleotide mutations relative to PAO1 in each of the QS genes of interest, to determine how frequently strains exhibit nucleotide polymorphisms across multiple QS genes. We then translated these sequences into protein sequences calculating putative amino acid sequence similarities using BLOSUM80 [41]. First, we compared genes found in each isolate against our reference strain, PAO1, normalized against the similarity of the reference against itself. We then calculated the mean dissimilarity score of all isolates compared to PAO1. Some isolates were missing genes due to sequencing errors or true truncations, the number of isolates with a given gene present was under 852 for all genes. All analyses, including translation steps were conducted in R version 4.3. All code and files are available on a publicly available database:

https://github.gatech.edu/koconnor36/Frequency_of_quorum_sensing_mutations_in_Pa2021

Creating an IPCD database using BLASTn. We pulled IPCD data from GenBank from the PRJNA325248 BioProject (https://www.ncbi.nlm.nih.gov/bioproject/325248), and downloaded contigs as a multifasta file. We used the makeblastdb/ command to generate a database of all isolate contigs.

Using BLASTn to find QS genes for each isolate. Using our generated database, we queried the PAO1 sequence for each gene found on Pseudomonas.com [61], against the database. We generated csv files for each gene which included the gene sequences for each isolate.

Comparing strains with nucleotide polymorphisms in multiple QS genes. We used the csv files for each gene generated from the BLASTn analysis to isolate all accession information of strains with <100% query coverage and <100% identity to the PAO1 sequence of each QS gene. For each QS gene, we used this list of NCBI accession IDs, corresponding to unique strains, to visualize the number of strains with nucleotide mutations in one or more genes with InteractiVenn [62]. We then calculated the number of strains and the percentage of strains in the IPCD database with at least one mutation in each QS gene. We generated accession lists of mutated strains for each QS gene using a custom R script (v.4.0.2) and generated Fig. 1 with InteractiVenn. All analyses were conducted in R version 4.3.

Translating nucleotide to amino acid sequence. We translated genes to proteins using a custom R script. We first queried only for sequences starting with a canonical ATG start codon. VqsR is an exception as it begins with the alternative start codon "GTG". We translated the sequences meeting these criteria using the translate function from the BioStrings R package (v.2.58.0) [63].

Calculating dissimilarity scores for isolates' QS proteins. All sequence analyses were performed in R (v.4.0.2) using the Biostrings package v.2.58.0. We compared isolate protein sequences to PAO1 protein sequences using BLOSUM80, a matrix designed to compare protein sequences within species.

Determining truncation rates for LasR and categorizing isolates by location. We determined the length of the reference LasR protein, from PAO1, compared to each isolate protein. If the isolate protein was less than 100% of the length of the PAO1 protein, we categorized it as truncated. Sequences were categorized as CF-originated (CF), environmental (ENV), or wound (WND). If the sequence was entered into IPCD as environmental, we adopted that label. Additionally, we included sequences labeled from animal hosts as environmental. For CF, we only included sequences with sources explicitly labeled as CF or cystic fibrosis. For wound, we included sequences labeled as wound, ulcer, and burn.

Protein mutation analysis using GAMMA: We used GAMMA [42] to find the mutations in QS genes for all isolates. We created a multifasta of genes: *lasR,I, rhlR,I, pqsA,B,C,D,E,H,L,R, qscR, rsaL, vqsR*, *mucA, rpsL, mexT, psdR* to query against the IPCD PRJNA325248 multifasta. We ran commands as described in the GAMMA GitHub [42] https://github.com/rastanton/GAMMA, and generated a GAMMA file with mutations reported for all genes in all IPCD isolates. All other sequences are available on our project Github https://github.gatech.edu/koconnor36/Frequency_of_quorum_sensing_mutations_in_Pa2021.

Phenotypic assays. Isolates sequenced as part of the IPCD were donated by the Brown lab at Georgia Tech. We cultured isolates on LB agar plates, and confirmed their identity by sequencing the *lasR* gene, using colony *OneTaq* PCR (New England Biolabs). For protease activity, we inoculated colonies in 5 mL of LB broth, and grew strains in biological triplicates for 16-18 hours at 37 °C, 200 rpm. We pelleted cells and used the supernatant to run the Pierce Fluorescent Protease

Assay Kit (Thermo). Readings were quantified using the TPCK Trypsin standard in triplicate, and normalized by strain optical density (OD at 600_{nm}). All readings were compared to NPAO1. For colony autolysis experiments, we inoculated colonies in 5 mL of LB broth, and grew strains for 16-18 hours at 37 °C, 200 rpm. We tested colony autolysis by spotting 5 µL of overnight cultures on LB agar plates, and growing colonies for 24 hours at 37 °C. We scanned images of colonies on plates and quantified lysis by eye, looking for iridescent sheen or an uneven colony surface caused by plaquing.

Author contributions. SPD and KO designed the study. KO, CYZ, and MM performed the *in silico* analysis of the data. KO performed the *in vitro* analysis. All authors contributed to the writing of the manuscript.

Competing interests. The authors declare no competing interests.

Funding and acknowledgements. We wish to thank The Cystic Fibrosis Foundation (DIGGLE20G0) and The National Institute for Health (R01AI153116) to SPD for funding. We also thank members of the Diggle Lab and Jon Gerhart for helpful discussion. We thank the Brown Lab at Georgia Tech for donating strains from the IPCD collection.

2.6 References

1. **Diggle SP, Whiteley M**. Microbe profile: Pseudomonas aeruginosa: Opportunistic pathogen and lab rat. *Microbiology (United Kingdom)* 2020;166:30–33.

2. **Smith EE, Buckley DG, Wu Z, Saenphimmachak C, Hoffman LR, *et al.*** Genetic adaptation by Pseudomonas aeruginosa to the airways of cystic fibrosis patients. *Proc Natl Acad Sci U S A* 2006;103:8487–8492.

3. **LaFayette SL, Houle D, Beaudoin T, Wojewodka G, Radzioch D, *et al.*** Cystic fibrosis–adapted Pseudomonas aeruginosa quorum sensing lasR mutants cause hyperinflammatory responses. *Sci Adv* 2015;1:1–15.

4. **Hansen SK, Rau MH, Johansen HK, Ciofu O, Jelsbak L, *et al.*** Evolution and diversification of Pseudomonas aeruginosa in the paranasal sinuses of cystic fibrosis children have implications for chronic lung infection. *ISME Journal* 2012;6:31–45.

5. **Ciofu O, Mandsberg LF, Bjarnsholt T, Wassermann T, Høiby N**. Genetic adaptation of pseudomonas aeruginosa during chronic lung infection of patients with cystic fibrosis: Strong and weak mutators with heterogeneous genetic backgrounds emerge in mucA and/or lasR mutants. *Microbiology (N Y)* 2010;156:1108–1119.

6. **Williams P, Cámara M**. Quorum sensing and environmental adaptation in Pseudomonas aeruginosa: a tale of regulatory networks and multifunctional signal molecules. *Curr Opin Microbiol* 2009;12:182–191.

7. **Galán-Vásquez E, Luna B, Martínez-Antonio A**. The Regulatory Network of Pseudomonas aeruginosa. *Microb Inform Exp* 2011;1:3.

8. **Lee J, Zhang L**. The hierarchy quorum sensing network in Pseudomonas aeruginosa. *Protein Cell* 2014;6:26–41.

9. **Whiteley M, Diggle SP, Greenberg EP, Wilson EO**. Bacterial quorum sensing: the progress and promise of an emerging research area. *Nature* 2017;551:313–320.

10. **Azimi S, Klementiev AD, Whiteley M, Diggle SP**. Bacterial Quorum Sensing during Infection. *Annu Rev Microbiol* 2020;74:201–219.

11. **Wagner VE, Bushnell D, Passador L, Brooks AI, Iglewski BH**. Microarray analysis of Pseudomonas aeruginosa quorum-sensing regulons: Effects of growth phase and environment. *J Bacteriol* 2003;185:2080–2095.

12. **Schuster M, Lostroh CP, Ogi T, Greenberg EP**. Identification, timing, and signal specificity of Pseudomonas aeruginosa quorum-controlled genes: A transcriptome analysis. *J Bacteriol* 2003;185:2066–2079.

13. **Fuqua WC, Winans SC, Greenberg EP**. Quorum sensing in bacteria: The LuxR-LuxI family of cell density- responsive transcriptional regulators. *J Bacteriol* 1994;176:269–275.

14. **Ding F, Oinuma KI, Smalley NE, Schaefer AL, Hamwy O, *et al.*** The Pseudomonas aeruginosa orphan quorum sensing signal receptor QscR regulates global quorum sensing gene expression by activating a single linked operon. *mBio*;9. Epub ahead of print 2018. DOI: 10.1128/mBio.01274-18.

15. **Schuster M, Greenberg EP**. A network of networks: Quorum-sensing gene regulation in Pseudomonas aeruginosa. *International Journal of Medical Microbiology* 2006;296:73–81.

16. **Rampioni G, Bertani I, Zennaro E, Polticelli F, Venturi V, *et al.*** The quorum-sensing negative regulator RsaL of Pseudomonas aeruginosa binds to the lasI promoter. *J Bacteriol* 2006;188:815–819.

17. **Rampioni G, Schuster M, Greenberg EP, Zennaro E, Leoni L**. Contribution of the RsaL global regulator to Pseudomonas aeruginosa virulence and biofilm formation. *FEMS Microbiol Lett* 2009;301:210–217.

18. **Liang H, Deng X, Ji Q, Sun F, Shen T, *et al.*** The Pseudomonas aeruginosa global regulator VqsR directly inhibits QscR To control quorum-sensing and virulence gene expression. *J Bacteriol* 2012;194:3098–3108.

19. **Juhas M, Wiehlmann L, Huber B, Jordan D, Lauber J, *et al.*** Global regulation of quorum sensing and virulence by VqsR in Pseudomonas aeruginosa. *Microbiology (N Y)* 2004;150:831–841.

20. **Gurney J, Azimi S, Brown SP, Diggle SP**. Combinatorial quorum sensing in pseudomonas aeruginosa allows for novel cheating strategies. *Microbiology (United Kingdom)* 2020;166:777–784.

21. **Cornforth DM, Popat R, McNally L, Gurney J, Scott-Phillips TC, *et al.*** Combinatorial quorum sensing allows bacteria to resolve their social and physical environment. *Proc Natl Acad Sci U S A* 2014;111:4280–4284.

22. **Dubern JF, Diggle SP**. Quorum sensing by 2-alkyl-4-quinolones in Pseudomonas aeruginosa and other bacterial species. *Mol Biosyst* 2008;4:882–888.

23. **Heeb S, Fletcher MP, Chhabra SR, Diggle SP, Williams P, *et al.*** Quinolones: From antibiotics to autoinducers. *FEMS Microbiol Rev* 2011;35:247–274.

24. **Gambello MJ, Iglewski BH**. Cloning and characterization of the Pseudomonas aeruginosa lasR gene, a transcriptional activator of elastase expression. *J Bacteriol* 1991;173:3000–3009.

25. **Kostylev M, Kim DY, Smalley NE, Salukhe I, Peter Greenberg E, *et al.*** Evolution of the Pseudomonas aeruginosa quorum-sensing hierarchy. *Proc Natl Acad Sci U S A* 2019;116:7027–7032.

26. **Feltner JB, Wolter DJ, Pope CE, Groleau M, Smalley NE, *et al.*** LasR Variant Cystic Fibrosis Isolates Reveal an Adaptable Quorum-. *mBio* 2016;7:e01513-16.

27. **Cruz RL, Asfahl KL, Bossche S van den, Coenye T, Crabbé A, *et al.*** RhlR-Regulated Acyl-Homoserine Lactone Quorum Sensing in a Cystic Fibrosis Isolate of Pseudomonas aeruginosa. *mBio*;11. https://doi.org/10.1128/mBio.00532-20 (2020).

28. **Thomason MK, Voichek M, Dar D, Addis V, Fitzgerald D, *et al.*** A rhli 5= UTR-derived sRNA regulates RhlR-dependent quorum sensing in Pseudomonas aeruginosa. *mBio*;10. Epub ahead of print 2019. DOI: 10.1128/mBio.02253-19.

29. **Chen R, Déziel E, Groleau MC, Schaefer AL, Greenberg EP**. Social cheating in a Pseudomonas aeruginosa quorum-sensing variant. *Proc Natl Acad Sci U S A* 2019;116:7021–7026.

30. **Groleau M, Taillefer H, Vincent AT, Constant P, Déziel E**. Pseudomonas aeruginosa isolates defective in function of the LasR quorum sensing regulator are frequent in diverse environmental niches . *Environ Microbiol* 2021;00:1–14.

31. **Oshri RD, Zrihen KS, Shner I, Omer Bendori S, Eldar A**. Selection for increased quorum-sensing cooperation in Pseudomonas aeruginosa through the shut-down of a drug resistance pump. *ISME Journal* 2018;12:2458–2469.

32. **Schweizer HP**. Efflux as a mechanism of resistance to antimicrobials in Pseudomonas aeruginosa and related bacteria: Unanswered questions. *Genetics and Molecular Research* 2003;2:48–62.

33. **Köhler T, Epp SF, Curty LK, Pechère JC**. Characterization of MexT, the regulator of the MexE-MexF-OprN multidrug efflux system of Pseudomonas aeruginosa. *J Bacteriol* 1999;181:6300–6305.

34. **Mukherjee S, Moustafa DA, Stergioula V, Smith CD, Goldberg JB, *et al.*** The PqsE and RhlR proteins are an autoinducer synthase–receptor pair that control virulence and biofilm development in Pseudomonas aeruginosa. *Proc Natl Acad Sci U S A* 2018;115:E9411–E9418.

35. **Farrow JM, Sund ZM, Ellison ML, Wade DS, Coleman JP, *et al.*** PqsE functions independently of PqsR-Pseudomonas quinolone signal and enhances the rhl quorum-sensing system. *J Bacteriol* 2008;190:7043–7051.

36. **García-Reyes S, Cocotl-Yañez M, Soto-Aceves MP, González-Valdez A, Servín-González L, *et al.*** PqsR-independent quorum-sensing response of Pseudomonas aeruginosa ATCC 9027 outlier-strain reveals new insights on the PqsE effect on RhlR activity. *Mol Microbiol* 2021;1113–1123.

37. **Freschi L, Vincent AT, Jeukens J, Emond-Rheault JG, Kukavica-Ibrulj I, *et al.*** The Pseudomonas aeruginosa Pan-Genome Provides New Insights on Its Population Structure, Horizontal Gene Transfer, and Pathogenicity. *Genome Biol Evol* 2019;11:109–120.

38. **Asfahl KL, Walsh J, Gilbert K, Schuster M**. Non-social adaptation defers a tragedy of the commons in Pseudomonas aeruginosa quorum sensing. *ISME Journal* 2015;9:1734–1746.

39. **Smalley NE, Schaefer AL, Asfahl KL, Perez C, Greenberg EP, *et al.*** Evolution of the Quorum Sensing Regulon in Cooperating Populations of Pseudomonas aeruginosa. *mBio* 2022;13:1–19.

40. **Altschul SF, Gish W, Miller W, Myers EW, Lipman DJ**. Basic local alignment search tool. *J Mol Biol* 1990;215:403–410.

41. **Henikoff S, Henikoff JG**. Amino acid substitution matrices from protein blocks. *Proc Natl Acad Sci U S A* 1992;89:10915–10919.

42. **Stanton RA, Vlachos N, Halpin AL**. GAMMA: a tool for the rapid identification, classification and annotation of translated gene matches from sequencing data. *Bioinformatics* 2021;1–3.

43. **Team Rs**. RStudio: Integrated Development Environment for R.

44. **Martin DW, Schurr MJ, Mudd MH, Govan JRW, Holloway BW, *et al.*** Mechanism of conversion to mucoidy in Pseudomonas aeruginosa infecting cystic fibrosis patients. *Proc Natl Acad Sci U S A* 1993;90:8377–8381.

45. **Deretic V, Martin DW, Schurr MJ, Mudd MH, Hibler NS, *et al.*** Conversion to mucoidy in Pseudomonas aeruginosa. *Bio/Technology* 1993;11:1133–1136.

46. **Weir TL, Stull VJ, Badri D, Trunck LA, Schweizer HP, *et al.*** Global gene expression profiles suggest an important role for nutrient acquisition in early pathogenesis in a plant model of Pseudomonas aeruginosa infection. *Appl Environ Microbiol* 2008;74:5784–5791.

47. **Dumas JL, van Delden C, Perron K, Köhler T**. Analysis of antibiotic resistance gene expression in Pseudomonas aeruginosa by quantitative real-time-PCR. *FEMS Microbiol Lett* 2006;254:217–225.

48. **D'Argenio DA, Wu M, Hoffman LR, Kulasekara HD, Déziel E, *et al.*** Growth phenotypes of Pseudomonas aeruginosa lasR mutants adapted to the airways of cystic fibrosis patients. *Mol Microbiol* 2007;64:512–533.

49. **D'Argenio DA, Calfee MW, Rainey PB, Pesci EC**. Autolysis and autoaggregation in Pseudomonas aeruginosa colony morphology mutants. *J Bacteriol* 2002;184:6481–6489.

50. **Déziel E, Lépine F, Milot S, He J, Mindrinos MN, *et al.*** Analysis of Pseudomonas aeruginosa 4-hydroxy-2-alkylquinolines (HAQs) reveals a role for 4-hydroxy-2-heptylquinoline in cell-to-cell communication. *Proc Natl Acad Sci U S A* 2004;101:1339–1344.

51. **Hazan R, Que YA, Maura D, Strobel B, Majcherczyk PA, *et al.*** Auto Poisoning of the Respiratory Chain by a Quorum-Sensing-Regulated Molecule Favors Biofilm Formation and Antibiotic Tolerance. *Current Biology* 2016;26:195–206.

52. **Marie-Christine Groleaua, Hélène Taillefera, Antony T. Vincentb PC and ED**. Pseudomonas aeruginosa isolates defective in function of the LasR quorum sensing regulator are frequent in diverse environmental niches. *bioRxiv*. Epub ahead of print 2021. DOI: https://doi.org/10.1101/2021.03.25.437011.

53. **de Kievit T, Seed PC, Nezezon J, Passador L, Iglewski BH**. RsaL, a novel repressor of virulence gene expression in Pseudomonas aeruginosa. *J Bacteriol* 1999;181:2175–2184.

54. **Rampioni G, Schuster M, Greenberg EP, Bertani I, Grasso M, *et al.*** RsaL provides quorum sensing homeostasis and functions as a global regulator of gene expression in Pseudomonas aeruginosa. *Mol Microbiol* 2007;66:1557–1565.

55. **Mould DL, Botelho NJ, Hogan DA**. Intraspecies signaling between common variants of pseudomonas aeruginosa increases production of quorum-sensing-controlled virulence factors. *mBio* 2020;11:1–16.

56. **Rumbaugh KP, Diggle SP, Watters CM, Ross-Gillespie A, Griffin AS, *et al.*** Quorum Sensing and the Social Evolution of Bacterial Virulence. *Current Biology* 2009;19:341–345.

57. **Azimi S, Roberts AEL, Peng S, Weitz JS, McNally A, *et al.*** Allelic polymorphism shapes community function in evolving Pseudomonas aeruginosa populations. *ISME Journal* 2020;14:1929–1942.

58. **Eldar A**. Social conflict drives the evolutionary divergence of quorum sensing. *Proc Natl Acad Sci U S A* 2011;108:13635–13640.

59. **LoVullo ED, Schweizer HP**. Pseudomonas aeruginosa mexT is an indicator of PAO1 strain integrity. *J Med Microbiol* 2020;69:139–145.

60. **Sandoz KM, Mitzimberg SM, Schuster M**. Social cheating in Pseudomonas aeruginosa quorum sensing. *Proc Natl Acad Sci U S A* 2007;104:15876–15881.

61. **Winsor GL, Griffiths EJ, Lo R, Dhillon BK, Shay JA, *et al.*** Enhanced annotations and features for comparing thousands of Pseudomonasgenomes in the Pseudomonas genome database. *Nucleic Acids Res* 2016;44:D646–D653.

62. **Heberle H, Meirelles VG, da Silva FR, Telles GP, Minghim R**. InteractiVenn: A web-based tool for the analysis of sets through Venn diagrams. *BMC Bioinformatics* 2015;16:1–7.

63. **Pagès H, Aboyoun P, Gentleman R DS**. Biostrings: Efficient manipulation of biological strings.

Chapter 3: A 'Goldilocks Zone' governs cooperation and cheating dynamics in *Pseudomonas aeruginosa* aggregates

Kathleen A O'Connor, Ryan Lowhorn, Samuel Brown, Stephen P. Diggle

3.1 Abstract

Bacterial pathogens use social behaviors to cooperate and modify their host environments. *Pseudomonas aeruginosa* is an opportunistic pathogen that uses chemical communication, termed quorum sensing, to regulate the expression of exoproteases necessary for living on protein food sources. The bacterium is best studied in the cystic fibrosis (CF) lung where it causes chronic infections. The CF lung is a spatially structured environment filled with extracellular DNA and mucin polymers where *P. aeruginosa* grows as free-floating multi-cellular aggregates. Despite primarily growing in spatially structured environments, bacterial social behaviors are most often studied in liquid culture or surface attached biofilms on petri plates, environments cells do not naturally encounter. Here we study social cheating in free-floating *P. aeruginosa* aggregates in liquid media with polymers, mimicking its growth in the CF lung. We manipulate the cell's surface hydrophobicity to change the proximity between cheater cells and cooperator cells. Cooperation appears to happen at close and intermediate distances, while cooperator-produced spite has less of an effect on cheaters when they're further apart. We found that cheaters best benefitted from cooperative behavior when they were an intermediate distance from cooperators, something we term the "goldilocks zone," where cells are close enough for cooperation but too far apart for spite.

We find that cell surface hydrophobicity, spiteful behaviors, and cell-to-cell proximity affect spatial and social dynamics in *P. aeruginosa* aggregates.

3.2 Introduction

The evolution of social traits and cooperative behaviors has puzzled researchers for decades. The evolution of cooperation is essential for the survival of many species in the face of biotic and abiotic stressors on Earth. However, once cooperation evolves, the evolution of non-cooperative 'cheating' individuals should in theory overwhelm the population and lead to the extinction of cooperative behaviors. In bacteria, cooperators contribute to publicly available common goods, frequently referred to as "public goods" [1]. These public goods are essential for the proliferation of a species when food is scarce or predators are present. Cheaters are individual cells which inherit mutations, eliminating or reducing social behaviors. These mutations free them from the biological requirement to cooperate, allowing them to divert resources to rapid reproduction, thereby increasing their fitness. Here, fitness refers to an individual's ability to produce offspring at a higher rate compared to non-relatives [2, 3]. The proliferation of cheaters floods the gene pool with the heritable non-cooperative trait, leading to the loss of cooperation - or so it is hypothesized. In practice, we see many cooperative traits maintained in animals and bacteria despite the spontaneous evolution of cheater individuals. How is this cooperation maintained?

In the animal kingdom, social individuals can selectively interact and benefit other known cooperators [4, 5]. Bacteria are less complex and unconscious single celled organisms, but they too must exclude cheater individuals to selectively benefit cooperators. Previous research has

shown that introducing spatial structure to bacterial populations maintains cooperation and decreases the fitness of cheaters via a process termed kin selection [6, 7]. It is hypothesized that this is because cheater and cooperator cells are father apart, growing in separate pockets of a spatially structured environment. However, the distance required to protect cooperators from the invasion of cheaters has not previously been defined.

A model system for studying these complex behaviors is *Pseudomonas aeruginosa,* an opportunistic pathogen with numerous social behaviors [8]. *P. aeruginosa* uses chemical signals to communicate via a process termed quorum sensing (QS), and excretes QS-dependent social products including exoproteases which break down large proteins, enabling close neighbors to also benefit [9–14]. Social behaviors in this bacterium have primarily been studied in liquid, well-mixed cultures where cheaters and cooperators both have unfettered access to public goods [15–19]. When cells are instead grown in solid medium, the fitness of cooperators decreases, theoretically due to an increased distance between cooperator-produced public goods and cheater cells [6, 7]. It is often assumed that cheaters will be most fit when closest to cooperators.

The field has investigated the effects of proximity on cooperation primarily using surface attached biofilms[20, 21]. Here, we explore free-growing, non-surface attached aggregates in liquid media with polymers, mimicking how cells grow in cystic fibrosis (CF) lung infections [22–29]. We recently discovered a role for the Δ*ssg* gene, a putative glycosyl transferase that leads to a hydrophobic cell surface when mutated, and novel aggregate formation [27, 30]. We saw this recent discovery as an opportunity to grow mixed cultures of *P. aeruginosa* where their cell surface hydrophobicity, rather than an abiotic solidifying agent, would determine the proximity between

cells. When grown together, hydrophilic wildtype *P. aeruginosa* and hydrophobic Δ*ssg* cells mix similarly to oil and water, forming distinct aggregates assorted by cell surface hydrophobicity. The difference in distance between cells with the same or different cell surfaces is minute – on the micron scale rather than the millimeters apart cells might be when grown as colonies on an agar plate. Bacteria are such small organisms that it is essential we study distance on the micron- rather than milli- or decimeter scale.

To study the importance of proximity on cooperation and a cell's ability to cheat, we worked with the cooperative trait QS, regulated by the *las* and *rhl* QS systems [31, 32]. Δ*lasR*Δ*rhlR* cells are unable to secrete extracellular exoproteases. As a result, they are unable to grow on protein food sources [15, 33]. Δ*lasR*Δ*rhlR* cells act as cheaters when grown on protein and are only able to grow in the presence of wildtype cooperator cells or externally supplied public goods. In addition to studying the effects of proximity and cell surface hydrophobicity on cheater fitness, we also wanted to see the impact cooperator-produced spite molecules had on cheater cells. While cooperation benefits the producer and receiver, spite harms both producer and receiver.

Through our experiments, we show the most fit cheaters are hydrophilic cheaters mixed with hydrophobic cooperators. We initially hypothesized that cheaters would need to share a cell surface hydrophobicity charge to cheat on cooperators, assuming that close proximity was required to share public goods. We found an intermediate distance between cheaters and cooperators resulted to the highest fitness for cheaters. We termed this the "goldilocks zone" where cheaters thrive at an intermediate distance from cooperators. Cooperation and spite appear to diffuse on different scales, and when cooperators lose spite, it has the biggest effect on closely aggregating cells. In

the rare case that cells are an intermediate distance apart, as is the case for hydrophobic cooperators and hydrophilic cheaters, cheaters are close enough to experience cooperation but too far apart to experience spite.

3.3 Materials and Methods

Experimental Conditions

We previously published that cell surface hydrophobicity dictates how *P. aeruginosa* cells aggregate when grown in liquid media with polymers. At the time we used SCFM2, a media with mucin and eDNA to mimic the environment of the CF lung. To simplify the design of our experiments, and to allow us to test social cheating in a spatially structured environment, we grew cells with eDNA as a polymer in a salt- and metal-based medium created as a hybrid between M9 salts and the metal components of OS medium, which we call "M9-metals". We added 1% BSA, a protein food source which requires cells to excrete QS-regulated exoproteases to grow; we additionally added 0.05% casamino acids (CAA) so the cells could grow to a high enough density to activate QS. We have termed M9-metals 1% BSA 0.05% CAA with 0.6 mg/mL eDNA as quorum sensing medium #2 (QSM2).

Experimental Setup and Growth Conditions for Imaging

We performed all experiments in biological triplicate. Cheater cells were labeled with mCherry and a Tn7-Trimethoprim (Tn7-Tp) resistance marker, and cooperator cells were labeled with GFP. We inoculated 5mL of LB broth 200 μg/mL Tetracycline in 50 mL conical tubes with fluorescently labeled cells. We grew cells shaking 200 rpm at 37C for 18 hours. We washed 1 mL of overnight

culture twice with PBS, vortexing the cells vigorously between each step throughout the remaining protocol. We diluted cells 1-in-10 in PBS after washing and measured the optical density at 600 nm. We prepared the structured media by mixing filter sterilized media with sterilized eDNA. We aliquoted 600 µL pre-mixed QSM2 media into 1.5 mL Eppendorf tubes, and aliquoted cells to a starting OD of 0.01. We then aliquoted 400 µL of each inoculum into 8-well confocal slides, and grew cells 22 hours before imaging and plating.

Cheater Fitness Quantification

After aliquoting 400 µL sample into confocal wells, we pipetted 20 µL sample into 96-well plates. Using PBS, we diluted the cells to 10^{-4} for t=0 plating. We spread plated 50 µL cells onto LB agar (LBA) and LBA-Trimethoprim (LBA-Tp) 500 µg/mL for total and cheater cell counts, respectively. We grew LBA plates 24 hours at 37C and LBA-Tp plates for 48 hours at 37C before counting. After imaging, we aliquoted all 400 µL sample into 2 mL screw cap sterilized tubes filled with 5 (*insert correct size*) mm metal balls. Using a micropipette, we washed confocal wells twice with 400 µL PBS and added wash to tubes. We bead-beated sample and washed diluent using a vortex at max speed for 45 seconds. We aliquoted 100 µL of diluted, bead-beated cells to a 96-well plate and measured the optical density using a plate reader (*model here*). For plating, we aliquoted 60 µL cells into 140 µL PBS in a 96-well plate, to account for the 3-fold PBS wash dilution. We diluted cells to 10^{-6} and spread plated 50 µL diluted cells on LB and LBA-Tp plates, and grew them at 37C.

Strain growth in QSM2

We grew PAO1 GFP, Δ*ssg* GFP, Δ*lasR*Δ*rhlR* mCherry Tn7-Tp, Δ*lasR*Δ*rhlR*Δ*ssg* mCherry Tn7-Tp in biological triplicate in LB broth 200 µg/mL Tetracycline overnight. We washed cells as described above, and aliquoted cells into 96-well plates with 100 µL QSM2. We grew cells stationary at 37C for 24 hours and then read the optical density 600 nm in a plate reader. We additionally created a Proteinase K (PK) titration by diluting PK 2-fold in wells from 2 µg/mL to 0.0625 µg/mL. For spatial structure quantification, we prepared cells in confocal wells as described in above and imaged the cells after 22 hours of growth.

Confocal Imaging

All images were taken on a Zeiss Airyscan 880 set to Zoom 1 for images that measure 134.95 µm x 134.95 µm. After growing cells for 22 hours, we imaged cells using an 63x oil-immersion lens. We took two 10 µm thick Z-stack images for each biological replicate. We adjusted laser strength and gain as needed for best imaging, as it was important to quantify location but not the brightness of cells. We saved all images as czi files.

Image Analysis: Fuji & MicrobeJ

First, we generated the x, y, and z position for each green and red cell using the Batch feature of MicrobeJ in Fiji (ImageJ 2). We used the following settings: under Experiment: "MultiThreading"; under Bacteria: "Channel 1", "Dark", and "Auto"; under Morphology: "Morphology 1 [Medial Axis]"; under Attributes: "Circularity: [0-max]"; under options: "Exclude on Edges" and "Segmentation." We then repeated the same analysis for Channel 2. We saved the generated data as csv files.

Image Analysis: R Studio & Spatstat

Code is available on our Github. We loaded Spatstat in R studio and read in csv files for the red and green channels. We created an empty matrix with the dimensions of our image file (134.95 x 134.95 x 10 μm^3) and saved it as "bb". Using a loop function, we found the nearest neighbor distance for cells of the same or opposite color using the "nndist" and "nncross" commands. We then found the mean nearest neighbor and cross neighbor distances for each image, and output that image as a csv. To calculate distance ratio we divided the average distance between green and red cells, by the average distance from one red cell to another. We graphed data using ggplot2 in R studio.

3.4 Results

Figure 1. We grew monocultures of PAO1 GFP, PAO1 mCherry, Δssg GFP, and Δssg mCherry and mixed them 50:50 in QSM2. We grew mixes of hydrophilic cells (PAO1 GFP 50:50 PAO1 mCherry; PAO1 mix), mixes of hydrophobic cells (Δssg GFP 50:50 Δssg mCherry; Δssg mix), and a mix of hydrophobic and hydrophilic cells (PAO1 GFP 50:50 Δssg mCherry). Cultures were inoculated into QSM2 at an OD of 0.01 and grew approximately 100-fold. We used a confocal microscope to take 10 μm thick Z-stack images, and assigned an X, Y, and Z location for each red and green cell. We then used Spatstat to find the nearest neighbor of each green cell to the nearest red cell and the nearest neighbor of each red cell from other red cells. We found the mean of the nearest neighbor distance and divided the mean nearest neighbor of red to green cell by the mean nearest neighbor distance of red to red cell – this became the "Mean Cross Distance Ratio." We observed that the hydrophilic mix had the lowest mean cross distance ratio, with red and green cells clustering close together and forming mixed aggregates. The hydrophobic mix was not significantly different from the hydrophilic mix. The mix of hydrophobic and hydrophilic cells was significantly larger than the hydrophilic mix, indicating that green and red cells of different cell surfaces were more separate.

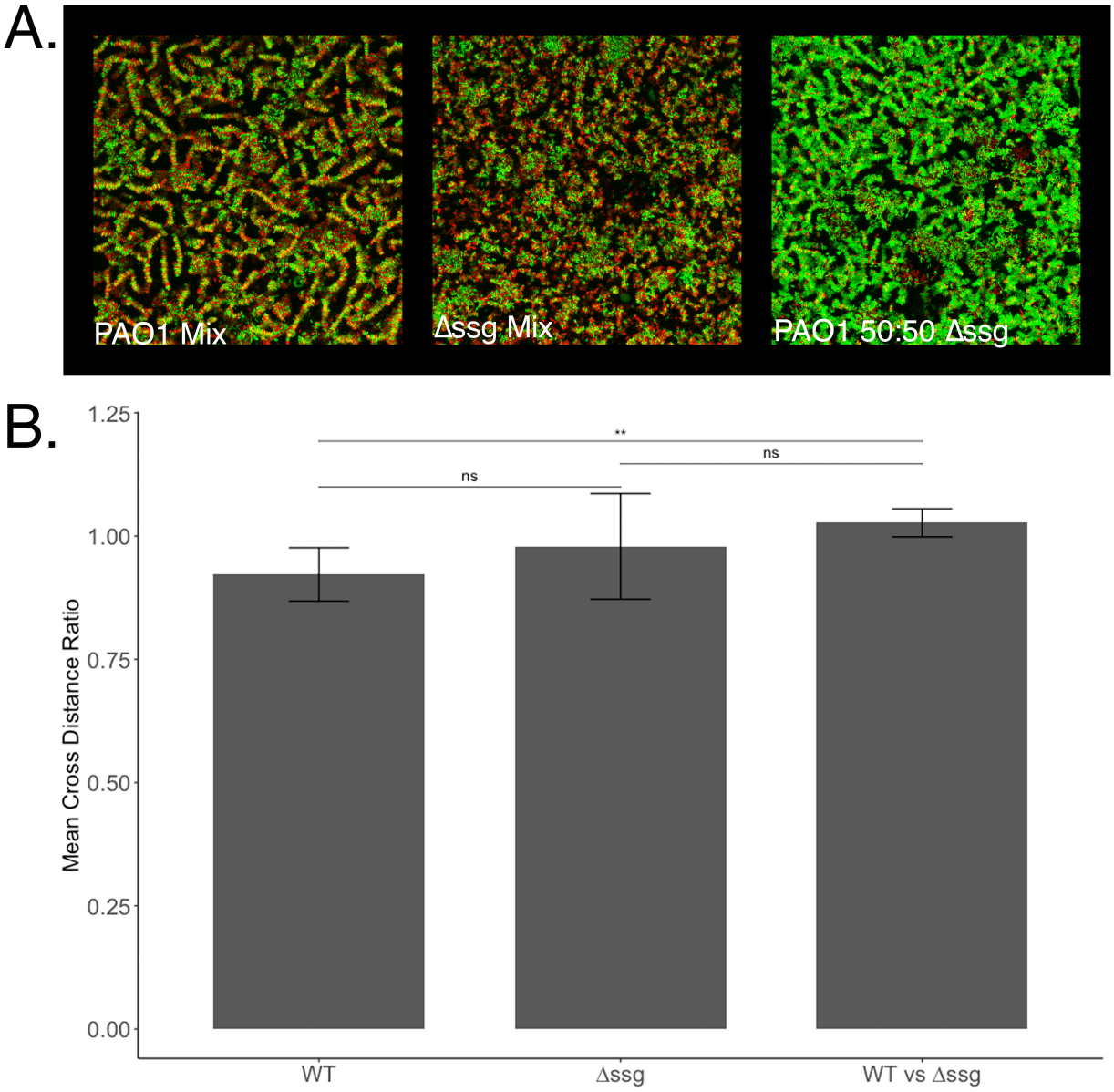

***P. aeruginosa* cells aggregate based on cell surface hydrophobicity charge.** We first grew liquid monocultures of mCherry labeled Δ*ssg*, GFP labeled Δ*ssg*, mCherry labeled PAO1 and GFP labeled PAO1, before mixing them at 50:50 ratio in QSM2, with a starting OD_{600} of 0.005 for each strain. We grew mixes of hydrophilic cells: PAO1 mCherry/PAO1 GFP, mixes of hydrophobic cells: Δ*ssg* mCherry/Δ*ssg* GFP, and a mix of hydrophilic and hydrophobic cells: PAO1 GFP/Δ*ssg*

mCherry (**Fig. 1A**). The distance ratio between green and red cells when PAO1 is mixed with itself was the smallest at 0.92 (**Fig. 1B**). When Δ*ssg* is mixed with itself, we found that cells were slightly further apart although not significantly so (**Fig. 1B**; ratio = 0.98 , p-adj > 0.05). We found that cells were significantly further apart when we mixed hydrophobic and hydrophilic cells with a ratio of 1.03 (**Fig. 1B**; p-adj compared to PAO1 mix = 0.009).

Hydrophilic cells are fitter than hydrophobic cells when mixed. While imaging, we observed that the hydrophilic/hydrophobic mixed cultures appeared to have more PAO1 growth than Δ*ssg* (**Fig 1A)**. Before mixing cells to test for cheating, we wanted to determine whether Δ*ssg* and PAO1 had the same fitness when mixed. We therefore tested invasion of Δ*ssg* into a PAO1-dominated culture or PAO1 into Δ*ssg*-dominated cultures. We also wanted to ensure that GFP labeled cells were not inherently fitter than mCherry labeled cells. We labeled Δ*ssg* with GFP and a Tn7-Gentamycin (Tn7-Gm) resistance marker, and PAO1 with mCherry and a Tn7-Tp marker. We mixed the cells 1:100, 1:10, 50:50, 100:1, 10:1 (Δ*ssg* GFP: PAO1 mCherry) in QSM2 and plated to t=0, t=22 hours and imaged cells (**Fig. 2A**). We found that PAO1 cells were fitter than Δ*ssg* when mixed and at all ratios, PAO1 was able to increase in frequency against Δ*ssg* (p=0.003, **Table 1**)*,* while Δ*ssg* was unable to increase in frequency against PAO1 (**Fig. 2B,** p=0.002, **Table 1**).

Figure 2. When we grew mixes of hydrophobic and hydrophilic cells (Fig 1A), we noted that we saw fewer hydrophobic cells at the imaging time point. Before beginning cheating experiments, we wanted to determine if there was an inherent fitness benefit for hydrophilic cells. We used PAO1 mCherry with a Tn7-Tp resistance marker and Δ*ssg* GFP with a Tn7-Gm resistance marker to track invasion of hydrophilic cells into hydrophobic populations or vice versa. We mixed cells (PAO1 : Δssg) 100:1, 10:1, 50:50, 1:10, 1:100 at a starting OD of 0.01 and allowed them grow 100-fold before imaging. We plated cells directly after inoculation and 22 hours later, after imaging and physically disrupting aggregates with bead beating on LBA to get total population counts, on LBA Tp500 to get PAO1 counts, and on LBA Gm200 to get Δ*ssg* counts. We found that PAO1 invaded Δssg populations in a frequency dependent manner, and had the highest fitness against Δssg at low starting frequencies. Δssg was unable to invade PAO1 populations at any starting frequency. We additionally tested invasion of PAO1 mCherry Tn7-Tp into Δ*wbpL* GFP

populations, an B-band mutant that forms similar aggregates to Δssg. We found that similarly to its invasion into Δssg, PAO1 had a frequency dependent fitness benefit against Δ*wbpL*, although it was less fit than when it competed against Δ*ssg*.

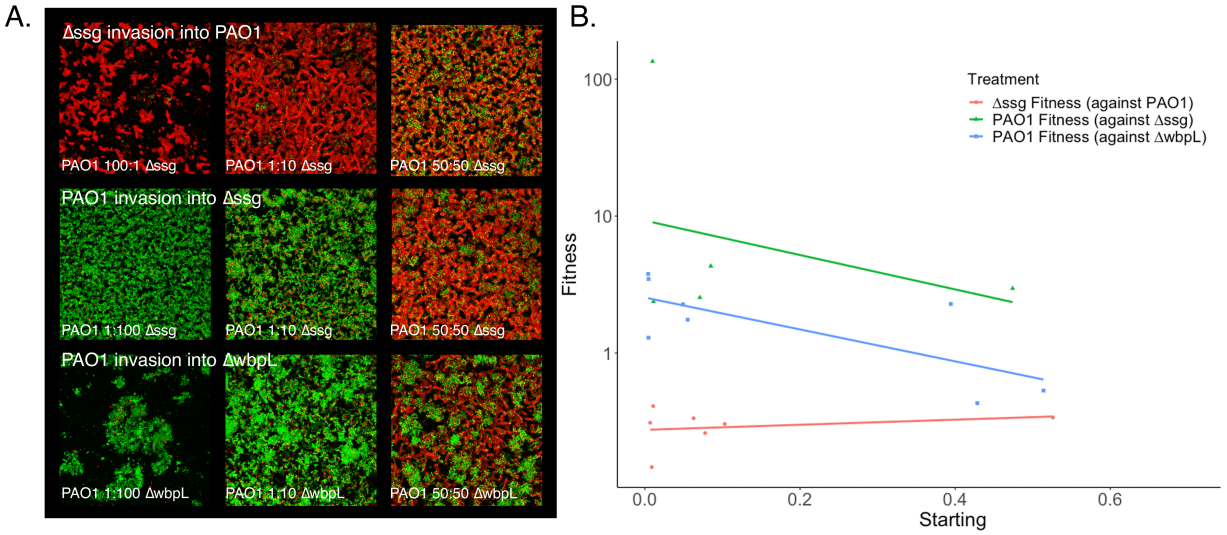

The estimated marginal means represents the average fitness, after accounting for other factors in the model. A value greater than 1 indicates a fitness advantage, while a value less than 1 indicates a fitness disadvantage. The confidence intervals provide a range within which the true mean fitness likely falls. If the entire confidence interval is above or below 1, it provides evidence of a significant fitness advantage or disadvantage, respectively.

Table 1: Estimated Marginal Means

Treatment	Estimated Mean	Standard Error	Lower 95% CI	Upper 95% CI	Degrees of Freedom	t-ratio	p-value
Δssg Fitness (against PAO1)	−0.925	0.241	−1.442	−0.407	14.000	−3.834	0.002
PAO1 Fitness (against Δssg)	1.032	0.282	0.428	1.636	14.000	3.662	0.003
PAO1 Fitness (against ΔwbpL)	0.218	0.225	−0.265	0.702	14.000	0.967	0.350

The role Δssg plays in cell surface hydrophobicity is a recent finding, and the gene has few publications detailing its physiological effects. To confirm that hydrophobic cells are less fit than

hydrophilic cells, we wanted to repeat our invasion experiment with a better studied mutant: Δ*wbpL*. We mixed mCherry labeled and Tn7-Tp marked PAO1 with GFP labeled Δ*wbpL* at a ratio of 1:100, 1:10, and 50:50 (**Fig. 2A**). We found that similarly to competition with Δ*ssg*, PAO1 was able to increase in abundance at low starting frequencies. While overall PAO1 is appears to be less fit against Δ*wbpL* than against Δ*ssg,* the finding is not significant ($p > 0.05$, **Table 1, Fig. 2B**).

Cheater cells grow poorly in QSM2. Before beginning cheating experiments, we wanted to ensure differential growth between cooperators and cheaters. We also wanted to ensure that when public goods (proteinase) were substituted in the media, the cheater growth defect would be alleviated. We found that in QSM2, PAO1 and Δ*ssg* grew significantly better than the cheaters in mono-culture (**Fig. 3**; PAO1 vs Δ*lasR*Δ*rhlR* p = .038; Δ*ssg* vs Δ*lasR*Δ*rhlR*Δ*ssg* p = 6.64e-4). When we titrated in public goods (Proteinase K; which degrades the BSA protein in QSM2), we found that Δ*lasR*Δ*rhlR* and Δ*lasR*Δ*rhlR*Δ*ssg* growth improved in a dose-dependent manner (**Fig. 3B.** We additionally imaged the four strains in QSM2 and found that Δ*lasR*Δ*rhlR* did not form stacking structures the way PAO1 does, and Δ*lasR*Δ*rhlR*Δ*ssg* forms clumping aggregates that look different than Δ*ssg* (**Fig. 3A**).

Figure 3. We tested the growth of cooperator (PAO1 GFP, Δ*ssg* GFP) and cheater strains (Δ*lasR*Δr*hlR* mCherry, Δ*lasR*Δ*rhlR*Δ*ssg* mCherry) in QSM2, our cheating medium. We found that cooperator strains grew significantly better than cheater strains. We additionally tested the impact of added public goods (proteinase K, which breaks down protein) on cheater growth. We titrated in proteinase K and found that it improved the growth of both cheaters. Although even at 2 μg/mL of proteainse K, the cheaters grow more poorly than cooperators.

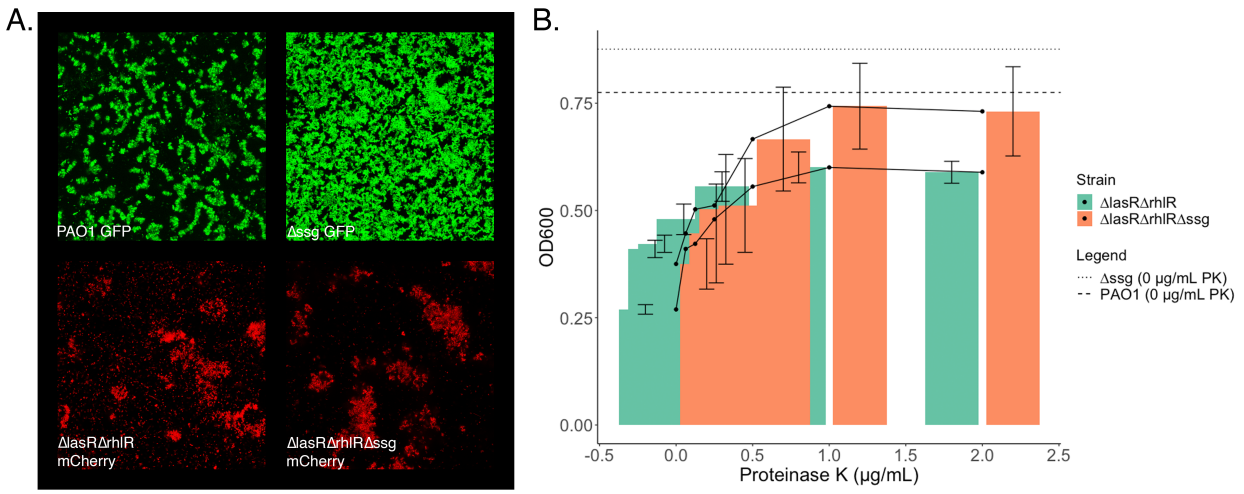

Fitness of Hydrophilic and Hydrophobic Cheater Cells.

We mixed cheater cells with cooperators at a ratio of 100:1, 10:1, and 50:50 (cooperator : cheater) in spatially structured media. We grew cells for 22 hours and then took Z-stack images on the confocal and plated for cheater fitness. We found that when we mixed cells of the same surface - PAO1 with Δ*lasR*Δ*rhlR* or Δ*ssg* with Δ*lasR*Δ*rhlR*Δ*ssg* – cheaters trended towards a frequency dependent fitness benefit at low starting frequencies, although the frequency dependent fitness benefit was only significant for PAO1 vs Δ*lasR*Δ*rhlR* ($p = 0.012$, **Fig. 4A, Table 2**). We then mixed cells with different cells surfaces together, anticipating that cells would be too distant from one another to cheat. We found that unlike when cells of the same surface were mixed, Δ*lasR*Δ*rhlR*Δ*ssg* were unable to cheat on PAO1 at any starting frequency ($p<0.001$, **Fig. 4A, Table 2**). We repeated the experiment with Δ*lasR*Δ*rhlR* cheaters with Δ*ssg* cooperators. We surprisingly found that Δ*lasR*Δ*rhlR* cells cheated on Δ*ssg* in a frequency-dependent manner, with cheaters having the highest fitness of any of the cheat-cooperator combinations (**Fig. 4A, Table 3**).

Figure 4. We tested 4 combinations of cooperators and cheats in QSM2, imaged cells after 22 hours of growth, and plated for cell counts at t=0 and t=22 hrs. We calculated the fitness of cheaters using the starting and end frequencies of cheaters, and plotted it against starting frequency of cheats. We

found that the hydrophilic-hydrophilic mix and the hydrophobic-hydrophobic mix of cooperators and cheaters resulted in a frequency dependent fitness benefit for cheaters. Cheaters were most fit at low starting frequencies. Δ*lasR*Δ*rhlR*Δ*ssg* cells cheated poorly against PAO1 as evidenced by the images – there are few red cheater cells – and by cheater fitness. Δ*lasR*Δ*rhlR* cheaters had high fitness against Δ*ssg*, despite having different cell surfaces. Cells of the same surface have low mean cross distance ratio, while cells with different cell surfaces have less mixing between green and red cells. Δ*lasR*Δ*rhlR*Δ*ssg* cells were very far away from PAO1 cooperators. Δ*lasR*Δ*rhlR* cells were an intermediate distance from PAO1; they had the greatest fitness so we suspected an intermediate distance is important for cheater fitness.

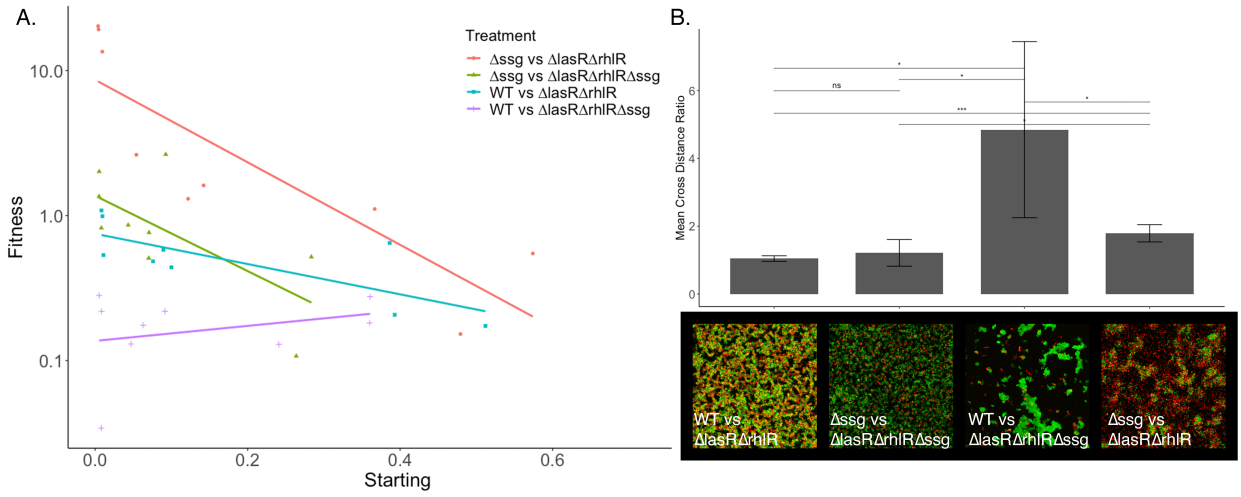

Table 2: Linear Regression Coefficients (Sum Contrasts) (Table Cont. on Page 94)

Variable	Coefficient	Standard Error	t-value	p-value
(Intercept)	0.326	0.128	2.548	0.017
Starting	−2.391	0.651	−3.675	< 0.001
Δssg vs ΔlasRΔrhlRΔssg	0.778	0.218	3.566	0.001
PAO1 vs ΔlasRΔrhlR	0.774	0.222	3.484	0.002
PAO1 vs ΔlasRΔrhlRΔssg	0.024	0.224	0.108	0.915
Starting: Δssg vs ΔlasRΔrhlRΔssg	0.772	0.809	0.955	0.348
Starting: PAO1 vs ΔlasRΔrhlR	−3.961	1.471	−2.693	0.012
Starting: PAO1 vs ΔlasRΔrhlRΔssg	−0.049	0.968	−0.050	0.960

Table 2: Linear Regression Coefficients (Sum Contrasts) (Table Cont. on Page 94)

Distance Between Hydrophobic and Hydrophilic Cells Varies.

We were surprised to find that Δ*lasR*Δ*rhlR* cells were fitter against Δ*ssg* than PAO1, despite having a different cell surface. We therefore wanted to quantify the distance between cells to understand why there were fitness differences. Using confocal microscopy, we imaged 50:50 mixed cultures of cooperators and cheats and determined the average distance of cheater cells to cooperator cells relative to how close they are to one another. For Δ*lasR*Δ*rhlR* and PAO1, the hydrophilic mix, we found a ratio of 1.04 μm (**Fig. 4B**). We determined the distance ratio for the hydrophobic mix of cheaters and cooperators: Δ*ssg* and Δ*lasR*Δ*rhlR*Δ*ssg* found a ratio of 1.21 μm (**Fig. 4B**); the distance ratio was more than the hydrophilic mix but not significantly so ($p > 0.05$). In addition to cheating poorly, Δ*lasR*Δ*rhlR*Δ*ssg* cells were very far apart from PAO1 compared to cells sharing a cell surface, with a distance ratio of 4.85 μm (**Fig. 4B**). We then mixed hydrophilic Δ*lasR*Δ*rhlR* cells with hydrophobic Δ*ssg* cooperators and found that cheaters had an intermediate distance between cooperators and cheats, with a distance ratio of 1.79 μm (**Fig. 4B**). These results could be because Δ*lasR*Δ*rhlR* cells are inherently more fit than Δ*ssg* because of their LPS structure, or it could be due to the distance between the cells. To further explore this, we reasoned that looking at spite behaviors might shed some light. Perhaps the combination of spite and cooperation has an impact on the fitness of cheaters at different distances from cooperators.

Table 3: Estimated Marginal Means

Treatment	Estimated Mean	Standard Error	Lower 95% CI	Upper 95% CI	Degrees of Freedom	t-ratio	p-value
Δssg vs ΔlasRΔrhlR	0.844	0.196	0.442	1.246	28.000	4.303	< 0.001
Δssg vs ΔlasRΔrhlRΔssg	0.078	0.226	−0.385	0.542	28.000	0.346	0.732
PAO1 vs ΔlasRΔrhlR	−0.042	0.189	−0.429	0.345	28.000	−0.223	0.825
PAO1 vs ΔlasRΔrhlRΔssg	−1.114	0.192	−1.508	−0.720	28.000	−5.793	< 0.001

Spite has a greater effect on cells sharing a cell surface.

To get a global view of possible spite behaviors, we used a cooperator with a Δ*pqsE* mutation, yielding cells that can no longer produce pyocyanin or hydrogen cyanide, two spiteful behaviors. We found that Δ*lasR*Δ*rhlR* cheater cells showed higher fitness against hydrophilic PAO1Δ*pqsE* cooperators than they did against PAO1, although fitness did not correlate with starting frequency (**Fig. 5, Table 4**).

Figure 5. After noticing that Δ*lasR*Δ*rhlR* cheated exceptionally well against Δ*ssg* despite being further apart due to their cell surfaces, we suspected that spiteful behaviors may play a role in determining cheater fitness. We tested the fitness of cheats against spite-deficient cooperators: Δ*pqsE*. In the absence of spite, Δ*lasR*Δ*rhlR* had a high mean fitness against ΔpqsE; over 5-fold higher than when cheating against spiteful PAO1 (**Table 5**).We found that Δ*lasR*Δ*rhlR* was much more fit against Δp*qsE* than against PAO1, indicating that spite was playing a role in low cheat fitness (cheating against PAO1 data was previously show in Fig 4A, p=0.007, **Table 6**). We then tested Δ*lasR*Δ*rhlR*Δ*ssg* cheating against Δ*pqsE*, in this case the cells have different cell surfaces. We saw a much smaller change where the hydrophobic cheat (less than 3-fold increase in mean fitness), likely because of its distance from the cooperator, was not as affected by the loss of spite (**Table 5**). The difference between ΔlasRΔrhlRΔssg cheating on PAO1 and ΔpqsE was not significant, indicating that spite has less of an effect on cells that are father apart (p> 0.05, **Table 6**). These findings indicated that spite happens on a small distance scale, and does not act on cells that are far from spiteful cooperators.

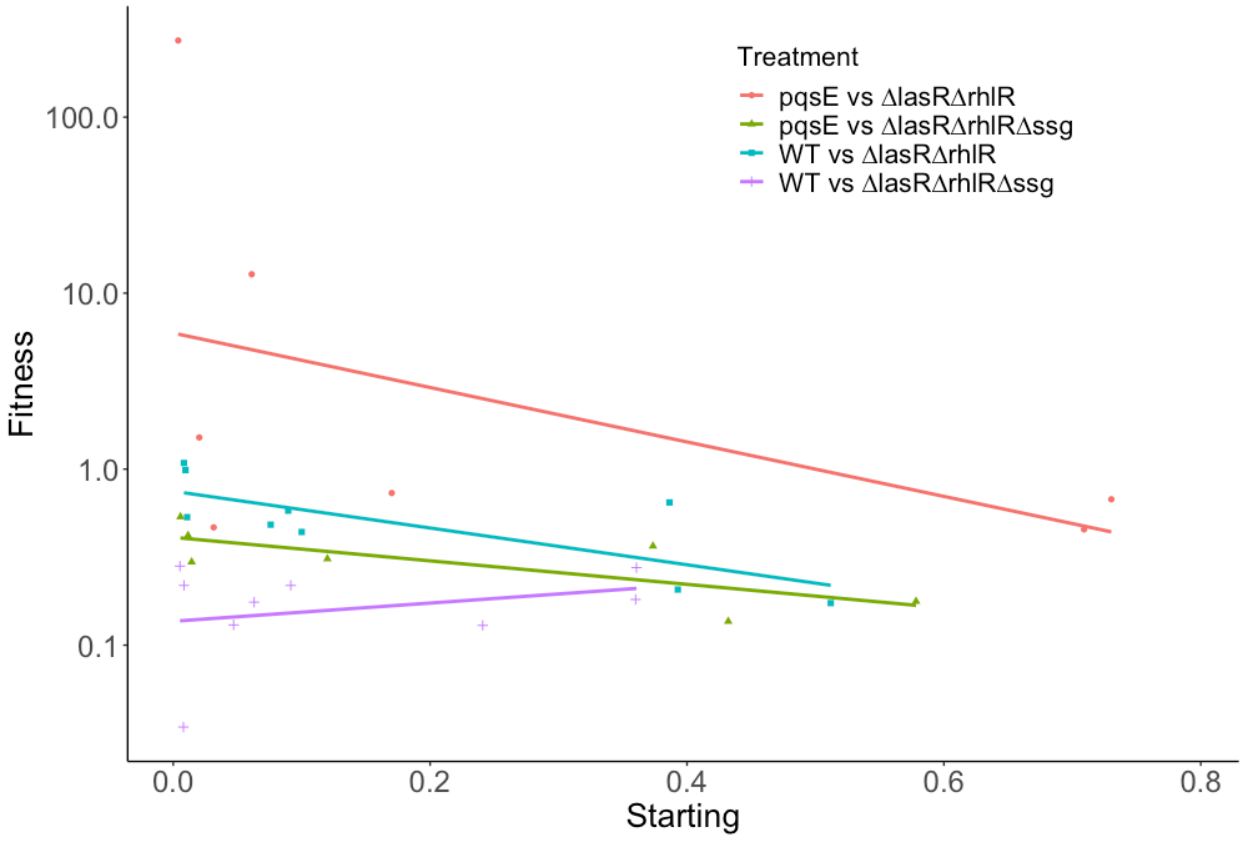

Table 4: Spiteful Cheating: Linear Regression Coefficients (Sum Contrasts) (Cont. Page 97)

Variable	Coefficient	Standard Error	t-value	p-value
(Intercept)	0.341	0.138	2.465	0.021
Starting	−1.364	0.521	−2.616	0.015
PAO1 vs ΔlasRΔrhlRΔssg	0.386	0.231	1.669	0.108
pqsE vs ΔlasRΔrhlR	−1.305	0.230	−5.663	< 0.001
pqsE vs ΔlasRΔrhlRΔssg	1.267	0.240	5.277	< 0.001
Starting: PAO1 vs ΔlasRΔrhlRΔssg	−1.347	0.891	−1.511	0.144
Starting: pqsE vs ΔlasRΔrhlR	1.983	1.092	1.816	0.082
Starting: pqsE vs ΔlasRΔrhlRΔssg	−0.428	0.724	−0.591	0.560

Table 5: Spiteful Cheating: Estimated Marginal Means

Treatment	Estimated Mean	Standard Error	Lower 95% CI	Upper 95% CI	Degrees of Freedom	t-ratio	p-value
PAO1 vs ΔlasRΔrhlR	0.216	0.190	−0.177	0.609	24.000	1.133	0.269
PAO1 vs ΔlasRΔrhlRΔssg	−0.847	0.205	−1.271	−0.424	24.000	−4.134	< 0.001
pqsE vs ΔlasRΔrhlR	1.270	0.219	0.817	1.723	24.000	5.792	< 0.001
pqsE vs ΔlasRΔrhlRΔssg	−0.303	0.217	−0.752	0.146	24.000	−1.393	0.177

In some cases cheaters had extremely high fitness against Δ*pqsE* cooperators. Δ*lasR*Δ*rhlR*Δ*ssg* aggregate far from PAO1 cells, so we hypothesized that they would not experience cooperation or spite. We hypothesized that mixing Δ*lasR*Δ*rhlR*Δ*ssg* cells with Δ*pqsE* would have little to no effect on cheater fitness. We found that Δ*lasR*Δ*rhlR*Δ*ssg* had low fitness (>1) at all starting frequencies when mixed with the non-spiteful hydrophilic cooperator ΔpqsE, however the cheater fitness was higher than when they were mixed with PAO1, and we saw a frequency dependent fitness benefit that wasn't present against PAO1 (**Fig. 5**).

Table 6: Spiteful Cheating Comparisons: Pairwise Comparisons of Estimated Marginal Means (Cont. on Page 98)

Comparison	Estimate	Standard Error	Lower 95% CI	Upper 95% CI	Degrees of Freedom	t-ratio	p-value
PAO1 vs ΔlasRΔrhlR - PAO1 vs ΔlasRΔrhlRΔssg	1.063	0.280	0.291	1.835	24.000	3.800	0.005
PAO1 vs ΔlasRΔrhlR - pqsE vs ΔlasRΔrhlR	−1.054	0.290	−1.856	−0.253	24.000	−3.631	0.007

Table 6: Spiteful Cheating Comparisons: Pairwise Comparisons of Estimated Marginal Means (Cont. on Page 98)

Comparison	Estimate	Standard Error	Lower 95% CI	Upper 95% CI	Degrees of Freedom	t-ratio	p-value
PAO1 vs ΔlasRΔrhlR - pqsE vs ΔlasRΔrhlRΔssg	0.518	0.289	−0.279	1.316	24.000	1.794	0.301
PAO1 vs ΔlasRΔrhlRΔssg - pqsE vs ΔlasRΔrhlR	−2.118	0.300	−2.946	−1.289	24.000	−7.054	< 0.001
PAO1 vs ΔlasRΔrhlRΔssg - pqsE vs ΔlasRΔrhlRΔssg	−0.545	0.299	−1.369	0.280	24.000	−1.822	0.288
pqsE vs ΔlasRΔrhlR - pqsE vs ΔlasRΔrhlRΔssg	1.573	0.309	0.721	2.425	24.000	5.093	< 0.001

3.5 Discussion

In this study, we explored the effects of proximity, cell surface hydrophobicity, and spite on cheating behaviors in mixed bacterial populations. Our investigation provides novel insights into the mechanisms underlying the dynamics of cheater fitness in spatially structured environments, shedding light on the complexities of social behaviors in bacterial aggregates.

We show that cell surface hydrophobicity charge serves as a key factor influencing the spatial distribution and fitness of bacterial cells. Cell surface hydrophobicity is determined by the lipopolysaccharide (LPS) structure of the *P. aeruginosa* cell [27]. LPS is frequently mutated when *P. aeruginosa* forms chronic infections in the CF lung [34–39]. Our lab previously published on

the effect Δ*ssg* and Δ*wbpL* mutations have on spatial structure, where cells become hydrophobic and form clumping aggregates instead of stacking aggregates [27]. When mixed together, hydrophobic and hydrophilic cells form distinct aggregates and are significantly further apart from each other than when hydrophilic cells are mixed with other like cells. We additionally find that hydrophilic cells are fitter than hydrophobic cells when they're mixed together, further underscoring the importance of cell surface properties.

Interestingly, the fitness dynamics observed in mixed populations of hydrophilic and hydrophobic cells deviated from our expectations in certain scenarios. Previous studies on spatial structure suggested that cheaters closest to cooperators would have the highest fitness, and we expected that as their mean cell-to-cell distance changed, they would have lower fitness [20, 21]. We found that when cheaters share the same surface with cooperators, they aggregate closely together and have intermediate fitness. Cheaters sharing the same surface as cooperators have a frequency-dependent fitness benefit and are only fitter than cooperators at low starting frequency. In liquid media, cells are well mixed and public goods are presumed to be freely available and widely distributed. When polymers are added, cells of the same cell surface closely intermingle in mixed aggregates. If cheater cells were indeed most fit at the closest proximity to cooperators, then we would expect high fitness for cheaters in aggregates – higher than reported in liquid media. However, we see relatively low fitness despite close-proximity, indicating that other factors beyond cooperation is at play. One factor might be that goods are more "private" when polymers are added, decreasing the fitness of even the most proximate cheats. We also suspected that cheaters with high proximity to cheaters were experiencing negative behaviors – spite produced by the cooperator.

In addition to mixing cells with the same surface, we mixed combinations of hydrophobic and hydrophilic cells to see the effects proximity had on social behaviors. When we mixed hydrophobic and hydrophilic cells for cheating experiments, we expected cheaters to have worse fitness than cells sharing the same cell surface. We instead found results were different for the two combinations of cells. First, hydrophobic cheaters have the lowest fitness against hydrophilic cooperators, and are the furthest apart. Whereas hydrophilic cheater cells exhibited unexpected fitness advantages when interacting with hydrophobic cooperators, surpassing their fitness against hydrophilic cooperators. This result could be due to the inherent fitness benefit hydrophilic cells have over hydrophobic cells, or it could be due spiteful behaviors from cooperators.

Our exploration of spiteful behaviors revealed that spite, controlled by *pqsE*, changes fitness dynamic and impacts the growth of both cheaters and cooperators [40–43]. Consistent with previous findings in liquid cultures, we show that spiteful behaviors contribute to the success of cooperator cells in spatially structured environments [42]. *pqsE* is a major regulator that has garnered recent attention in the QS field, and it regulates behaviors beyond spite. Future studies will look at individual spite behaviors such as hydrogen cyanide or pyocyanin production on the effects of cheater fitness in spatial structure. We show that when cells share the same cell surface, the loss of spite has a large effect on the fitness of cheaters. However, when cells have different cell surfaces, and accordingly are further apart, spite has less of an impact on cheater fitness. This led us to conclude that spite happens on a small distance scale than cooperation, resulting in a "goldilocks zone" where cheaters are exposed to cooperation but not spite. We illustrate this in **Fig. 6**, where cells are fittest in an intermediate zone where they experience cooperation but not spite.

Figure 6. Here we present a schematic of the "goldilocks zone" hypothesis we explore in this paper. We propose that cooperation works on a close and intermediate distance scale, providing public benefit to cheaters that are nearby cooperators. However, at a close distance, cheaters are also exposed to spite which only acts on a close distance scale. At close distances, cheaters are exposed to spite and cooperation, leading to low frequency dependent fitness – they are in the "spite zone". At an intermediate distance, cheaters are exposed to cooperation but not spite, so they have the highest fitness – the "goldilocks zone." At large distances, cheaters are too far away to experience spite or cooperation and as a result are in an "asocial dead zone."

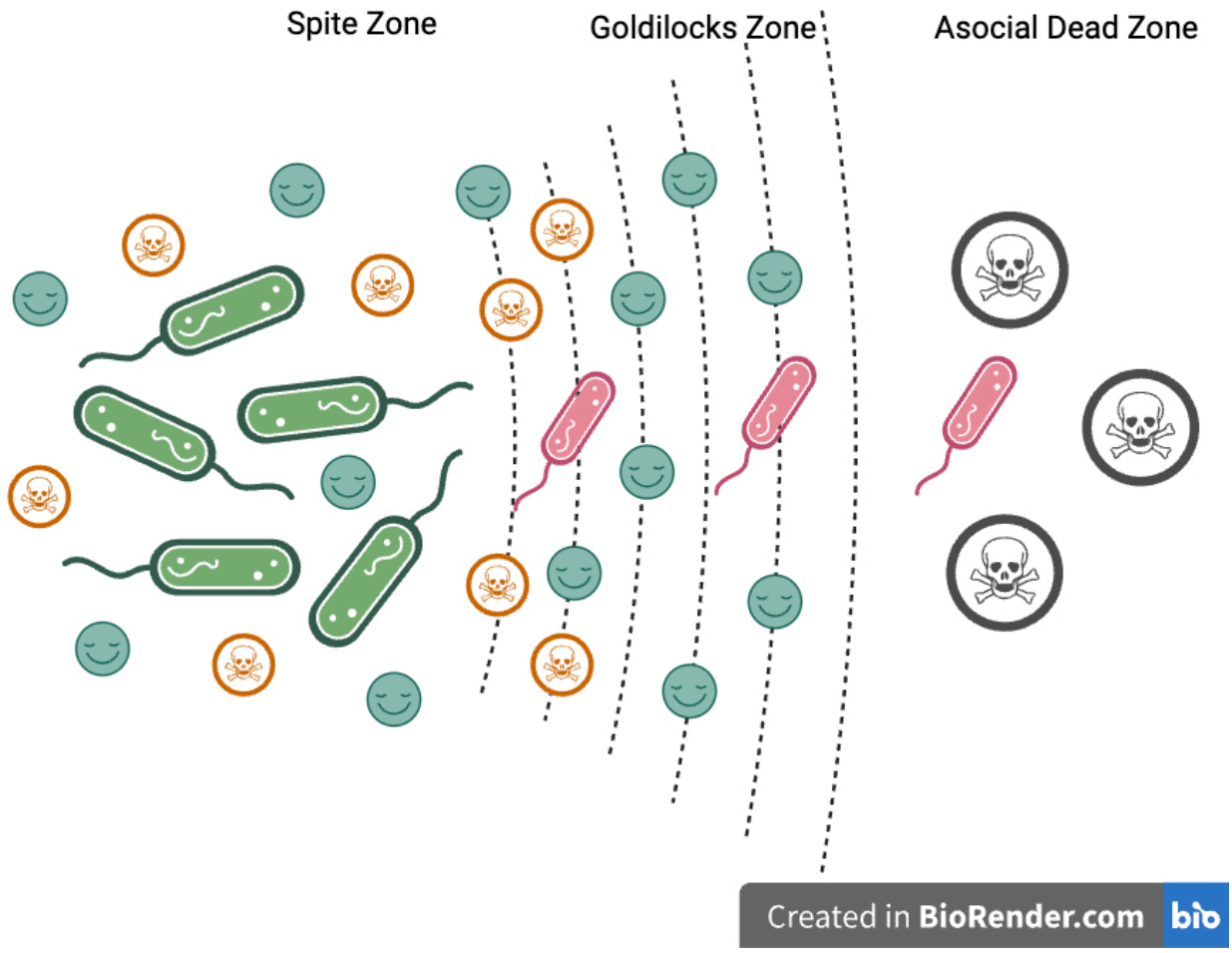

In summary, our study highlights the complexities of bacterial interactions in spatially structured environments, emphasizing the significance of cell surface properties, cell-to-cell proximity, and spiteful behaviors. Our findings contribute to a deeper understanding of the mechanisms governing the success of cheating behaviors and cooperative interactions in spatially structured bacterial populations. Moreover, our work underscores the complexity of bacterial social dynamics in real-

world environments, such as the CF lung, where frequent mutations in QS and cell surface can significantly impact the spatial organization and fitness of microbial populations.

3.6 References

1. **Mankiw NG**. *Principles of microeconomics*. 7th ed. Cengage; 2014.
2. **Hartl DL**. *A Primer of Population Genetics and Genomics*. 4th ed. Oxford University Press; 2020.
3. **Darwin C**. *On the Origin of Species*. Revised Ed. Oxford University Press; 2009.
4. **Gerald S. Wilkinson**. Reciprocal food sharing in the vampire bat Gerald. *Nature* 1984;13:576.
5. **Griffin AS, West SA**. Kin Discrimination and the Benefit of Helping in Cooperatively Breeding Vertebrates. *Science (1979)* 2003;302:634–636.
6. **Hol FJH, Galajda P, Nagy K, Woolthuis RG, Dekker C, *et al.*** Spatial Structure Facilitates Cooperation in a Social Dilemma: Empirical Evidence from a Bacterial Community. *PLoS One* 2013;8:2–11.
7. **Mund A, Diggle SP, Harrison F**. The Fitness of Pseudomonas aeruginosa Quorum Sensing Signal Cheats Is Influenced by the Diffusivity of the Environment. 2017;8:1–8.
8. **Diggle SP, Whiteley M**. Microbe profile: Pseudomonas aeruginosa: Opportunistic pathogen and lab rat. *Microbiology (United Kingdom)* 2020;166:30–33.
9. **Waters CM, Bassler BL**. Quorum sensing: Cell-to-cell communication in bacteria. *Annu Rev Cell Dev Biol* 2005;21:319–346.

10. **Popat R, Cornforth DM, McNally L, Brown SP**. Collective sensing and collective responses in quorum-sensing bacteria. *J R Soc Interface*;12. Epub ahead of print 2015. DOI: 10.1098/rsif.2014.0882.

11. **Papenfort K, Bassler BL**. Quorum sensing signal-response systems in Gram-negative bacteria. *Nat Rev Microbiol* 2016;14:576–588.

12. **Schuster M, Joseph Sexton D, Diggle SP, Peter Greenberg E**. Acyl-homoserine lactone quorum sensing: From evolution to application. *Annu Rev Microbiol* 2013;67:43–63.

13. **Williams P, Cámara M**. Quorum sensing and environmental adaptation in Pseudomonas aeruginosa: a tale of regulatory networks and multifunctional signal molecules. *Curr Opin Microbiol* 2009;12:182–191.

14. **Scholz RL, Peter Greenberg E**. Positive autoregulation of an Acyl- homoserine lactone quorum-sensing circuit synchronizes the population response. *mBio* 2017;8:1–12.

15. **Diggle SP, Griffin AS, Campbell GS, West SA**. Cooperation and conflict in quorum-sensing bacterial populations. *Nature* 2007;450:411–414.

16. **Kostylev M, Kim DY, Smalley NE, Salukhe I, Peter Greenberg E, *et al.*** Evolution of the Pseudomonas aeruginosa quorum-sensing hierarchy. *Proc Natl Acad Sci U S A* 2019;116:7027–7032.

17. **Sandoz KM, Mitzimberg SM, Schuster M**. Social cheating in Pseudomonas aeruginosa quorum sensing. *Proc Natl Acad Sci U S A* 2007;104:15876–15881.

18. **Perlin MH, Clark DR, McKenzie C, Patel H, Jackson N, *et al.*** Protection of Salmonella by ampicillin-resistant Escherichia coli in the presence of otherwise lethal drug concentrations. *Proceedings of the Royal Society B: Biological Sciences* 2009;276:3759–3768.

19. **Bacun-Druzina V, Cagalj Z, Gjuracic K**. The growth advantage in stationary-phase (GASP) phenomenon in mixed cultures of enterobacteria. *FEMS Microbiol Lett* 2007;266:119–127.

20. **Butaitė E, Kramer J, Kümmerli R**. Local adaptation, geographical distance and phylogenetic relatedness: Assessing the drivers of siderophore-mediated social interactions in natural bacterial communities. *J Evol Biol* 2021;34:1266–1278.

21. **Tai JSB, Mukherjee S, Nero T, Olson R, Tithof J, *et al.*** Social evolution of shared biofilm matrix components. *Proc Natl Acad Sci U S A* 2022;119:1–10.

22. **Bjarnsholt T, Alhede M, Alhede M, Eickhardt-Sørensen SR, Moser C, *et al.*** The in vivo biofilm. *Trends Microbiol* 2013;21:466–474.

23. **Alhede M, Kragh KN, Qvortrup K, Allesen-Holm M, van Gennip M, *et al.*** Phenotypes of non-attached pseudomonas aeruginosa aggregates resemble surface attached biofilm. *PLoS One*;6. Epub ahead of print 2011. DOI: 10.1371/journal.pone.0027943.

24. **Darch SE, Kragh KN, Abbott EA, Bjarnsholt T, Bull JJ, *et al.*** Phage inhibit pathogen dissemination by targeting bacterial migrants in a chronic infection model. *mBio*;8. Epub ahead of print 2017. DOI: 10.1128/mBio.00240-17.

25. **Kragh KN, Alhede M, Jensen P, Moser C, Scheike T, *et al.*** Polymorphonuclear leukocytes restrict growth of Pseudomonas aeruginosa in the lungs of cystic fibrosis patients. *Infect Immun* 2014;82:4477–4486.

26. **Kragh KN, Hutchison JB, Melaugh G, Rodesney C, Roberts AEL, *et al.*** Role of multicellular aggregates in biofilm formation. *mBio*;7. Epub ahead of print 2016. DOI: 10.1128/mBio.00237-16.

27. **Azimi S, Thomas J, Cleland SE, Curtis JE, Goldberg JB, *et al.*** O-specific antigen-dependent surface hydrophobicity mediates aggregate assembly type in pseudomonas aeruginosa. *mBio*;12. Epub ahead of print 2021. DOI: 10.1128/mBio.00860-21.

28. **Bjarnsholt T, Jensen PØ, Fiandaca MJ, Pedersen J, Hansen CR, *et al.*** Pseudomonas aeruginosa biofilms in the respiratory tract of cystic fibrosis patients. *Pediatr Pulmonol* 2009;44:547–558.

29. **Palmer KL, Aye LM, Whiteley M**. Nutritional cues control Pseudomonas aeruginosa multicellular behavior in cystic fibrosis sputum. *J Bacteriol* 2007;189:8079–8087.

30. **Veeranagouda Y, Lee K, Cho AR, Cho K, Anderson EM, *et al.*** Ssg, a putative glycosyltransferase, functions in lipo- and exopolysaccharide biosynthesis and cell surface-related properties in Pseudomonas alkylphenolia. *FEMS Microbiol Lett* 2011;315:38–45.

31. **Kiratisin P, Tucker KD, Passador L**. LasR , a Transcriptional Activator of Pseudomonas aeruginosa Virulence Genes , Functions as a Multimer. 2002;184:4912–4919.

32. **Ochsner UA, Koch AK, Fiechter A, Reiser J**. Isolation and characterization of a regulatory gene affecting rhamnolipid biosurfactant synthesis in Pseudomonas aeruginosa. *J Bacteriol* 1994;176:2044–2054.

33. **O'connor K, Zhao CY, Mei M, Diggle SP**. Frequency of quorum-sensing mutations in Pseudomonas aeruginosa strains isolated from different environments. *Microbiology (United Kingdom)* 2022;168:1–12.

34. **Deretic V, Schurr MJ, Yu H**. Pseudomonas aeruginosa, mucoidy and the chronic infection phenotype in cystic fibrosis. *Trends Microbiol* 1995;3:351–356.

35. **Chester IR, Meadow PM, Pitt TL**. The relationship between the O antigenic lipopolysaccharides and serological specificity in strains of Pseudomonas aeruginosa of different O serotypes. *J Gen Microbiol* 1973;78:305–318.

36. **Hancock REW, Mutharia LM, Chan L, Darveau RP, Speert DP, *et al.*** Pseudomonas aeruginosa isolates from patients with cystic fibrosis: A class of serum-sensitive, nontypable strains deficient in lipopolysaccharide O side chains. *Infect Immun* 1983;42:170–177.

37. **Ojeniyi B, Bék L, Høiby N**. Polyagglutinability Due to Loss of O-Antigenic Determinants in Pseudomonas Aeruginosa Strains Isolated from Cystic Fibrosis Patients. *Acta Pathologica Microbiologica Scandinavica Series B: Microbiology* 1985;93 B:7–13.

38. **Penketh A, Pitt T, Roberts D, Hodson ME, Batten JC**. The relationship of phenotype changes in Pseudomonas aeruginosa to the clinical condition of patients with cystic fibrosis. *American Review of Respiratory Disease* 1983;127:605–608.

39. **Varga JJ, Barbier M, Mulet X, Bielecki P, Bartell JA, *et al.*** Genotypic and phenotypic analyses of a Pseudomonas aeruginosa chronic bronchiectasis isolate reveal differences from cystic fibrosis and laboratory strains. *BMC Genomics* 2015;16:1–27.

40. **García-Reyes S, Soberón-Chávez G, Cocotl-Yanez M**. The third quorum-sensing system of Pseudomonas aeruginosa: Pseudomonas quinolone signal and the enigmatic PqsE protein. *J Med Microbiol* 2020;69:25–34.

41. **Groleau M, de Oliveira Pereira T, Dekimpe V, Déziel E**. PqsE Is Essential for RhlR-Dependent Quorum Sensing Regulation in Pseudomonas aeruginosa. *mSystems* 2020;5:1–13.

42. **Yan H, Asfahl KL, Li N, Sun F, Xiao J, *et al.*** Conditional quorum-sensing induction of a cyanide-insensitive terminal oxidase stabilizes cooperating populations of Pseudomonas aeruginosa. *Nat Commun* 2019;10:1–7.

43. **Letizia M, Mellini M, Fortuna A, Visca P, Imperi F, *et al.*** PqsE Expands and Differentially Modulates the RhlR Quorum Sensing Regulon in Pseudomonas aeruginosa. *Microbiol Spectr*;10. Epub ahead of print 2022. DOI: 10.1128/spectrum.00961-22.

Chapter 4: Amendment: Supplementary and Preliminary Results

Kathleen O'Connor, Ryan Lowhorn, Stephen P. Diggle

4.1 Introduction

The following section comprises of work relating to Chapter 3 that serves as either supplementary data useful for future Diggle lab students, or data that was too preliminary to be included in the Chapter. Chapter 3 in its current state is a complete manuscript for the purpose of this thesis, but will be amended before publication. A portion of the following data may be included for publication.

4.2 Results

Decreasing the Carbon Source Negatively Impacts Cheater Fitness

Previous experiments in liquid media have shown that decreasing carbon source concentration leads to higher cheat fitness [1]. Cheaters have an increased ability to invade cooperator populations when nutrients are low, likely because of the higher Cost (C) for cooperators. We wanted to test if this would be the case in spatially structured populations. We created media with 50% carbon concentration: BSA 0.5% and CAA 0.025%, and performed cheating experiments with Δ*lasR*Δ*rhlR* against Δ*ssg*. We chose this combination because Δ*lasR*Δ*rhlR* were the cheats with the greatest fitness benefit against Δ*ssg*. We found that decreasing the carbon source positively impacted cheater fitness, similar to what is seen in liquid studies (Figure S1).

Figure S1. We tested the effects of carbon source limitation on Δ*lasR*Δ*rhlR* cheating on Δ*ssg*. In previous liquid experiments, we see that limiting carbon will decrease the fitness of cheaters. Here in spatial structure, we found that limiting carbon increases the fitness of cheaters.

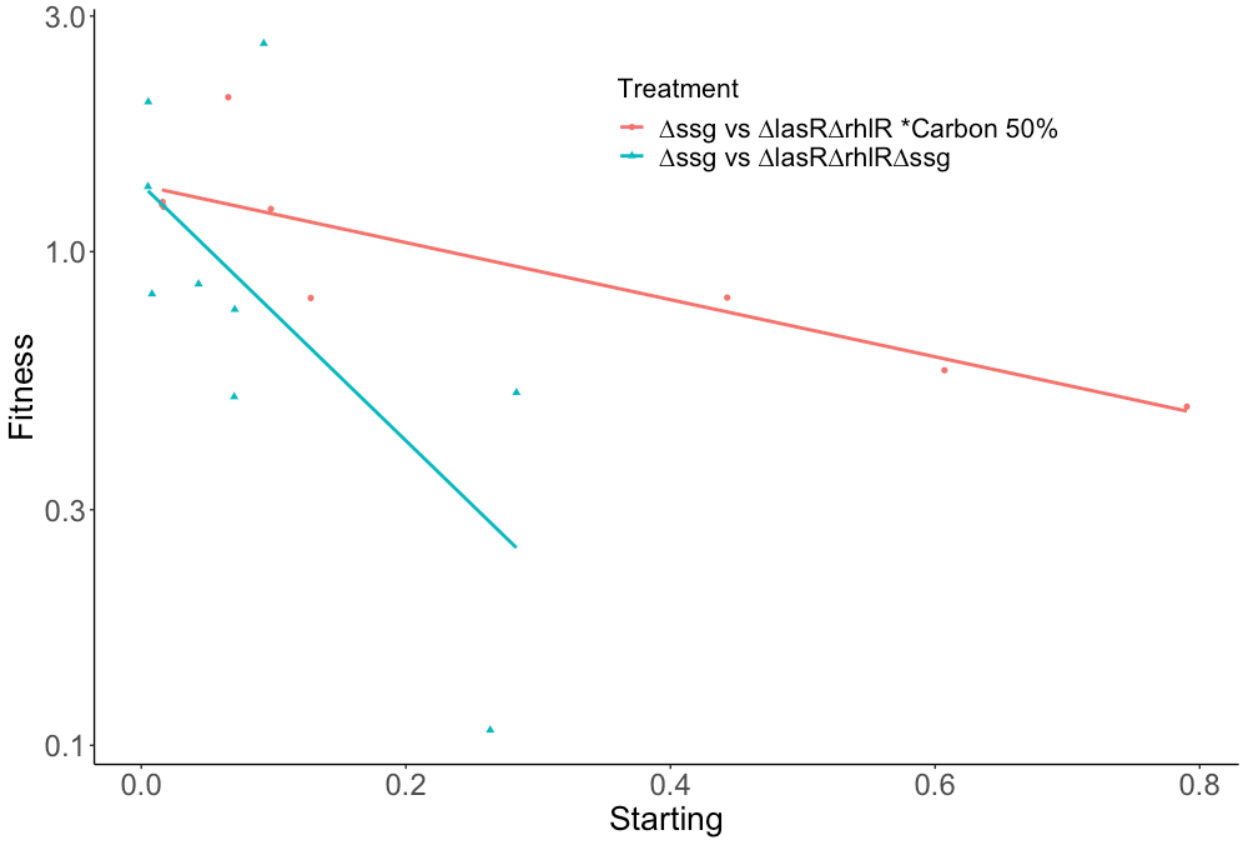

Hydrogen Cyanide is Essential for Cheating

We mixed hydrophilic Δ*lasR*Δ*rhlR* cheaters with hydrophilic PAO1Δ*hcnABC* cooperators unable to produce hydrogen cyanide. We expected that Δ*lasR*Δ*rhlR* cells would cheat better in the absence of spiteful hydrogen cyanide production; surprisingly, we found the opposite (Figure S2). Δ*lasR*Δ*rhlR* cells had lower fitness against PAO1Δ*hcnABC* than they did against PAO1.

Figure S2. When mixing ΔlasRΔrhlR with hydrogen cyanide negative cooperators, we expected to see improved fitness of cheaters. In fact, cheaters had worse fitness against PAO1Δ*hcnABC* than they did against wildtype cooperators. Hydrogen cyanide appears to be essential for cheater proliferation as evidenced by the few cheater cells seen in images (A) and the low fitness found using plating (B).

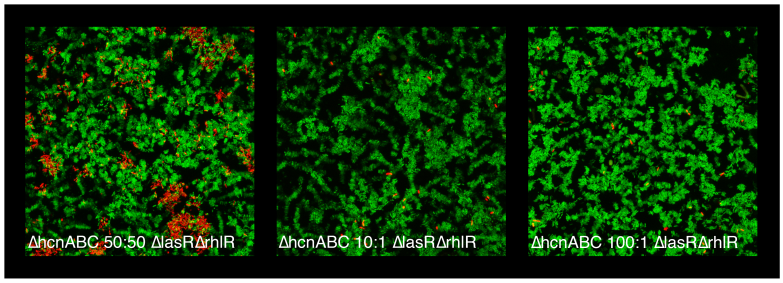

A.

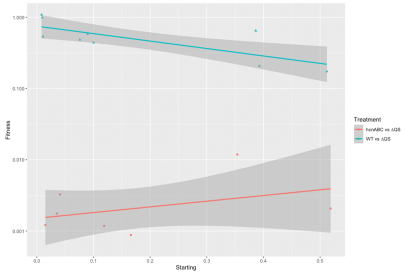

B.

MicrobeJ Analysis Proves Useful for A Portion of Image Analysis

To assess cheater frequency, we plated for total population counts and cheater counts at t=0 and t=22 hours. The cells form multi-cellular aggregates so it is essential to break cells up using bead beating. The fitness counts were determined using plate counts. To analyze cell-to-cell proximity, we used MicrobeJ, an ImageJ plug-in to segregate cells and assign them an x, y, and z position in space. We wanted to determine if MicrobeJ would accurately count cells, so we compared MicrobeJ counts to plate counts. We used a sample that had plate counts and images produced on the same day: Δ*ssg* vs Δ*lasR*Δ*rhlR*; note that there are two image files for each plate count. We found the total number of red cells (cheaters) and divided that by the total number of red and green cells (total population) to find the ratio. We found that for 1:10 and 1:100 mixes of cheaters and cooperators, the MicrobeJ counts were highly inaccurate (Table S1). We determined the proximity between cells using the 50:50 mixes, and we found that the ImageJ ratio was closer to the Plating frequency. Before publication, we will investigate an alternative method to count cells or voxels.

Table S1. We used MicrobeJ to count red and green cells for each image (Condition), and plated for cell counts. The MicrobeJ ΔQS Frequency was calculated by dividing the sum of red cells by the total of red and green cells. Plating frequency was determined by dividing Δ*lasR*Δ*rhlR* counts on Tp500 LBA plates by total LBA counts.

Condition	Red Cells	Green Cells	MicrobeJ ΔQS Freq	Plating ΔQS Freq
ssg10-1lasRrhlR-bsa0.5caa0.025_rep1_image1	2556	2283	0.53	0.11
ssg10-1lasRrhlR-bsa0.5caa0.025_rep1_image2	835	5108	0.14	0.11
ssg10-1lasRrhlR-bsa0.5caa0.025_rep2_image1	1093	19874	0.05	0.12
ssg10-1lasRrhlR-bsa0.5caa0.025_rep2_image2	3838	14000	0.22	0.12
ssg10-1lasRrhlR-bsa0.5caa0.025_rep3_image1	1964	2020	0.49	0.13
ssg10-1lasRrhlR-bsa0.5caa0.025_rep3_image2	1300	9109	0.12	0.13
ssg100-1lasRrhlR-bsa0.5caa0.025_rep1_image1	395	2505	0.14	0.02
ssg100-1lasRrhlR-bsa0.5caa0.025_rep1_image2	240	3194	0.07	0.02
ssg100-1lasRrhlR-bsa0.5caa0.025_rep2_image1	449	3465	0.11	0.02
ssg100-1lasRrhlR-bsa0.5caa0.025_rep2_image2	495	5438	0.08	0.02
ssg100-1lasRrhlR-bsa0.5caa0.025_rep3_image1	220	1977	0.1	0.02
ssg100-1lasRrhlR-bsa0.5caa0.025_rep3_image2	331	3745	0.08	0.02
ssg50-50lasRrhlR-bsa0.5caa0.025_rep1_image1	1943	5061	0.28	0.39
ssg50-50lasRrhlR-bsa0.5caa0.025_rep1_image2	1803	4122	0.3	0.39
ssg50-50lasRrhlR-bsa0.5caa0.025_rep2_image1	6650	3150	0.68	0.65
ssg50-50lasRrhlR-bsa0.5caa0.025_rep2_image2	4756	2563	0.65	0.65
ssg50-50lasRrhlR-bsa0.5caa0.025_rep3_image1	8201	3617	0.69	0.47
ssg50-50lasRrhlR-bsa0.5caa0.025_rep3_image2	3542	2547	0.58	0.47

4.3 References

1. **Sexton DJ, Schuster M**. Nutrient limitation determines the fitness of cheaters in bacterial siderophore cooperation. *Nat Commun* 2017;8:230.

Conclusion

In this thesis, I explored the variation and social dynamics of QS in *P. aeruginosa*. *P. aeruginosa* is an important pathogen, responsible for antibiotic resistant chronic and acute infections, and additionally serves as a common model for QS studies. It has a highly complex interconnected series of QS systems that regulate virulence traits and are essential for the cell to establish itself in new environments. QS variation in *P. aeruginosa* has become a hot topic as labs have revealed that many environmental and infection isolates have differently regulated QS systems compared to lab strains. Beyond studying the intricate dynamics regulating QS in *P. aeruginosa*, the field has also looked at QS as a social trait. QS allows the cell to respond to changes in cell density, and it regulates both cooperation and spite – social behaviors that either help or harm neighbors. The field began by studying intra-species social behaviors in liquid culture, and has now expanded to inter-species interactions, and interactions in spatially structured environments. Through my research, I found that QS in *P. aeruginosa* is a complex behavior that is highly variable across isolates and its social dynamics are strongly impacted by spatial structure.

Using the International Pseudomonas Consortium Database (IPCD), I queried over 800 strains of *P. aeruginosa* to investigate the frequency of QS gene mutations across different environments. In searching through isolates from the environment, the CF lung, and wounds, I found that some QS genes were conserved while others were highly variable. Consistent with previous studies, I found that not only was LasR the most variable protein, but LasR varied in isolates outside of the CF lung, with highly divergent protein sequences found in wound and environmental isolates. The negative regulator of the *las* system, RsaL was highly conserved. It was striking that LasR, which

hierarchical activates QS in most strains was commonly lost and mutated, while the negative regulator RsaL was conserved. These results indicate that there must be a fitness benefit to suppressing or losing QS activity across different environments. The *las* system, made up of LasR and LasI were more variable than their homologs: RhlR and RhlI. Transcriptional regulators for the AHL systems, RhlR and LasR were more variable than signal synthases, RhlI and LasI. Lengthy *pqs* system genes *pqsH*, *pqsL*, and *pqsA* were highly variable, likely due to their length – more amino acid residues means more opportunities for mutations.

In addition to looking at the protein sequences, I looked at QS-associated phenotypic traits of 12 isolates from the IPCD. Loss of protease secretion and colony autolysis are traits that have long been associated with *lasR*- mutants isolated from the CF lung. The *las* and *rhl* systems control protease secretion, and since *las* hierarchically regulates *rhl* in most strains, loss of *las* often leads to loss of protease secretion. I found that *las* protein sequence correlated with protease secretion in some strains, but there were *lasR*- strains with high protease secretion. In 2 strains with low protease secretion and wildtype LasR, I found that they had the same RhlI mutation, indicating that RhlI, and not solely *las* affects colony protease secretion. Colony autolysis and colony sheen are also associated with *lasR*- mutants from the CF lung, but they are not traits solely determined by *las* system mutation. A similar type of sheen has been documented in Δ*pqsL* strains and is due to HHQ accumulation, the precursor of the PQS molecule. I reasoned that if I deleted *pqsA*, the first step in the pathway to making *pqs* system intermediates, I would lose the colony autolysis phenotype in Δ*lasR* mutants. In lab strains, we see colony autolysis in Δ*lasI*, Δ*lasR*, Δ*pqsH* and Δ*pqsL* due to an accumulation of HHQ or HQNO. When Δp*qsA* is deleted in these strains, the above mutants revert back to a typical colony form with no autolysis. In strains from the IPCD,

colony autolysis could sometimes be attributed to LasR protein sequence, but other times it was due to *pqs* system mutations. For both protease secretion and colony autolysis, more than one QS system is responsible for the phenotype.

After looking at the variation in QS proteins across *P. aeruginosa* isolates, I focused on the impact QS mutation has on social dynamics in spatial structure. I found that aggregate formation and proximity are important for QS social dynamics in *P. aeruginosa*. The outside of a wildtype PAO1 *P. aeruginosa* cell is hydrophilic due to its lipopolysaccharide (LPS) structure. When the B-band portion of the O-antigen is mutated - the outermost portion of the LPS – then the cell becomes hydrophobically charged. Mutations in the *ssg* or *wbpL* genes lead to a mutated B-band and hydrophobic cell surface. *P. aeruginosa* cells form distinct aggregate types in liquid media with polymers depending on their cell surface hydrophobicity. Hydrophilic cells form "stacking" or tube-like aggregates due to entropic de-aggregation, where cells are pushed side-to-side into aggregates by polymers. Hydrophobic cells form distinctly different aggregates of irregular size and shape due to their sticky texture in hydrophilic medium; we call these "clumping" aggregates. When mixing labeled red and green cells that are both hydrophilic, cells form mixed aggregates with close mixing between red and green. The same happens when mixing labeled red and green hydrophobic cells – they form mixed aggregates. However, when combining labeled hydrophilic and hydrophobic cells, they form distinct stacking and clumping aggregates, and there is reduced mixing between red and green cells. I took advantage of these differences in aggregation to test how proximity affects social behaviors in spatially structured populations of *P. aeruginosa.*

P. aeruginosa engages in QS signaling to control cooperation and spite behaviors. Cooperation takes many forms - here we focus on protease secretion, a public good that is susceptible to non-cooperating cheats. In liquid cultures, cooperators and cheats co-mingle, leading to an overgrowth of cheaters and loss of the cooperative trait. Previous research in spatial structure has suggested that proximity is important for cheating, however the exact distance that social behaviors play out on needs to be defined. I looked at the effects of aggregate type and cooperation and spite on *P. aeruginosa* intra-species interactions. To study this, I looked at cheating on QS-controlled protease secretion by QS-null cheaters: Δ*lasR*Δ*rhlR* cells. I manipulated the distance between cells in spatial structure by mixing cells with different cell surfaces that formed independent aggregates. I tested 3 conditions where cheaters were either very close to cooperators, an intermediate distance apart, or far from cooperators. I found that cheaters were most fit at an intermediate distance from cooperators, indicating that another factor in addition to cooperation, such as spite, might be at play. In looking at spite behaviors controlled by *pqsE*, I found that spite works on a smaller distance scale than cooperation. This results in a "goldilocks zone" where cheaters thrive at an intermediate distance from cooperators where they are exposed to cooperative goods but not spite.

Future Works

P. aeruginosa is highly variable pathogen that diversifies and adapts during chronic infection in human hosts. An important factor in its ability to cause infection is how its QS system functions. I found that some aspects of QS are highly conserved, while others are highly variable. Interestingly, despite being thought of as essential for infection, there appears to be a fitness benefit to losing QS activity in multiple environments. The system is no strictly hierarchical and traits that were previously attributed to the *las* system are co-regulated by the *pqs* or *rhl* systems. Much of our understanding of QS as a social trait comes from studies in liquid cultures. In liquid medium, QS as a cooperative trait is quickly lost to cheat invasion. Once spatial structure is introduced, cheaters have less of a benefit. The field believed that fitness loss was due to increased distance between cooperators and cheaters, or due to decreased diffusion in solid medium. I found that factors such as proximity and spite are important for cheater fitness in spatially structured medium. The work described in Chapter 2 is incomplete as written. I explored the effect of spite on cheaters using the *pqsE* gene, a global regulator controlling pyocyanin and hydrogen cyanide production. However, the *pqsE* controls many genes beyond those two spite genes so it is important to look specifically at individual spite behaviors: pyocyanin production (*phzM*) and hydrogen cyanide production (*hcnABC*). In addition to the work I propose doing to complete the work described in Chapter 2 for publication, it is important for the field to look at spite as a cheatable trait. The field has clearly established that cooperative behaviors in bacteria are widely cheatable, but as a field we haven't yet tested cheating on spite behaviors. The field should also investigate the effect of b, "benefit" as part of Hamilton's rule affecting the maintenance of cooperation. Works have looked at C and r (Cost and relatedness), but not yet the benefit received from cooperation. Beyond studying social

aspects of QS, the field should further explore QS regulatory mechanisms. The past 5 years has seen an influx of papers on *pqs* and *rhl* system regulation and the way the two interact without *las*. In the introduction I propose two mechanisms that allow for the evolution of *rhl* independent function, and the field should explore those mechanisms to better understand QS regulation. The work explored in Chapters 1 and 2 of this thesis increase our understanding of the variation in *P. aeruginosa* QS and the effects of spatial structure on its social dynamics. It is essential that we continue studying social behaviors in spatial structure because our world is spatially structured. We must also continue exploring the social dynamics spite behaviors which are understudied compared to cooperation.